Precision targeting of *pten*-null triple-negative breast tumors guided by electrophilic metabolite sensing

Xuyu Liu, Marcus J. C. Long, Benjamin D. Hopkins, Chaosheng Luo,
Lingxi Wang, and Yimon Aye*

SUPPLEMENTARY INFORMATION

Supplementary Figure Legends

Figure S1. MK-G exhibits overall reduced covalent labeling compared to MK-HNE and preference toward Akt2-binding. The HEK293T cells ectopically expressing the indicated Halo-Akt-variants were treated with either 5 μM of indicated compounds or DMSO in 3% FBS for 48 hours before cell lysis and Click-coupling with Cy5-azide. M, molecular weight markers (in kDa). Anti-Halo and anti-actin anti-bodies were used to assess relative expression of Halo-Akt(n) transgenes and lysate loading, respectively. Representative data from experiments where MK-G was compared with **(a)** MK-HNE and MK-2206, and **(b)** MK-2206 alone. (n = 4 independent biological replicates). **Inset** in **(a)** shows chemical structures of compounds used. Rectangular box indicates the corresponding Cy5-signal of Halo-Akt(n), used in the quantification. Also see **Fig. 1b-c**.

Figure S2. Dose-responsive covalent association analysis of Akt2- vs. Akt3-labeling in cells by MK-HNE. HEK293T cells transiently transfected with pCS2+8-plasmids encoding either His_6-Halo-Akt3 *(left panel)* or His_6-Halo-Akt2 *(right panel)* were treated with MK-HNE at indicated concentrations over 24 hr period in 3% FBS prior to cell lysis and Click coupling assay using Cy5-azide. M, molecular weight markers (in kDa). Rectangular box indicates the corresponding Cy5 signal of Halo-Akt(n), used in the quantification (see inset). Anti-Halo and anti-actin antibodies probe expression of Halo-Akt(n) protein and lysate loading, respectively. **Inset:** quantification of relative Cy5-signal intensity on the Halo-Akt(n)-band. [Error bars indicate s.e.m.; technical replicates: n = 14 (left panel); n = 6 (right panel); independent biological replicates: n ≥ 4 (left panel); n = 3 (right panel)]. The relative fluorescent intensity (RFI) is calculated from the following equations:

$$RFI = \{(Cy5_{(X\ \mu M)} / Halo_{(X\ \mu M)}) \div (Cy5_{(25\ \mu M)}/Halo_{(25\ \mu M)})\} \div (\text{corresponding plateau})$$

Data in each plot are fit to the following equations:
(one-site-binding model):

$$\boldsymbol{RFI} = \boldsymbol{B_{max}} \times \frac{[I]}{\boldsymbol{K_i} + [I]}$$

where B_{max} is the signal intensity corresponding to maximum binding on Halo-Akt(n) thereby, yielding: $K_{i(\text{Halo-Akt3})}$ = 7.3 μM, $K_{i(\text{Halo-Akt2})}$ = 23.8 μM

Figure S3. MK-HNE labels endogenous Akt. Native HEK293T cells were treated with 5 μM MK-HNE or an equivalent volume of DMSO in 3% FBS for 12 h prior to cell lysis. A fraction of each sample was used for the input blot. The remaining cell lysates were subjected to Click coupling with biotin-azide followed by streptavidin enrichment. Western blot analysis was performed using anti-pan-Akt antibody (Cell Signaling: C67E7). Independent biological replicates: DMSO, n = 3; MK-HNE, n = 3.

Figure S4. Effects of MK-HNE and MK-2206 on Halo-Akt2 kinase activity. Also see **Figure 2. Inset**: Schematic representation of the ratiometric FRET-based AktAR reporter assay. Phosphorylation of a peptide substrate (within the region indicated by maroon curve) by Akt isozymes allows a phospho-peptide binding domain (also within the same region marked by maroon curve) to bind the phosphorylated substrate resulting in an increase in FRET (indicated by a blue lightning-bolt). Thus, drop in ratiometric FRET signal reports on downregulation of Akt(n)-specific enzymatic activity in cells ectopically co-overexpressing AktAR and corresponding Halo-Akt(n). Black wavy arrow: 458 nm excitation, green wavy arrown: YFP signal, blue wavy arrow: CFP signal, wherein the relative size of the green and blue arrows represents the relative magnitude of emission. Representative confocal images of HEK293T cells expressing AktAR and Halo-Akt2 under indicated treatment conditions are shown. Cells were excited using an Argon laser (458 nm). Images were obtained using cyan (463–498 nm) and yellow (525–620 nm) channels. Scale bar: 10 μm. Quantitation of YFP/CFP ratio of individual cells was performed using Image-J. Error bars indicate 5-95% confidence intervals, boxes show upper and lower quartiles, and central bar shows median with *n* = 303, 150, 406 (24 h); 77, 198, 122 (48 h); 163, 144, 98 (withdrawal). Cells per condition were from 3 independently replicated sets at different passage numbers. Two-tailed unpaired *t*-test was applied.

Figure S5. MK-HNE manifests a different mechanism of Akt-pathway regulation relative to MK-2206.

(a) Western blot analysis of Akt-T305 phosphorylation following cell treatment with indicated compounds. Left: representative data. Right: quantitation (relative pT305 signal intensity normalized to Halo). Two-tailed unpaired *t*-test was applied. Error bars indicate mean ± s.e.m. (Independent biological replicates: DMSO, n = 5; MK-2206, n = 4; MK-HNE, n = 6).

(b) Quantitation from a similar treatment of cells but lysates were analyzed by ratiometric-sandwich ELISA assays. Two-tailed unpaired *t*-test was applied. Error bars indicate mean ± s.e.m. (DMSO, n = 4, MK-2206, n = 3, MK-HNE, n = 4).

Figures S6. MK-NE and MK-FNE covalently labels Akt3 to an extent similar to MK-HNE. HEK293T cells were transfected with Halo-Akt3 for 20 h, then treated with the indicated compound (5 μM, 48 h). After this time, cells were lysed and the labeling was assayed by Click coupling using Cy5-azide.

(a) Representative data: Top: in-gel fluorescence data with Cy5-azide. M, molecular weight ladder (in kDa). Rectangular box indicates the Cy5 signal of Halo-Akt3, which used in the quantification. Bottom: western blots probing for Halo and actin, respectively. Inset: structures of indicated compounds.

(b) Quantitation: relative Cy5-signal intensity normalized by Halo-expression levels. Two-tailed unpaired *t*-test was applied. Error bars indicate mean ± s.e.m. (MK-NE, n = 4; MK-HNE, n = 4; MK-FNE, n = 4).

Figures S7. Covalent or reversible inhibition by MK-HNE, MK-NE, and MK-G, analyzed by NADH-coupled Akt3-kinase-activity assays. Also see **Figure 3(a)-(c)**. See methods for details. [Note: specific activity of the commercial source of recombinant human Akt3 (Active Motif, 31147) varies batch-to-batch, rendering differences in the amount of product formed (Y-axis values) despite the same enzyme concentration deployed in each assay].

(a) and **(b):** Progress curves show dose-dependent inhibition of recombinant-human-Akt3 (0.15 μM) by MK-HNE (a) and MK-NE (b), respectively. Solid curves: best non-linear fits using Eq(i) (see (e); the same equations are also shown in **Fig. 3**). Error bars indicate s.e.m. (n=3 technical replicates). For biological replicates, n=2 for (a); and n=3 and 2, respectively, for 1, 5 and 10 μM; and 0, 2 and 40 μM for (b).

(c) and **(d):** k_{obs} [derived from Eq(ii) in (e)] against respective inhibitor concentration. Data were fit to Eq(iii) in (e). (Error bars indicate s.e.m.; n ≥3 biological replicates). Insets show chemical structures of the two compounds.

(e) Fitting analysis associated with data in (a)—(d).

(f) Progress curves show dose-dependent inhibition of recombinant-human-Akt3 (0.15 μM) by MK-G. Solid curves: best linear fits using Eq(iv) [see (h)]. Error bars indicate s.e.m.

For biological replicates, n = 5 for 0 μM, n = 4 for 10 and 20 μM, and n = 3 for 30, 50 and 100 μM.

(g) k_i [derived from Eq(iv); see (h)] against respective inhibitor concentration. k_0 derived from enzymatic rate in the saturated substrate conditions. Data were fit to Eq(vi) in (h). (Error bars indicate s.d.; n ≥3 biological replicates). Inset shows chemical structure of MK-G.

(h) Fitting analysis associated with data in (a)—(d).

Figures S8. Dominant loss of Akt3-kinase activity measured by AktAR-ratiometric-FRET reporter assays [also see **Fig. 3(d)-(e), S4**-inset, and **S9**]. HEK293T cells were co-transfected with AktAR-reporter-plasmid and an equivalent amount of a plasmid mix containing Halo-Akt3(wt:C119S) in the indicated ratios. After 12-h, cells were treated (48-h) with MK-FNE (5 μM) or DMSO; washed twice with drug-free media; and allowed to recover over another 24-h in compound-free media (indicated as: "withdrawal"). The Akt kinase activities corresponding to 24-h and 48-h treatment time as well as that of 24-h cell recovery in drug-free media were measured using ratiometric FRET analysis in live cells. Representative images of HEK293T cells expressing AktAR and Halo-Akt3(wt:C119S) (in 25:75, 10:90 and 0:100 ratio) are shown. See **Fig. 3(e)** for image-J quantitation of YFP/CFP-emission ratios after 24-h-recovery in drug-free media. Equation shown in the inset was applied for the quantification of ratiometric FRET signal (see **Fig. 3e**).

Figure S9. Inhibition analysis in cells co-expressing Akt2 and Akt3C119S measured by AktAR-ratiometric-FRET reporter assays. HEK293T cells were co-transfected with AktAR-reporter-plasmid and an equivalent amount of a plasmid mix containing Halo-Akt2:Halo-Akt3C119S in the indicated ratio. After 12-h, cells were treated (48-h) with MK-FNE (5 μM) or DMSO; washed twice with drug-free media; and allowed to recover over another 24-h in compound-free media (indicated as: "withdrawal"). The Akt kinase activities corresponding to 24-h and 48-h treatment time as well as that of 24-h cell recovery in drug-free media were measured using ratiometric FRET analysis in live cells (see **inset** in **Fig. S4**). Representative images of HEK293T cells expressing AktAR and Halo-Akt2:Halo-Akt3C119S (in 100:0, 50:50, 25:75 and 0:100 ratio) are shown in **(a), (c)**

and **(e)**. The corresponding quantification are shown in **(b), (d)** and **(f)**. Data were normalized to the respective DMSO-treated samples subjected to otherwise identical conditions. Error bars indicate 5-95% percentile of data. *P* values are from two-tailed unpaired *t*-test. In dot plot **(b),** *n* (cell no. from left to right) = 139, 176, 164, 142. In dot plot **(d),** *n* (cell no. from left to right) = 76, 121, 159, 140. In dot plot **(f),** *n* (cell no. from left to right) = 170, 158, 148, 72. Data were collected from 3 independent sets of cells at different passage numbers. **Inset** below shows the equation applied for the quantification of ratiometric FRET signal in (b), (d) and (f).

Figures S10. Effects of MK-2206, MK-HNE, and MK-FNE on cell proliferation in continuous treatment vs. withdrawal conditions. MDA-MB-468 cells were treated with the indicated compound at its EC_{60} concentration for 48 hours [MK-2206 (2 μM), MK-FNE (3 μM), and MK-HNE (6 μM)]. For half of the samples, the media containing the compound were then removed and cells were allowed to recover for a further 24 h [denoted as "wd" (withdrawal)], whereas for the other half, cells were cultured in the new media containing the same concentration of the compound for another 24 h. The percentage of growth is normalized to DMSO-treated cells over 72 h subjected to the same handling procedure. Two-tailed unpaired *t*-test was applied. Error bars indicate mean ± s.e.m. (Number of independent biological replicates: MK-2206 and MK-2206 wd, n = 8, MK-HNE and MK-HNE wd, n =8, MK-FNE and MK-FNE wd, n = 8).

Figures S11. Absence of synergism between MK-2206 and HNE-amide in the effects on MDA-MB-468 cell proliferation.

Proliferation assessment of MDA-MB-468 cells was analysed following 72-h treatment with MK-2206 and/or HNE-amide at indicated concentrations. Identical final concentration of vehicle (DMSO) replaced the absence of the other compound, where applicable. The percentage of growth is normalized to DMSO-treated cells over 72 h which was set as 100%. Two-tailed unpaired *t*-test was applied. Error bars indicate mean ± s.e.m. (Independent biological replicate: n = 8)

Figures S12. Differential effects of MK-2206 and MK-FNE on MK-2206-resistant T47D cell proliferation.

(a) Native T47D-cells (denoted as wild-type "wt") and T47D-cells raised in MK-2206-containing media (known as MK2206-resistant cells, and denoted as "MK-res") were

treated with MK-2206 or MK-FNE over 72 h at the indicated concentrations. Solid curves represent the best non-linear fit to equation below. Error bars indicate s.e.m.; n = 8 independent biological replicates from 2 independent sets of cells at different passage numbers.

$$\%\ Viable\ cells = \frac{1}{1+\left(\frac{[I]}{EC_{50}}\right)^{n}} \times 100\ \%$$

The fold increase in resistance of T47D(MK-res) relative to T47D(wt) against each compound was calculated using the equation below.

$$Fold\ increase\ in\ resistance = \frac{EC_{50(MK\text{-}res)}}{EC_{50(wt)}}$$

(b) Western blots probing for endogenous Akt isoforms and gapdh, respectively. Bottom: quantitation (relative Akt isoform signal intensity normalized to gapdh). Two-tailed unpaired *t*-test was applied. Error bars indicate mean ± s.e.m. (Independent biological replicates: Akt1: wt, n = 3, MK-res, n = 4; Akt2: both wt and MK-res, n = 3; Akt3: wt, n = 3, MK-res, n = 4).

Figure S13. Western blot validation of Akt-isoform-specific knockdown in MDA-MB-468 cells. Representative data: Top blots: western blots probing for endogenous Akt isoforms upon the corresponding siRNA knockdown or control siRNA treatment, and gapdh. Denoted numbers on the side are the ladder marker (kDa). *Bottom:* quantitation [relative western blot signal intensity for respective Akt(n) normalized to gapdh]. Error bars indicate mean ± s.e.m. Precise *P* values are annotated. Independent biological replicates from 2 independent sets of cells at different passage numbers: Akt3: siAkt3-1 and -2, n = 10, siCont-1 and siCont-2, n = 8; Akt2: siAkt2-1 and -2, n = 5, siAkt2-3, n = 4, siAkt2-4 and -5, n = 6, siCont-1, n = 9, siCont-2, n = 3, siCont-3, n = 6; Akt1: siAkt1-1, n = 5, siAkt1-2, n = 6, siCont-1 and -2, n = 6. See supplementary methods for target sequences of relevant siRNAs.

Figure S14. Incorporation efficiency analysis in heavy amino-acid-labeled MDA-MB-468 cells and comparison of enriched hits in this study with the known Akt-substrates from PhosphoSitePlus® database. Also see **Fig. 5**. **(a)** Frequency distribution plot (shown in %) of histones and histones-associated proteins incorporated

with the heavy amino acids, $^{13}C_6$,$^{15}N_2$-lysine and $^{13}C_6$,$^{15}N_4$-arginine, enriched from 'heavy' MDA-MB-468 cells following Shechter et al.'s protocol[1]. **(b)** The Venn diagram shows the protein hits found in the MK-2206 and MK-FNE treatment groups against the known Akt substrates recorded in PhosphoSitePlus® database (denoted as PSP) [2].

Figure S15. Predicted Akt-phosphorylation sites of KIFC1, JUP and Grsf1 proteins. The number on either side denotes the flanking residue numbers of the corresponding amino-acid sequence. T/S residues highlighted in red are the predicted phosphorylation sites based on the canonical Akt-phosphorylation-site sequence RXXT/S that antibody recognizes. ***a*** designates the sequence wherein phosphorylation of the highlighted T/S residue has been found in high-throughput phosphoproteomic studies reported in PhosphoSitePlus® database [2].

Figure S16. Western blot validation of Grsf1- and JUP-shRNA-knockdown in MDA-MB-468 cells. Top: representative blots probing the respective endogenous protein expression level in indicated shRNA knockdown lines or knockdown-control (shCont). See **Fig. 5d** for the corresponding data regarding KIFC1. Either vinculin or actin was used as a loading control. Denoted numbers on the side of the blots are the ladder mass (kDa). Bottom: quantitation (relative signal intensity of the band corresponding to protein of interest, normalized to loading control). Precise *P* values are annotated. (shGrsf1: shCont-1, n = 10, siCont-2, n = 9, shGrsf1-1, n = 6, shGrsf1-2 and 3, n = 9. JUP: shCont-1 and -2, n = 6, shJUP-1 and -2, n = 6, shJUP-3, n = 4).

Figure S17. Relative gene expression levels of Akt isoforms, KIFC1, and Grsf-1 in breast tumor. The RNA-seq data are gathered from GDC and TCGA patient database and shown here as heat maps. The relative scale of RNA-seq read intensity is shown at the bottom of each heat map. The magnitude of deviation from the average expression level is represented by the difference in color intensity. Gene-gene Pearson correlation analysis between each gene pair and the corresponding Akt isoform is shown in the table below as *r*-value together with the corresponding statistical significance (*P*-value, two-tailed analysis). Images were created with UCSC Xena.[3]

Figure S18. Relative gene expression levels of Akt isoforms, and KIFC1, Grsf-1 in lung adenocarcinoma. The RNA-seq data are gathered from GDC and TCGA patient database and shown here as heat maps. The relative scale of RNA-seq read intensity is shown at

the bottom of each heat map. The magnitude of deviation from the average expression level is represented by the difference in color intensity. Gene-gene Pearson correlation analysis between each gene pair and the corresponding Akt isoform is shown in the table below as *r*-value together with the corresponding statistical significance (*P*-value, two-tailed analysis). Images were created with UCSC Xena.[3]

Figure S19. Relative gene expression levels of Akt isoforms, KIFC1, and Grsf-1 in stomach cancer. The RNA-seq data are gathered from GDC and TCGA patient database and shown here as heat maps. The relative scale of RNA-seq read intensity is shown at the bottom of each heat map. The magnitude of deviation from the average expression level is represented by the difference in color intensity. Gene-gene Pearson correlation analysis between each gene pair and the corresponding Akt isoform is shown in the table below as *r*-value together with the corresponding statistical significance (*P*-value, two-tailed analysis). Images were created with UCSC Xena.[3]

Figure S20. Relative gene expression levels of Akt isoforms, KIFC1, and Grsf-1 in colorectal carcinoma. The RNA-seq data are gathered from TCGA patient database and shown here as heat maps. The relative scale of RNA-seq read intensity is shown at the bottom of each heat map. The magnitude of deviation from the average expression level is represented by the difference in color intensity. Gene-gene Pearson correlation analysis between each gene pair and the corresponding Akt isoform is shown in the table below as *r*-value together with the corresponding statistical significance (*P*-value, two-tailed analysis). Images were created with UCSC Xena.[3]

Figure S21. Relative gene expression levels of Akt isoforms, KIFC1, and Grsf-1 in melanoma. The RNA-seq data are gathered from GDC and TCGA patient database and shown here as heat maps. The relative scale of RNA-seq read intensity is shown at the bottom of each heat map. The magnitude of deviation from the average expression level is represented by the difference in color intensity. Gene-gene Pearson correlation analysis between each gene pair and the corresponding Akt isoform is shown in the table below as *r*-value together with the corresponding statistical significance (*P*-value, two-tailed analysis). Images were created with UCSC Xena.[3]

Figure S22. Tumor growth inhibition by MK-2206 and MK-FNE in MDA-MB-468 xenograft mice. Mice bearing MDA-MB-468 xenografts on both flanks were treated with either vehicle (DMSO), or 200 mg/kg of indicated compounds twice a week. **(a)-(c)**, Individual tumor-size was monitored and data were represented as fold change and fit by linear regression, with y-axis-intercept = 1.

(a) and **(b):** Results after the first seven days of treatment **(a)**. Data were fit by linear regression, restricting the vertical intercept to be 1. The resultant growth slopes were plotted in **(b)**. (± s.e.m., n = 14). Two-tailed unpaired *t*-test was applied. Precise *P* values are annotated above lines.

(c) Results on Day-9. The corresponding growth-slope plot was shown in **Fig. 6b**.

(d) The tumor growth data were plotted as absolute tumor volumes vs. days.

(f) Dot plot showing the individual tumor volumes in each treatment group at Day-0.

Supplementary information for biological assays

General materials and methods

All primers were from IDT. Phusion HotStart II polymerase was from ThermoFisher Scientific. All restriction enzymes and alkaline phosphatase were from NEB. All Halo clones were contained in a pFN21a vector (Kazusa Collection) or the PCS2+8 vector (both of which drive expression from a CMV promoter). Complete EDTA free protease inhibitor was from Roche. Quick Start™ Bradford 1× dye reagent was from Bio-Rad. Cyanine5 (Cy5) azide and Cu(TBTA) were from Lumiprobe. Dithiothreitol (DTT), TCEP-HCl, were from Goldbio Biotechnology. BiotindPEG®11-azide was from Quanta Biodesign. Streptavidin sepharose beads were from GE Healthcare. Bovine Serum Albumin (BSA) powder was from ThermoFisher Scientific. Bioreagent grade MK-2206 (S1078), GDC-0068 (S2808) and GSK-690693 (S1113) were from Selleckchem. 10 mM stocks of the inhibitors were prepared in DMSO and stored in aliquots at −80 °C. Reagent grade MK-2206 was from eNovation. Ethylenediaminetetraacetic acid disodium salt dehydrate (EDTA, A15161) and sodium fluoride (NaF, A13019) were from Alfa Aesar. Triton X-100 (A4975) was from PanReac Appli Chem. All other chemicals/reagents were from Sigma-Aldrich, unless otherwise stated. Recombinant Akt3 protein (31147) was from Active Motif. Fat-free powdered milk was from Shaws.

HEK293T cells were purchased from American Type Culture Collection (ATCC). MDA-MB-468 and BT-549 Cell lines were gifts from the Cantley lab, Weill Cornell Medicine. MDA-MB-231, Hs578T, TSE and 3T3 cell lines were gifts from the Cerione lab, College of Veterinary Medicine, Cornell University Medical Center. T47D and T47D MK-2206-resistant lines were gifts from the Toker lab, Harvard Medical School. Cell lines were validated to be free of mycoplasma contamination using Venor™GeM Mycoplasma Detection Kit (MP0025, Sigma-Aldrich) every three months. All cell lines were used as polyclonal mixtures, below passage 10. 1 X DPBS (21600010), 1 X Trypsin (TrypLE™, 12605028), 100 X non-essential amino acids (11140035), 100 X sodium pyruvate (11360070), 100 X penicillin-streptomycin (15140148), and Minimum Essential Medium (MEM)+Glutamax (41090093), Roswell Park Memorial Institute (RPMI, 11875093) medium, Dulbecco's modified Eagle's medium (DMEM， 11965-092) and SILAC drop-off DMEM (88364) were from Life Technologies. FBS was from Sigma-Aldrich (F2442). TransIT-2020 transfection reagent was from Mirus Bio LLC. Polyethylenimine, linear, MW 25,000 (PEI) was from Polysciences (23966-1). All tissue-

culture treated plasticwares were from CellTreat. For all confocal imaging experiments, Zeiss LSM 710 or Leica SP8 FLIM confocal microscope was used. Imaging plate (35 mm glass bottom dish) was from Cellvis (D35-20-0-N). Quantification of fluorescence intensity was performed using ImageJ software (NIH, version 1.50 g). In-gel fluorescence imaging of western blots and Coomassie-stained gels were performed using Bio-Rad Chemi-Doc MP or Vilber Fusion FX. Imaging of histological sections and tissue slices were performed on a Leica DFC7000T stereomicroscope fitted with a Flu-combi lens. Densitometric quantitation was performed using ImageJ (NIH). Cy5 excitation source was detected using epi-illumination and 695 % 28 nm emission filter. Cell counting was conducted using Countess II FL (A25750). Tumors were cryosectioned with Cryostat Leica CM3050/S and parafilm-mounted on glass slides before hematoxylin and eosine (H&E) staining.

General cell culturing conditions and harvesting

HEK293T cell line was cultured in MEM medium; TSE cell line was cultured in RPMI medium; SILAC MDA-MB-468 cell lines were cultured in SILAC drop-off DMEM medium. All other cell lines were cultured in DMEM medium. Complete medium in the following sections stands for the culturing medium supplemented with 10% fetal bovine serum (FBS, Sigma-Aldrich, F2442) and 1% of a stock solution containing 10,000 IU/ml penicillin, and 10,000 µg/ml streptomycin, 100 mM sodium pyruvate (final concentration 1 mM) and 100 X non-essential amino acid (ThermoFisher scientific, 1140076) with the exception of RPMI complete medium, in which no sodium pyruvate and non-essential amino acid supplements were added, and DMEM complete medium without the addition of sodium pyruvate and non-essential amino acids were used for culturing 3T3 cells. The cell culture was placed in an incubator at 37 °C under humidified atmosphere containing 5% CO_2. Rinse medium stands for the corresponding complete medium without FBS. Cells were harvested with TrypLE™ (Gibco® by Life Technologies™, 12605-028) followed by the addition of the corresponding complete medium to quench trypsin activity.

General procedure for HEK293T cell transfection

HEK293T Cells were split in a 6-well plate (for example). After reaching 60% confluence, cells were transfected with a solution containing 2.5 µg of the designated plasmids in the

stated ratio and 7.5 μL TransIT® 2020 in MEM medium (200 μL). After 18-22 h, the medium was replaced with the fresh complete medium without transfection mixture.

General procedure for cell lysis and lysate collection

Cells were lyzed in the lysis buffer of 50 mM HEPES (pH 7.6), 100 mM NaCl, 1 mM TCEP and 1% Triton X-100 solution as well as 1 X Roche EDTA-free Protease inhibitor by rapid freeze-thaw three times. To maintain target protein phosphorylation state for western blotting or phospho-Akt substrate enrichment for SILAC proteomics study, 5 mM sodium orthovanadate and 20 mM NaF were also added to the lysis buffer. Cell debris was removed and the supernatant was collected after centrifugation at 20,000 *g* for 10 min at 4 °C. Protein concentration was determined using Bradford assay relative to BSA as standard.

General procedure for SDS-PAGE

10% SDS PAGE gels were prepared according to the Bio-Rad protocol. The prepared samples were diluted with 4X reducing Laemmli loading buffer (with 6% mercaptoethanol), and loaded into wells (30─40 μL for a 10-well lane) and electrophoresis was carried out using 120 V for 10 min followed by 150 V until the run was completed.

In-gel fluorescence assay

HEK293T cell transfection with the designated plasmid encoding HaloTag-Akt(n) fusion gene was conducted as described above. After transfection, the medium was aspirated and replaced with fresh 2 mL MEM supplemented with 3% FBS containing inhibitor at the designated concentration or an equivalent final volume of DMSO. The plates were incubated at 37 °C for the indicated period of time. Cells were then harvested and lyzed according to the general procedure. A portion of the lysate was made up to 21 μL final volume containing, in final concentrations, 5% *t*-BuOH, 2 mM TCEP, 1% SDS, 1 mM $CuSO_4$, 0.1 mM Cu(TBTA), 10 μM Cy5 azide, and 1.0 mg/mL lysate protein. The samples were incubated at 37 °C for 30 min and subsequently quenched with 8 μL of 4X reducing Laemmli sample buffer containing 6% β-mecaptoethanol. After an additional 5-min incubation at rt, samples were resolved on a 10% SDS-PAGE gel. After electrophoresis, the gel was rinsed three times with ddH_2O and imaged on Bio-Rad Chemi-doc MP or Vilber Fusion FX imager. Where applicable, the gel was transferred to a PVDF membrane for western blot analysis.

Western blotting

The proteins in gel were transferred onto a PVDF membrane in Towbin buffer at 90 V for 2 h at 4 °C or at 33 V overnight at 4 °C. The membrane was blocked with 5% milk (or BSA) in 100 mM Tris pH 7.6, 150 mM NaCl, 0.1% Tween (TBS-T1) and probed with various antibodies at the indicated dilutions, typically in 1% BSA in TBS-T1 overnight in 4 ºC cold room for primary; then washed three times in TBS-T1 at 10-min interval and probed with secondary antibody for 1 h at rt; washed two times in TBS-T1 followed by one wash in 100 mM Tris pH 7.6 and 150 mM NaCl solution (TBS). Proteins were visualized using Pierce™ ECL Western Blotting Substrate (32106, ThermoFisher), Pierce™ ECL2 Western Blotting Substrate (32132, ThermoFisher) or SuperSignal™ Western Blot Enhancer (46640, ThermoFisher), depending on the signal strength.

ELISA

Anti-Halo antibody at 1 µg/mL concentration in sodium bicarbonate buffer (pH 9.6) was added to a 96-well white plate (80 µL per plate) at 4 °C for 24 h. After this, the incubation buffer was removed and wells were washed once with TBS-T2 (100 mM Tris, 150 mM NaCl, 0.03% Tween-20) and then blocked in 5% BSA in TBS-T2 (280 µL per well) for 3–5 h at rt. After this time, BSA was washed away using TBS-T2, then wells were filled with 150 µL blocking buffer (1% BSA, 1 mM sodium orthovanadate, 5 mM NaF). HEK293T cells were transfected with Halo-Akt3 and TransIT 20-20 mixture, and lyzed according to the general procedure. 100 µg of each lysate (quantified by Bradford relative to BSA) was added to each well. This amount of lysate was shown to saturate binding of the plate, thus the amount of phosphorylated protein detected is a function of the ratio of phosphorylated to non-phosphorylated protein in the lysate. The mixture was incubated at 4 °C overnight. After this time, wells were washed with TBS-T2 three times, then the solution of phospho-Akt (Thr308) antibody (1:1,000 dilution in 1% BSA in TBS-T2) was added and incubated overnight at 4 °C. After this time, wells were washed and HRP-conjugated secondary antibody was added in 1% BSA in TBS-T2. After incubation for 1 h at rt, wells were washed three times with TBS-T2 for 15 min then once with TBS for 20 min, after which 50 µL TBS was added to each well. HRP was detected using an autoinjector program on a Cytation3 plate reader (Biotek). Femto ELISA substrate was used, injecting 50 µL Femto ELISA substrates 1 and 2 per well. Signals were calculated relative to that of wells coated in antibody but treated with untransfected cell lysate.

Biotin-azide pulldown of endogenous Akt kinases from mammalian lysate.

HEK293T cells were split in 100 cm^2 plates. After reaching 60% confluence, media were aspirated and replaced with fresh 10 mL rinse media supplemented with 3% FBS, doping with 5 μM MK-HNE in DMSO or an equivalent volume of DMSO for 24 h. Cells were harvested, washed with chilled 1 X DPBS twice and once with chilled 50 mM HEPES (pH 7.6) before being flash frozen. Cell lysis was performed in 300 μL lysis buffer as described above, and the lysate was subsequently diluted to 10 mg/mL with lysis buffer and subjected to click reaction with biotin-azide for 30 min at 37 °C. The final concentrations of each component were: 2 mM TCEP, 5% *t*-BuOH, 1% SDS, 1 mM $CuSO_4$, 0.1 mM Cu(TBTA), 200 μM biotin-azide and 9.1 mg/mL lysate protein. The lysate proteins were precipitated by adding four volumes of ethanol pre-chilled at −20 °C. The sample was vortexed and incubated at −80 °C overnight. The precipitant was collected by centrifugation at 20,000x *g* for 30 min at 4 °C and washed twice with pre-chilled ethanol, then once with acetone. The pellet was re-suspended in100 μL 50 mM HEPES (pH 7.6), 8% LDS and 0.5 mM EDTA and dissolved by vortexing and heating at 42 °C for 5 min. LDS was diluted to a final concentration of 0.5% by diluting the sample with 50 mM HEPES (pH 7.6) and added to 50 μL of high-loading streptavidin bead suspension, which were pre-equilibrated with 50 mM HEPES (pH 7.6) and 0.5% LDS. The sample was incubated with beads for 2–3 h at rt with end-over-end rotation, after which the supernatant was removed after centrifugation at 500x *g* for 3 min. The beads were washed three times with 400 μL of 50 mM HEPES (pH 7.6) containing 0.5% LDS with end-over-end rotation at rt for 30 min during each wash. Bound proteins were eluted by boiling the beads at 98 °C for 10 min with 30 μL of 4 X Laemmli loading buffer containing 6% β-mercaptoethanol. The sample was subjected to SDS-PAGE and transferred to a PVDF membrane for western blot analysis.

FRET assay in live mammalian cells.

HEK293T cells were plated in imaging plates (D35-20-0-N, Cellvis) at 60% confluence. After 24 h, cells in each plate were transfected with 1 μg AktAR reporter plasmid and 1 μg plasmid of the designated HaloTag fusion Akt gene or Akt3 and Akt3C119S gene mixture in PCS2+8 vector, using TransIT 2020 (6 μL). After 12 h-transfection, cells were treated with 5 μM inhibitor in DMSO or an equivalent final volume of DMSO in rinse medium containing 3% FBS and incubated for 24 h before imaging. FRET imaging was performed using a Zeiss LSM 710 confocal microscope as previously described. Briefly, a 458 nm argon laser was used for excitation. The signals in the cyan channel

(463–498 nm) and the yellow channel (525–620 nm) were recorded. Cells were continued to incubate in drug medium for another 24 h before next imaging. The medium was aspirated and cells were gently rinsed with 3% FBS in rinse medium twice over the next hour. Fresh rinse medium supplemented with 3% FBS was added and cells were imaged again after 24 h. For quantification, the mean CFP and YFP signal intensity was measured using ImageJ by drawing a freehand circle around the cells, and the ratio image was calculated. Data analysis was performed using Prism software.

NADH-coupled Akt activity assay

To a 96-well plate with varying amounts of indicated inhibitors was added the kinetic assay mixture containing, in final concentrations, 50 mM HEPES (pH 7.6), 100 mM NaCl, 10 mM $MgCl_2$, 5 mM phosphoenolpyruvate, 500 μM NADH, 100 μM crosstide (the Akt substrate, cat. No. sc-471145, Santa Cruz), pyruvate kinase (24-40 units/mL), lactate dehydrogenase (36-56 units/mL), 4 mM TCEP, 500 μM ATP. The solution was allowed to equilibrate at rt for 5 min followed by the addition of recombinant Akt3 protein (Active Motif, 31147, 0.4 μg, 150 nM). The resulting solution was mixed thoroughly by pipetting. The progress of phosphorylation was monitored by reading absorbance at 340 nm over the course of study. Data analysis was performed using Prism software.

General procedure for cell viability assay

Indicated cell lines were plated in a 96-well plate containing the corresponding complete medium as described above (100 μL per well) at a density of 3,000-5,000 cells per well for 12 h. This is followed by the addition of inhibitor at varying concentrations in rinse medium (100 μL). Cells were allowed to grow for 72 h and 100 μL of the culture medium was removed from each well. This was followed by the addition of 10 μL alamarBlue® reagent to each well. The fluorescence emission signals at 590 nm were read by Cytation 3 cell imaging multi-mode reader (BioTeK) using an excitation wavelength of 560 nm. Data analysis was performed using Prism software.

Assay for drug synergism with Akt isoform-specific knockdown

MDA-MB-468 cells were plated in a 6-well plate to reach 80% confluence. At 12-h post seeding, cells were transfected with 75 pmol siRNA selectively targeting the indicated Akt isoform or control siRNA using Lipofectamine 3000 (7.5 μL). After 10-12 h, culture medium was aspirated and the cells were harvested with TrypLE™ Express followed by

the addition of an equal volume of the complete medium. Cells were counted and plated in a 96-well plate at a density of 3,000-5,000 cells per well in complete culture medium. The cells continued to grow for 12 h before addition of an equivalent volume of rinse medium containing varying concentrations of inhibitions or an equivalent volume of DMSO. The cells continued to grow for 72 h before adding 1/10th volume of alamarBlue® reagent to the culture medium. The fluorescence emission signals at 590 nm were read by Cytation 3 cell imaging multi-mode reader (BioTeK) using an excitation wavelength of 560 nm. Data analysis was performed using Prism software.

Drug effect persistence assay

MDA-MB-468 cells were plated in a 96-well plate at a density of 3,000-5,000 cells per well for 10 h before the addition of varying concentrations of inhibitors. Cells were allowed to grow for 48 h. The cell medium was aspirated and the cells were washed once with DMEM rinse medium. Cell growth continued in DMEM rinse medium with 5% FBS for 24 h before adding 1/10th volume of alamarBlue® reagent to the culturing medium. The fluorescence emission signals at 590 nm were read using a Cytation 3 cell imaging multi-mode reader (BioTeK) using an excitation wavelength of 560 nm. Data analysis was performed using Prism software.

SILAC MDA-MB-468 cell preparation

MDA-MB-468 cell lines were maintained and passaged six times in SILAC DMEM medium supplemented with 10% dialyzed FBS (F0392, Sigma-Aldrich), 1 X sodium pyruvate and 1 X pen-strep as well as doping with SILAC heavy-isotope labelled amino acids [$^{13}C_6$ $^{15}N_2$ L-lysine, 0.8 mM (608041, Sigma-Aldrich) and $^{13}C_6$ $^{15}N_4$ L-arginine, 0.5 mM (608033, Sigma-Aldrich)] to generate SILAC heavy cells, or light-isotope labelled amino acids [L-lysine, 0.8 mM (L8662, Sigma-Aldrich) and L-arginine, 0.5 mM (A8094, Sigma-Aldrich)] for SILAC light cells.

Cell cycle analysis using flow cytometry

MDA-MB-468 cells in a 6-well plate at 10% confluence were treated with the indicated compound at EC_{60} or EC_{80} concentration for 72 h at 37 °C. Negative control contained the equivalent volume of DMSO. Cells were grown and analyzed in separate batches of 1-2 replicates per condition that were run 2-3 times each. At the indicated time post compound treatment, the culture medium was aspirated and the adherent cells were

detached from the plate using trypsin, quenched with complete media, centrifuged (700 g), washed once with PBS, centrifuged (700 g), resuspended in PBS, then fixed with 70% ethanol for 24 h. The cell suspensions were spun down at 1,000 g and washed with 500 μl of PBS twice. Each cell pellet was treated with 500 μL staining solution containing 50 μl of Ribonuclease A (≥70 Kunitz units/mg proteins, R6513, Sigma-Aldrich) and 50 μl of a propidium iodide (PI, 1 mg/ml, Sigma-Aldrich) solution in PBS with 1% BSA. The resulting solution was incubated for 30 min at room temperature in the dark with agitation.

The stained cells were assayed on BD LSR II. FlowJo® was used to deconvolute the signals. Cells were grouped first by forward and side scatter (area), then that group was regrouped using forward (width) versus forward (area) scatter to give single cells. Cells were than analyzed using cellular DNA content to quantitate the percentage of cells in the respective phases (G_1, S, G_2/M and sub-G_0) of the cell cycle. Each time the data points were compared with the control set for each batch.

Protein enrichment by phospho-Akt substrate antibody (sepharose bead conjugate, 110B7E) for SILAC proteomics analysis

Heavy SILAC MDA-MB-468 cells were harvested and plated in a 150mm-cell culture dish at 60% confluence. Cells were maintained in SILAC DMEM medium supplemented with 5% dialyzed FBS, 1 X sodium pyruvate and 1 X pen-strep and doping with the additive of heavy-isotope labelled amino acids [$^{13}C_6$ $^{15}N_2$ L-lysine, 0.8 mM (608041, Sigma-Aldrich) and $^{13}C_6$ $^{15}N_4$ L-arginine, 0.5 mM (608033, Sigma-Aldrich)] for 24 h. The medium was aspirated and the same culturing medium with the addition of the small-molecule compound of interest at EC_{60} concentration (3.2 μM MK-FNE or 2.2 μM MK-2206) was added. Cells were incubated for 36 h at 37 °C. The light SILAC MDA-MB-468 cells were subject to the same culturing conditions with the exception of using light-isotope labelled L-lysine (0.8 mM L8662, Sigma-Aldrich) and L-arginine (0.5 mM, A8094, Sigma-Aldrich) as the amino acid additive for culturing medium, and DMSO as the small-molecule compound in final equal volume to the MK-FNE or MK-2206 solution. The heavy and light SILAC cells were counted and combined in 1:1 ratio. The resulting cell mixture was spun down and washed twice with 1 X DPBS, and washed once with 50 mM HEPES (pH 7.6) before subject to cell lysis. The protein lysate (~ 400 μL, 1 mg/mL) was added to 30 μL of phospho-Akt substrate antibody immobilized on sepharose beads, incubated with end-over-end rotation overnight at 4°C. The mixture was spun for 30 sec (500 g) at 4 °C and

the beads were washed five times with lysis buffer (500 μL) at 10-min interval. Bound proteins were eluted by boiling the beads at 98 °C for 10 min with 30 μL of 4 X Laemmli loading buffer containing 6% β-mercaptoethanol. The resulting protein mixture was resolved on gradient SDS-PAGE gel (4561096, Bio-rad).

In-gel trypsin digestion of SDS gel bands

The protein bands from the SDS-PAGE gel (5 gel slices for each of the 4 samples) were cut into ~1 mm cubes and subjected to in-gel digestion followed by extraction of the tryptic peptide as reported previously [4]. The excised gel pieces were washed consecutively in 400-800 µL distilled water, 100 mM ammonium bicarbonate (Ambic)/acetonitrile (1:1) and 100% acetonitrile. The gel pieces were reduced with 100-300 µL of 10 mM DTT in 100 mM Ambic for 1 hr at 56 °C, alkylated with 100-300 µL of 55 mM Iodoacetamide in 100 mM Ambic at room temperature in the dark for 60 mins. Repeated wash steps as described above, the gel slices were dried and rehydrated with 100-200 µL trypsin in 50 mM Ambic, 10% ACN (5 ng/µL) at 37 °C for 16 hrs. The digested peptides were extracted twice with 200-300 µl of 50% acetonitrile, 5% FA and once with 200-300 µl of 90% acetonitrile, 5% FA. Extracts from each sample were combined, filtered with 0.22 um spin filter (Costar Spin-X from Corning Incorp) and lyophilized.

Nano LC/MS/MS Analysis on Orbitrap Fusion:

The SILAC tryptic digests were reconstituted in 50 µL of 0.5% FA estimated at 0.1 µg/µL for nanoLC-ESI-MS/MS analysis, which was carried out using an Orbitrap FusionTM TribridTM (Thermo-Fisher Scientific, San Jose, CA) mass spectrometer equipped with a nanospray Flex Ion Source, and coupled with a Dionex UltiMate3000RSLCnano system (Thermo, Sunnyvale, CA) [4-5]. The tryptic peptide samples (10 µL) were injected onto a PepMap C-18 RP nano trap column (5 µm, 100 µm i.d x 20 mm, Dionex) with nanoViper Fittings at 20 µL/min flow rate for on-line desalting. The peptides were separated on a PepMap C-18 RP nano column (2 µm, 75 µm x 25 cm) at 35 °C, in a 120 min gradient of 5% to 38% acetonitrile (ACN) in 0.1% formic acid at 300 nL/min and followed by an 8 min ramping to 90% ACN-0.1% FA and a 9 min hold at 90% ACN-0.1% FA. The column was re-equilibrated with 0.1% FA for 25 min prior to the next run. The Orbitrap Fusion is operated in positive ion mode with spray voltage set at 1.6 kV and source temperature at 275°C. External calibration for FT, IT and quadrupole mass analyzers was performed. In data-dependent acquisition (DDA) analysis, the instrument was operated using FT mass analyzer in MS scan to select precursor ions followed by 3 second “Top Speed” data-

dependent CID ion trap MS/MS scans at 1.6 m/z quadrupole isolation for precursor peptides with multiple charged ions above a threshold ion count of 10,000 and normalized collision energy of 30%. MS survey scans at a resolving power of 120,000 (fwhm at m/z 200), for the mass range of m/z 375-1575. Dynamic exclusion parameters were set at 50 s of exclusion duration with ±10 ppm exclusion mass width. All data were acquired under Xcalibur 3.0 operation software (Thermo-Fisher Scientific).

SILAC proteomics data analysis:

All MS and MS/MS raw spectra were processed and searched using Sequest HT software within the Proteome Discoverer 2.2.0.388 (PD 2.2, Thermo Scientific). The *Homo sapiens* NCBI UniprotKB.fasta database containing 20,153 entries downloaded on October 17, 2016 was used for database searches. The database search was performed under a search workflow with the "Precursor Ions Quantifier" node for SILAC 2plex (Arg10, Lys8) quantitation. The default setting for protein identification in Sequest node were: two mis-cleavages for full trypsin with fixed carbamidomethyl modification of cysteine, variable modifications of 10.008 Da on Arginine and 8.014 Da on lysine, N-terminal acetylation, methionine oxidation and deamidation of asparagine and glutamine residues. The peptide mass tolerance and fragment mass tolerance values were 10 ppm and 0.6 Da, respectively. Only high confidence peptides defined by Sequest HT with a 1% FDR by Percolator were considered for the peptide identification. The mass precision for expected standard deviation of the detected mass used to create extracted ion chromatograms was set to 3 ppm. The SILAC 2-plex quantification method within PD 2.2 was used with unique + razor peptides only to calculate the heavy/light ratios using pairwise ratio based for all identified proteins without normalization and exclude the deamidation modification. The final protein group list was further filtered with two peptides per protein in which only #1-ranked peptides within top scored proteins were used.

Lentiviral Production in 6-well plates

HEK293T cells were seed at 0.24 x 10^6 cells/mL (2 mL per well) in antibiotic-free DMEM complete medium in a 6-well plate. Cells were maintained in a humidified, 5% CO_2 incubator at 37 °C for 24 h. The cells had reached 70-80% confluence next day. To a mixture of the packaging plasmid (pCMVR8.74psPAX2, 500 ng), the envelop plasmid (pCMV-VSV-G, 50 ng) and the pLKO vector containing the shRNA of interest (500 ng) in 250 μL Opti-MEM medium was added *Trans*IT-2020 reagent (7.5 μL) and the resulting mixture was incubated at rt for 30 min. The transfection mix was carefully transferred to

the HEK293T cells followed by incubation at 37 °C for 18 h. The medium was exchanged with DMEM rinse medium (2.5 mL per well) supplemented with high FBS (20% FBS) and the cells were incubated at 37 °C for another 24 h. The virus in 2.5 mL high-FBS DMEM rinse medium were then harvested and passed through a 0.48 μm filter to remove cells. The resulting lentivirus solution was used immediately for infection.

Lentiviral Infection in 6-well plates

MDA-MB-468 cells were seed at 0.24 x 10^6 cells/mL (2 mL per well) in antibiotic-free DMEM complete medium in a 6-well plate. Cells were maintained in a humidified, 5% CO_2 incubator at 37 °C for 24 h. The cells had reached 80-90% confluence next day. The medium was aspirated. A mixture of polybrene (53 μg) and 0.6 mL of the lentivirus solution in high-FBS DMEM complete medium (final volume 6.6 mL) was added to each well. Cells were incubated overnight and the medium was replaced with new DMEM complete medium, and incubated for another 24 h. Over the following two days, the MDA-MB-468 cells were incubated with DMEM complete medium-containing puromycin (1.5 μg/mL) and the medium was replaced as needed. The infected MDA-MB-468 cells were continuously passaged and selected in puromycin medium (1 μg/mL) until the third cell passage was completed.

Cell viability assay for studying the combinatorial effect of AZ-82 and MK-FNE or MK-2206 treatment

Indicated cells were plated in a 96-well plate containing complete DMEM (100 μL per well) with a density of 3,000-5,000 cells per well for 12 hours followed by the addition of varying concentrations of each inhibitor in rinse medium (50 μL) or the equivalent volume of rinse medium containing the corresponding amount of DMSO. The cells were allowed to grow for 72 hours and 100 μL of the culture medium was removed from each well. This was followed by the addition of 10 μL alamarBlue® reagent to each well. The fluorescence emission signals at 590 nm were read by Cytation 3 cell imaging multi-mode reader (BioTeK) using an excitation wavelength of 560 nm. Data analysis was performed using Prism software.

Gene-gene Pearson correlation analysis of clinical carcinoma database

The analysis of relative gene expression levels found in GDC and/or TCGA patient databases was completed with UCSC Xena (https://xena.ucsc.edu/), closely following the recommended guidelines established by the developers. The RNA-seq data are gathered from the patient databases and shown here as heat maps.

***In vitro* microsomal stability assay (experiments conducted by WuXi AppTec)**

2 μL of a 10 mM compound or control solution (10 mM) was diluted with DMSO (18 μL) followed by further dilution in MeOH/water solution (180 μL, 1:1 v/v ratio). 20 μL of this solution was diluted with 180 μL of 100 mM potassium phosphate solution (pH 7.4) to afford the compound working solution (10 μM). 10 μL of the working solution (or 10 μL of 100 mM potassium phosphate solution as negative control) was mixed with 80 μL of CD-1 mouse liver microsomes (0.625 mg/mL) in potassium phosphate solution in each well. The resulting solution was incubated at 37 ^{o}C for 10 min followed by the addition of 10 μL cofactor solution containing 10 mM NADPH and 10 mM $MgCl_2$ to start the reaction. Chilled acetonitrile (400 μL) containing 200 ng/mL Tolbutamide and 200 ng/mL Labetalol was added at indicated time points to stop the reactions. Samples were centrifuged and 100 μL of each supernatant was mixed with 300 μL water and submitted for LCMS-MS analysis. The compound half-life of elimination was calculated based on the equation of first order kinetics shown here:

$ln C_t = -kt + ln C_0$,

where C_0 is the initial compound absorbance signal in LC and sets to be 1, C_t is the corresponding absorbance signal at a given time point in LC, and k is the first order kinetic constant.

$t_{1/2} = \ln 2/k = 0.693/k$,

where $t_{1/2}$ is the half-life of the added molecule.

	MK-2206	**MK-HNE**	**MK-FNE**	**MK-NE**
k (min^{-1})	-0.008 ± 0.002	-0.024 ± 0.001	-0.045 ± 0.004	-0.029 ± 0.007
$t_{1/2}$ (min)	85.8 ± 17.0	28.7 ±1.4	15.4 ± 1.4	24.7 ± 5.7

Drug efficacy test in an MDA-MB-468 xenograft mouse model (conducted by Washington Biotechnology, Inc., following ethical standards for animal studies of the Office for Laboratory Animal Welfare (OLAW), division of the US Public Health Service as administered by the US National Institutes of Health)

42 athymic nude mice (SOP 1910, SOP 1920, female, 5-6 weeks old) were housed in filter-topped cages layered with autoclaved bedding. The following animal handling procedures were carried out in a laminar flow hood and each mouse was ear-tagged (SOP 810) for individual identification. MDA-MB-468 cells in 0.1 ml PBS with 20% Matrigel were injected subcutaneously (SOP 1610) into both flanks (1 $x10^7$ cells per flank). Recording of tumor volume began seven days later and mice were sorted into 5 groups of 7 mice with similar average tumor volumes (based on the right flank). Dosing regimen commenced as described below in the table below. Dosing regimen was carried out based on a pilot escalating maximum tolerable dose study that showed no toxicity up to 400 mg/kg.

The measurement of tumor volume was carried out three times a week (Mon, Wed and Fri). The weight of each mouse was recorded on the same day. The mice in each treatment group were dosed twice a week with the test material (Mon and Thur) until day 17, which was the last day of all compound treatments. After completing tumor measurement on day 18, two mice in each treatment group were randomly selected and euthanized. The organs and tumors were harvested for subsequent immunohistological staining and whole-mount chemical fluorescence studies. On day 21 (four days after treatment ceased), blood glucose measurement of each mouse was conducted by cutting the tail and blood examination with glucose strip (One Touch Ultra, Lot #: 4467886). Tumor volume measurement of the remaining mice in each group was continued without compound administration until day 57, after which all the remaining mice were euthanized and their tumors and organs were harvested.

Table

Group	# Mice	Material[a]	Dose (mg/kg)	Administration	Frequency[c]
Group 1	7	DMSO	Equivalent volume	PO[b]	Twice a week
Group 2	7	**MK-2206**	200	PO	Twice a week
Group 3	7	**MK-HNE**	200	PO	Twice a week
Group 4	7	**MK-FNE**	200	PO	Twice a week

[a]Test materials in DMSO solution (400 mg/mL) or the equal volume of DMSO were diluted with 30% Captisol to afford 80 mg/mL solution before feeding to mice.

[b]PO= Oral gavage (SOP 1651)

[c]Test materials dosed twice a week, over 17 days.

Tumor preservation for subsequent histology analysis (conducted by Washington Biotechnology Inc. following ethical standards for animal studies of the Office for Laboratory Animal Welfare (OLAW), division of the US Public Health Service as administered by the US National Institutes of Health)

Harvested mouse tumors on day 18 were cut into half. One half was preserved in 10% neutral buffered formalin at ambient temperature until needed. The other half was further cut into five sections, each of which was preserved in 2 mL RNAlater solution. After in refrigerator overnight, RNAlater solution was aspirated and tumor sections were preserved at -80 ^{o}C or on dry ice until needed.

Tumor whole-mount epifluorescence imaging

Tumors in formalin were aspirated and washed with PBS three times followed by the addition of methanol, and permeated in methanol at −20 °C for 24 h. Tumors were then washed three times in PBS at 10-min intervals. This was followed by two washes in 50 mM HEPES (pH 7.6) for 30 min each. Tumors were then exposed to a Click reaction cocktail containing (in final concentration): 50 mM HEPES (pH 7.6), *t*-BuOH (5%), $CuSO_4$ (1.1 mM), sodium ascorbate (10 mM, made as a 100 mM stock in 500 mM HEPES (pH 7.6) with no further pH adjustment), and Cy5-azide (10 μM). The mixture was shaken at rt for 1 h, then washed 3 times in PBT (1 x PBS with 0.015% Tween-20) at 10-min interval. After third wash, tumors were incubated in PBS overnight at 4 °C. Tumors were then washed with 1 x PDT (1 x PBS, 1% DMSO, 0.3% Triton X-100) continuously at 8-hour intervals over three days. After the final wash, tumors were incubated in 1 x PBT for 30 min before imaging on 2% agarose gel.

H&E staining

Tumor slice was paraffin-fixed on a glass slide. The glass slide was placed in a staining rack, deparaffinised by washing with xylene, 100% ethanol, 70% ethanol, and rehydrated in tap water. The tumor section was placed in Harris Hematoxylin (Gill II PAP 1) solution for 5 min and washed briefly in tap water. The slide was dipped into 1% acid-ethanol solution several times to destain, and washed in running tap water. The slide was left in eosine-phloxine working solution for 1 min, washed in water, dehydrated by washing with 70% ethanol, 100% ethanol and xylene. The section was mounted with cover slip and ready for imaging.

Summaries and validation of antibodies

WB, western blot.
ELISA, enzyme-linked immunosorbent assay.
IP, immunoprecipitation

Name	Catalog number, Supplier	Application	Dilution	Incubation time (h)
Anti-Halo monoclonal antibody	G9211, Promega	WB, ELISA	1:1,000 in 1% BSA in TBS-T1	2 (WB, rt); Overnight (ELISA, 4 °C)
Phospho-Akt (Thr308) antibody	9275, Cell Signaling	WB, ELISA	1:1,000 in 1% BSA in TBS-T1	16 (WB, 4 °C) Overnight (ELISA, 4 °C)
Akt3 monoclonal antibody (4059, Cell Signaling)	4059, Cell Signaling	WB	1:1,000 in 1% BSA in TBS-T1	16 (4 °C)
Akt2 (D6G4) Antibody	3063, Cell signaling	WB	1:1,000 in 1% BSA in TBS-T1	16 (4 °C)
Akt (pan) (C67E7) monoclonal antibody (4691, Cell Signaling)	4691, Cell Signaling	WB	1:1,000 in 1% BSA in TBS-T1	16 (4 °C)
Anti-AKT1 antibody [4D6]	Ab124341, Abcam	WB	1:1,000 in 1% BSA in TBS-T1	16 (4 °C)
Monoclonal anti-β-actin-peroxidase antibody	A3854, Sigma-Aldrich	WB	1:15,000 in 1% milk in TBS-T1	1 (rt)
Monoclonal anti-gapdh−Peroxidase	G9295, Sigma-Aldrich	WB	1:15,000 in 1% milk in TBS-T1	1 (rt)
Anti-rabbit IgG, HRP-linked antibody	7074, Cell Signaling	WB	1:5,000 in 1% BSA in TBS-T1	1 (rt)
Anti-mouse IgG, HRP-linked antibody	7076, Cell Signaling	WB	1:5,000 in 1% BSA in TBS-T1	1 (rt)
Anti-Vinculin antibody [EPR8185]	Ab129002, Abcam	WB	1:5,000 in 1% BSA in TBS-T1	3 (rt)
Phospho-Akt Substrate (RXXS*/T*) rabbit monoclonal antibody [110B7E]	9614, Cell Signaling	WB	1:1,000 in 1% BSA in TBS-T1	16 (4 °C)
Sepharose bead conjugated phospho-Akt Substrate (RXXS*/T*) rabbit monoclonal antibody [110B7E]	9646, Cell Signaling	IP	15 μL bead suspension per 200 μL cell lysate	Overnight (4 °C)

Gapdh and actin antibodies have been used very commonly by us and others, and serve as loading controls. All other antibodies were validated by comparison to untransfected, knockdown lines or lines transiently overexpressing target protein (or HaloTag fusion target protein), in which the expected band(s) were depleted or upregulated (consistent with the experimental conditions).

The following siRNAs were used in individual Akt-isoform gene silencing:

siRNA	Catalog Number	Target Sequence	Manufacturer
siCont-1	SC-44230, siRNA-B	N.A. (not applied)	Santa Cruz
siCont-2	SC-44233, siRNA-E	N.A. (not applied)	Santa Cruz
siCont-3	SC-37007, siRNA-A	N.A. (not applied)	Santa Cruz
siAkt1-1	42811	*Sense:* GGCUCCCCUCAACAACUUCTT *Antisense:* GAAGUUGUUGAGGGGAGCCTC	ThermoFisher
siAkt1-2	J-003000-11-0002	ACAAGGACGGGCACAUUAA	Horizon Discovery
siAkt2-1	103305	*Sense:* GGAUGAAGUCGCUCACACATT *Antisense:* UGUGUGAGCGACUUCAUCCTT	ThermoFisher
siAkt2-2	J-003001-11-0002	GUGAAUACAUCAAGACCUG	Horizon Discovery
siAkt2-3	D-003001-05-0002	GUACUUCGAUGAUGAAUUU	Horizon Discovery
siAkt2-4	D-003001-08-0002	GCAGAAUGCCAGCUGAUGA	Horizon Discovery
siAkt2-5	D-003001-21-0002	GAGUAGAAUAAUCGUCUUU	Horizon Discovery
siAkt3-1	J-003002-14-0002	GAAGAGGGGAGAAUAUAUA	Horizon Discovery
siAkt3-2	J-003002-16-0002	GACAGAUGGCUCAUUCAUA	Horizon Discovery

The following shRNAs from Sigma-Aldrich Mission® were used in the designated gene silencing:

Name	Catalogue #	Sequence
shKIFC1-1	TRCN0000047142	CCGGTGTGTCCCTATGTCTATGTATCTCGAGATACATAGACATAGGGACACATTTTTG
shKIFC1-2	TRCN0000336650	CCGGCAGGTGGAATTGCAGGAAGAACTCGAGTTCTTCCTGCAATTCCACCTGTTTTTG
shKIFC1-3	TRCN0000336591	CCGGCGGGAAACACAGGCCATTAACCTCGAGGTTAATGGCCTGTGTTTCCCGTTTTTG
shJUP-1	TRCN0000300091	CCGGGATCATGCGTAACTACAGTTACTCGAGTAACTGTAGTTACGCATGATCTTTTTG
shJUP-2	TRCN0000300090	CCGGCCTGCCTTCTTCTTGTGTCTTCTCGAGAAGACACAAGAAGAAGGCAGGTTTTTG
shJUP-3	TRCN0000083710	CCGGGTGCTGAAGATTCTGGTGAATCTCGAGATTCACCAGAATCTTCAGCACTTTTTG
shGrsf1-1	TRCN0000353957	CCGGCGGTATGTGGAAGTGTATGAACTCGAGTTCATACACTTCCACATACCGTTTTTG
shGrsf1-2	TRCN0000348994	CCGGGACTGAACATAGTAGACATTACTCGAGTAATGTCTACTATGTTCAGTCTTTTTG
shGrsf1-3	TRCN0000109078	CCGGCAGCGGTATGTGGAAGTGTATCTCGAGATACACTTCCACATACCGCTGTTTTTG

Supplementary information for syntheses and compound characterizations

General materials and methods related to synthesis and chemical analysis:

Unless otherwise stated, reactions were carried out under N_2 or Ar. Standard syringe and cannulating techniques were applied for transferring reagents to the reaction flask. Reaction progress was monitored with glass-backed thin-layer chromatography (TLC) plates pre-coated with silica UV254 and visualised by UV at λ = 254 or 365 nm, vanillin, 5% H_2SO_4, or potassium permanganate dip. Silica gel 60 (particle size 0.040-0.065 mm) was used in flash chromatography with the ratio of solvents indicated in the relevant experimental section. All solvents used were either analytical or HPLC grade. MK-2206 for chemical synthesis was from eNovation Chemicals. ^{1}H and ^{13}C NMR spectra were recorded on a Bruker Avance 500 (500 MHz for ^{1}H and 125 MHz for ^{13}C) spectrometer and referenced to the residual solvent peaks of deuterated solvents. The data is reported as chemical shift (δ), multiplicity (app = apparent, s = singlet, d = doublet, t = triplet, q = quartet, dd = doublet of doublet, ddt = doublet of doublet of triplet, td = triplet of doublet, m = multiplet), coupling constant (*J* Hz) and relative integral. UPLC-MS analysis was performed on a Shimadzu UPLC-MS Nexera X2 instrument containing a LC-30AD pump and an SPD-M30A photodiode array detector coupled to a Shimadzu 2020 mass spectrometer (ESI) operating in positive mode. Separations were performed on an Acquity UPLC® XBridge column (1.7 mm, 2.1 × 50 mm column (C18)) at a flow rate of 0.6 mL min^{-1} using Eluent A and B (Eluent A: 0.1% formic acid in water, Eluent B: 0.1% formic acid in acetonitrile).

General procedure for *t*-butyldimethylsilyl (TBDMS) ether protection

To a solution of alcohol (1.0 mmol, 1.0 eq.) in DMF (5 mL) on ice was added imidazole (4.0 mmol, 4.0 eq.) and *t*-butyldimethylsilyl chloride (3.0 mmol, 3.0 eq.), and the resulting solution was stirred overnight at room temperature. The crude reaction mixture was poured into 0.1 M HCl solution (50 mL) and extracted with Et_2O (3 × 10 mL). The combined organic extracts were dried over Na_2SO_4, filtered and concentrated in vacuo.

General procedure for coupling lipid acid to MK-2206

To a solution of acid (0.06 mmol, 2.0 eq.) in DMF (1.0 mL) at 0 °C was added EDC•HCl (14 mg, 0.07 mmol, 2.2 eq.) and *i*PrEt$_2$N (23 μL, 0.13 mmol, 17 mg, 4.0 eq.). After 5 min, a solution of **MK-2206** (15 mg, 0.03 mmol, 1.0 eq.) in DMF (1.0 mL) with *i*PrEt$_2$N (11 μL, 0.07 mmol, 9 mg, 2.0 eq.) was added dropwise. The resulting reaction mixture was

warmed to room temperature and stirred overnight. The crude reaction mixture was poured into water (20 mL) and extracted with EtOAc (3 × 10 mL). The organic fractions were combined, dried and concentrated in vacuo.

General procedure for deprotection of *t*-butyldimethylsilyl (TBDMS) ethers

The TBDMS ether (0.014 mmol) was added to TFA/MeOH (9:1 v/v, 10 mL) and stirred for 4 h. The solvent was evaporated under a stream of compressed gas overnight. The crude mixture was re-suspended in 0.1 M NaOH solution (20 mL) and extracted with EtOAc (3 x 20 mL). The organic fraction was dried over Na_2SO_4, filtered and evaporated in vacuo.

Syntheses and characterizations:

Synthesis of MK-HNE

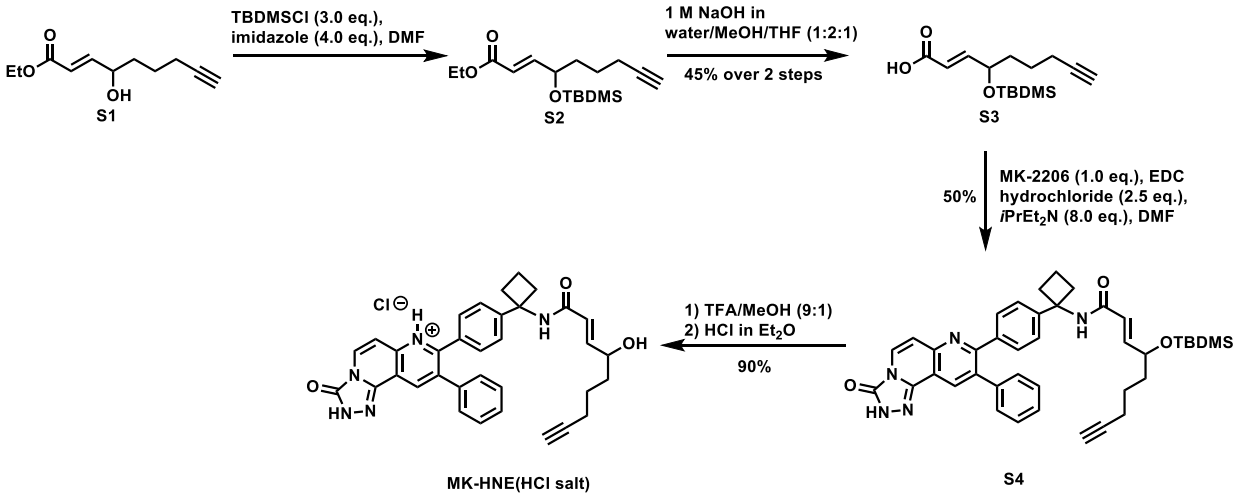

Ethyl (E)-4-((tert-butyldimethylsilyl)oxy)non-2-en-8-ynoate (S2)

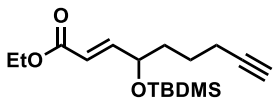

The alcohol protection reaction of **S1** with *t*-butyldimethylsilyl chloride was carried out following the general procedure described above. The crude product **S2** was subject to the following reaction without purification.

Ethyl (E)-4-((tert-butyldimethylsilyl)oxy)non-2-en-8-ynoate (S3)

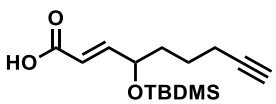

To a solution of crude ester **S2** (205 mg, 0.65 mmol, 1.0 eq.) in MeOH/THF (2:1 v/v, 30 mL) was added 4 M NaOH solution (10 mL) dropwise. The reaction mixture was stirred

at room temperature until TLC analysis indicating reaction completion. 3 M HCl solution was added dropwise until pH 2.0. This is followed by extraction with Et_2O (3 x 20 mL). The organic fractions were combined and concentrated in vacuo. The crude product was purified by flash chromatography (10:1 v/v, hexane:Et_2O with 1% AcOH) to afford the desired product **S3** as yellow oil (130 mg, 45% over 2 steps). **^{1}H NMR** (400 MHz, $CDCl_3$) δ 7.03 (dd, *J* = 15.5, 4.4 Hz, 1H), 6.01 (dd, *J* = 15.5, 1.5 Hz, 1H), 4.39 (app. q, *J* = 4.9 Hz, 1H), 2.22 (td, *J* = 6.9, 2.7 Hz, 2H), 1.95 (t, *J* = 2.7 Hz, 1H), 1.74-1.64 (m, 1H), 1.62-1.54 (m, 4H), 0.91 (s, 9H), 0.07 (s, 3H), 0.04 (s, 3H). **^{13}C NMR** (125 MHz, $CDCl_3$) δ 153.4, 119.3, 84.1, 71.1, 68.8, 36.1, 25.9, 23.7, 18.5, 18.3, -4.5, -4.8.

^{1}H NMR spectrum of acid S3

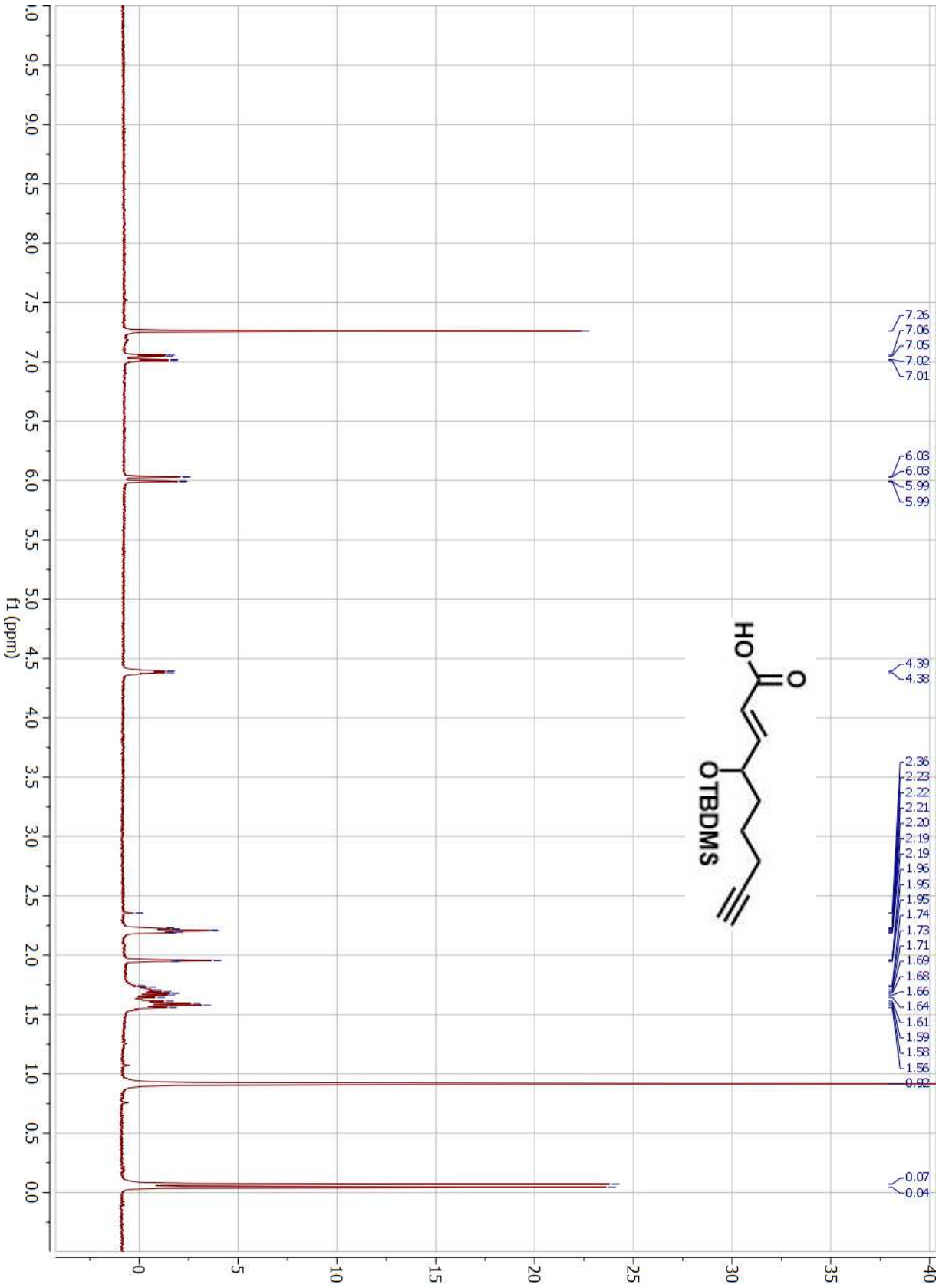

^{13}C NMR spectrum of acid S3

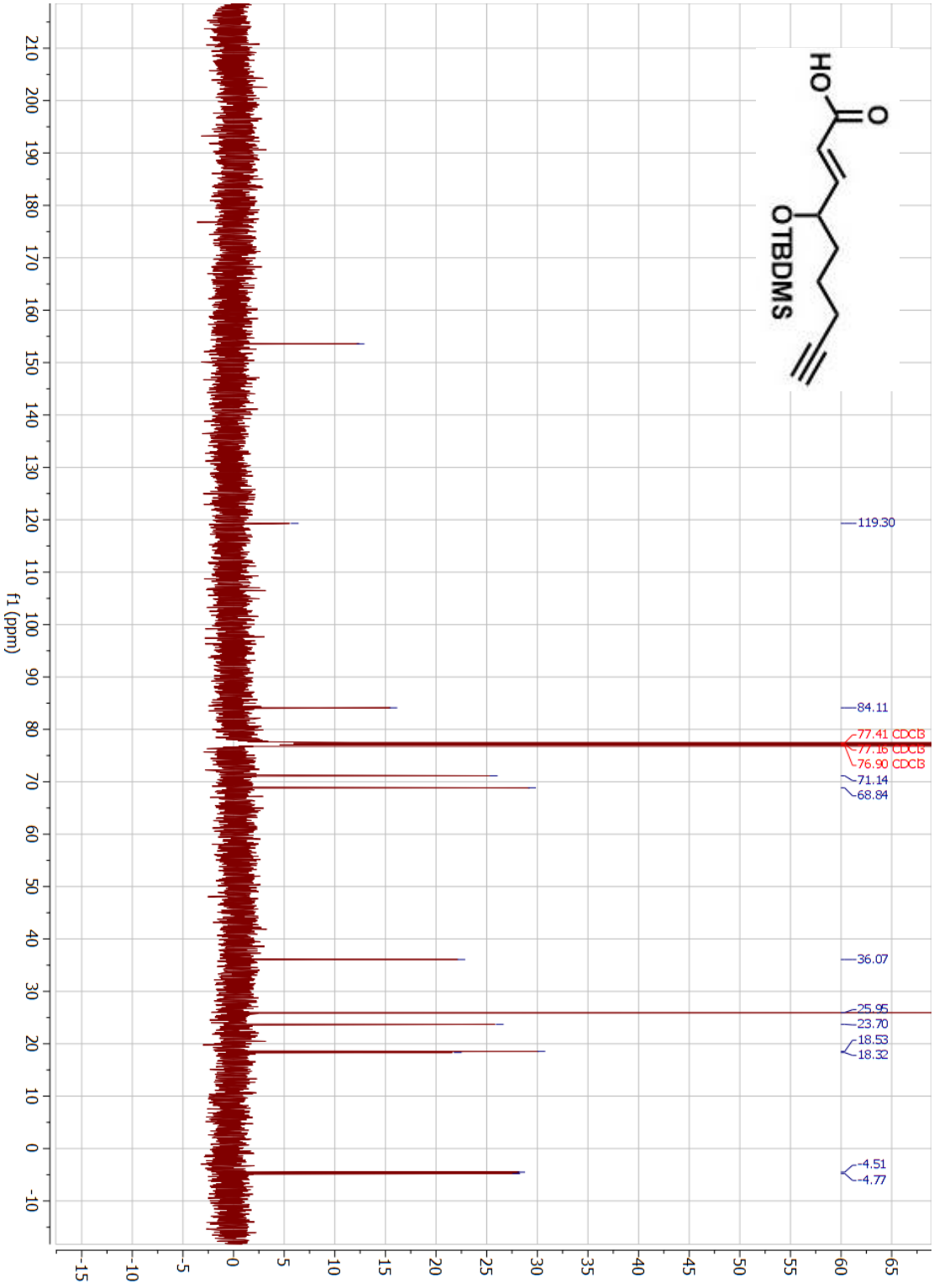

(E)-4-((tert-butyldimethylsilyl)oxy)-N-(1-(4-(3-oxo-9-phenyl-2,3-dihydro-[1,2,4]triazolo[3,4-f][1,6]naphthyridin-8-yl)phenyl)cyclobutyl)non-2-en-8-ynamide (S4)

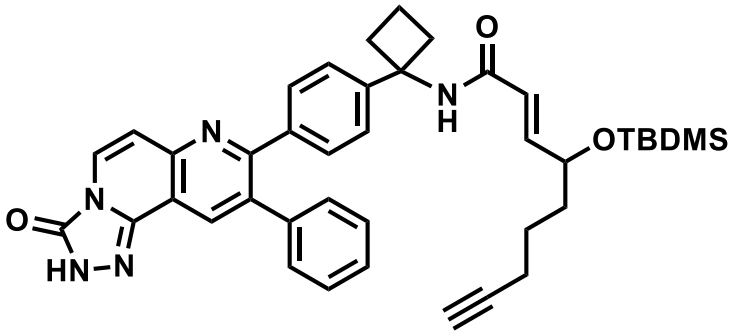

The coupling reaction of **S3** and **MK-2206** was carried out following the general procedure described above. The crude product was purified by flash chromatography (4:1 v/v, toluene:Et_2OAc) to afford the desired product **S4** as white solid (10 mg, 50%). **^{1}H NMR** (500 MHz, $CDCl_3$) δ 9.35 (s, 1H), 8.52 (s, 1H), 7.81 (d, *J* = 7.6 Hz, 1H), 7.45 (d, *J* = 8.5 Hz, 2H), 7.41 (d, *J* = 8.4 Hz, 2H), 7.35-7.33 (m, 3H), 7.30 (m, 2H), 7.09 (d, *J* = 7.6 Hz, 1H), 6.78 (dd, *J* = 15.1, 4.3 Hz, 1H), 5.92 (dd, *J* = 15.1 Hz, 1H), 5.14 (s, 1H), 4.37 (m, 1H), 2.74–2.58 (m, 4H), 2.21 (td, *J* = 7.2, 2.6 Hz, 2H), 2.12 (m, 1H), 1.96 (t, *J* = 2.6 Hz, 1H), 1.88 (dt, *J* = 8.4, 4.8 Hz, 1H), 1.74–1.62 (m, 1H), 1.64–1.55 (m, 4H), 0.94 (s, 9H), 0.09 (s, 3H), 0.07 (s, 3H). **^{13}C NMR** (125 MHz, CD_3OD) δ164.52, 160.26, 150.46, 147.98, 146.58, 145.92, 141.54, 138.75, 137.70, 136.11, 132.71, 129.93, 129.58, 128.58, 127.92, 125.64, 123.15, 122.35, 116.25, 113.84, 84.13, 71.10, 68.59, 59.65, 55.99, 36.26, 34.11, 29.71, 25.92, 23.55, 18.43, 18.24, 15.49, -4.51, -4.84.

^{1}H NMR spectrum of **S4**

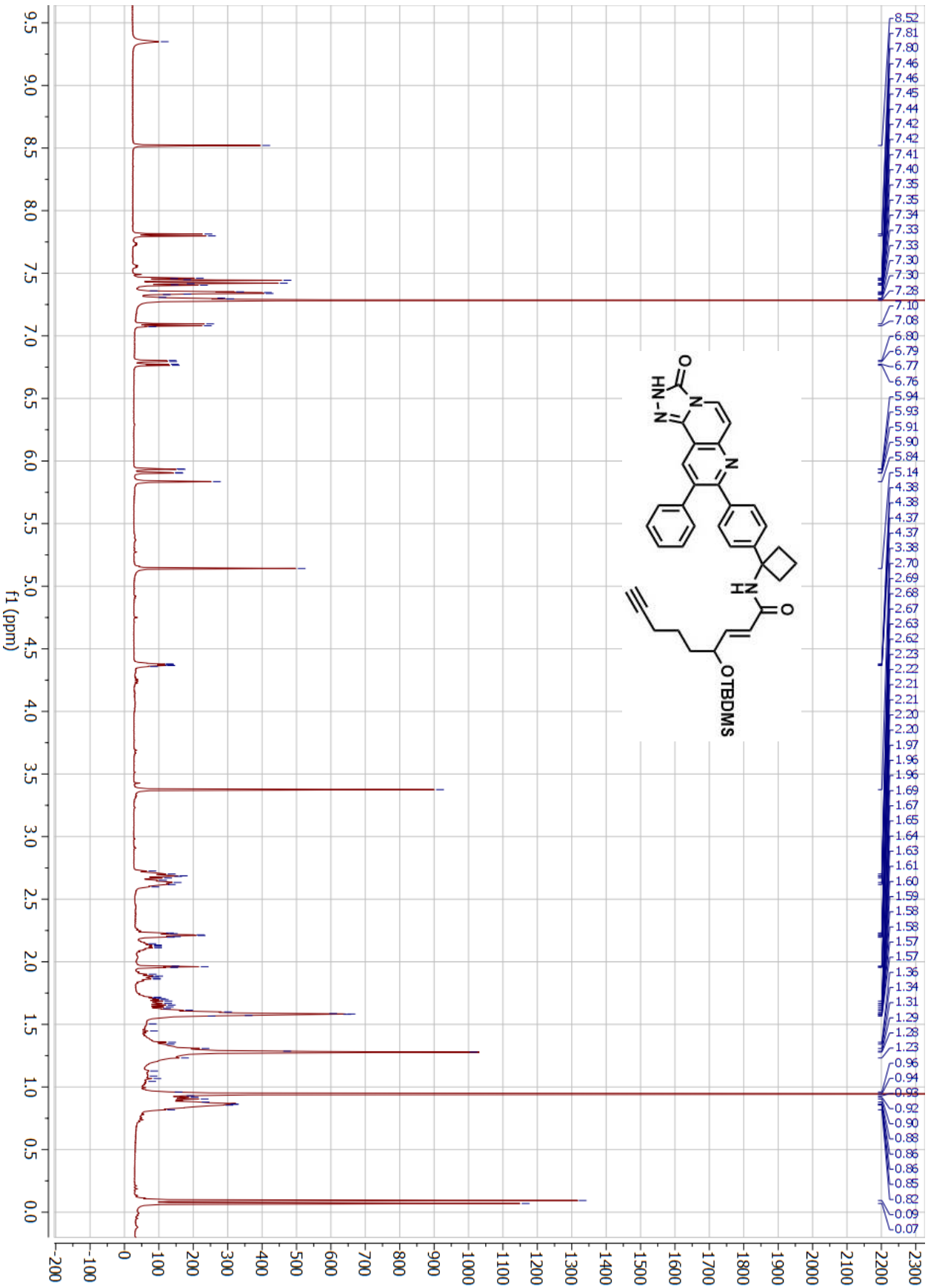

^{13}C NMR spectrum of **S4**

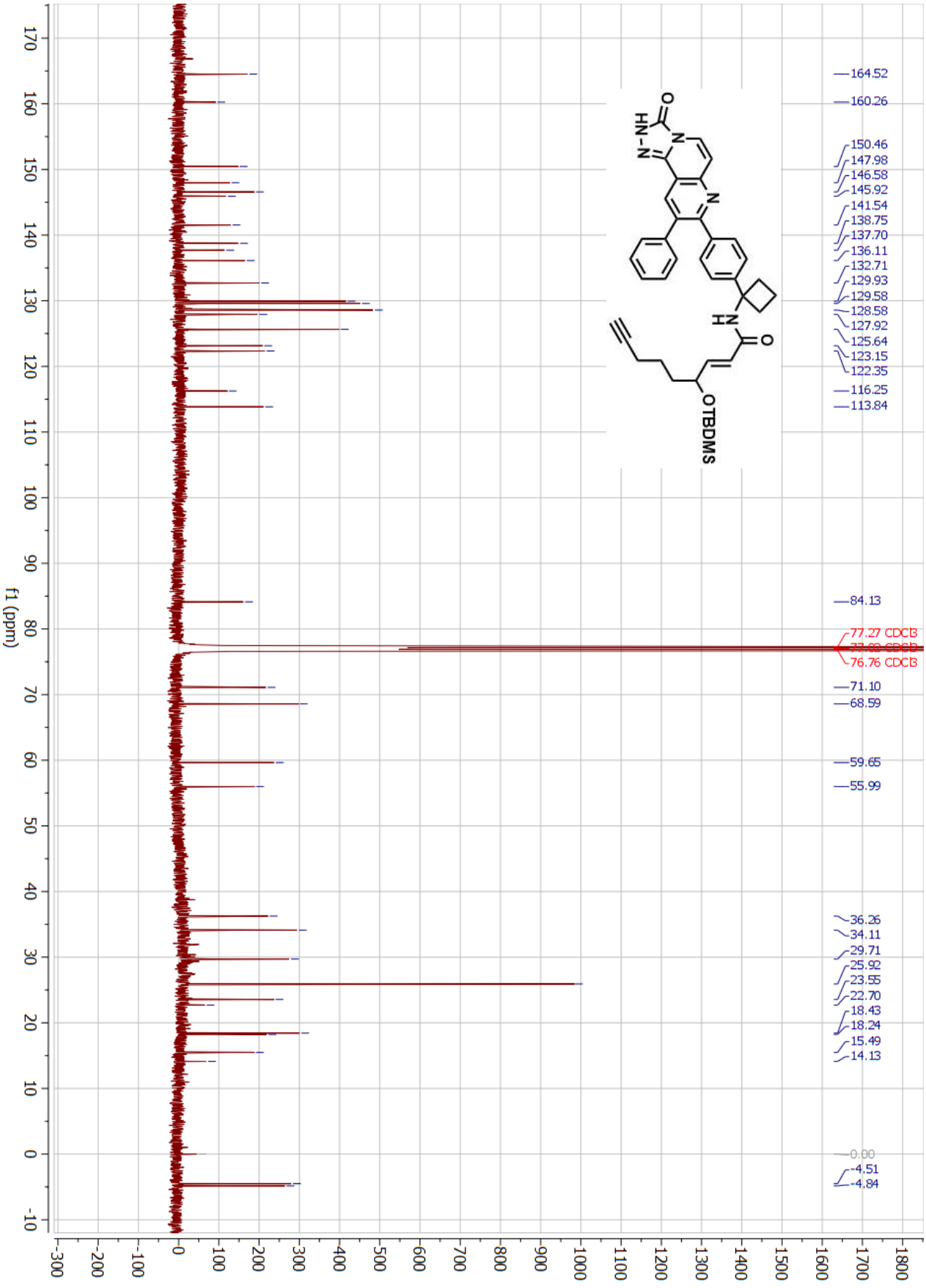

(E)-8-(4-(1-(4-hydroxynon-2-en-8-ynamido)cyclobutyl)phenyl)-3-oxo-9-phenyl-2,3-dihydro-[1,2,4]triazolo[3,4-f][1,6]naphthyridin-7-ium chloride (MK-HNE)

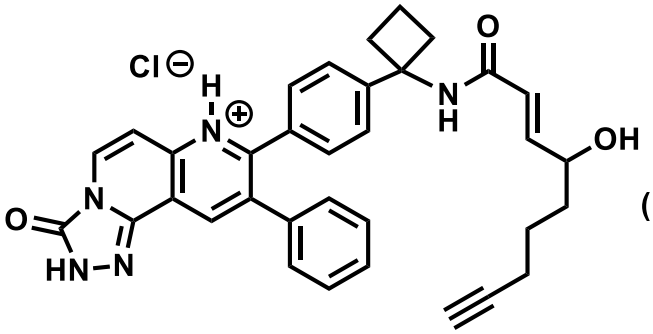

(MK-HNE, HCl salt)

Silyl ether deprotection reaction was carried out following the general procedure described above. The resulting crude product was re-dissolved in CH_2Cl_2 and precipitated by slow addition of 1 M HCl in Et_2O to afford **MK-HNE** as yellow HCl salt (7.5 mg, 90%). **^{1}H NMR** (500 MHz, CD_3OD) δ 8.97 (s, 1H), 8.15 (d, *J* = 7.5 Hz, 1H), 7.53 (d, *J* = 7.7 Hz, 2H), 7.47 (d, *J* = 7.9 Hz, 2H), 7.42-7.38 (m, 3H), 7.40–7.31 (m, 2H), 7.18 (d, *J* = 7.5 Hz, 1H), 6.69 (dd, *J* = 15.4, 5.1 Hz, 1H), 6.20 (dd, *J* = 15.4 Hz, 1H), 4.25 (m, 1H), 2.63–2.55 (m, 4H), 2.26–2.20 (m, 3H), 2.17-2.12 (m, 1H), 1.99–1.92 (m, 1H),1.71–1.57 (m, 4H); **^{13}C NMR** (125 MHz, CD_3OD) δ 165.90, 150.67, 148.87, 145.94, 138.93, 138.00, 137.28, 135.96, 129.76, 129.47, 128.67, 128.56, 128.09, 125.65, 125.59, 122.23, 118.75, 105.96, 83.25, 69.86, 68.42, 59.20, 35.39, 33.80, 33.75, 24.17, 17.50, 15.16. Analytical UPLC of MK-HNE: Retention time, 2.6 min (0 to 100% Eluent B over 5 min, λ = 230 nm). Mass spectrum (ESI+) of MK-HNE: Calculated mass for $C_{34}H_{32}N_5O_3^+$ $[M+H]^+$: 558.3; Mass found $[M+H]^+$: 558.2. HRMS (ESI+) *m/z* calcd. for $C_{34}H_{32}N_5O_3$ $[M+H]^+$ 558.2505, found 558.2509.

^{1}H NMR spectrum of MK-HNE (HCl salt)

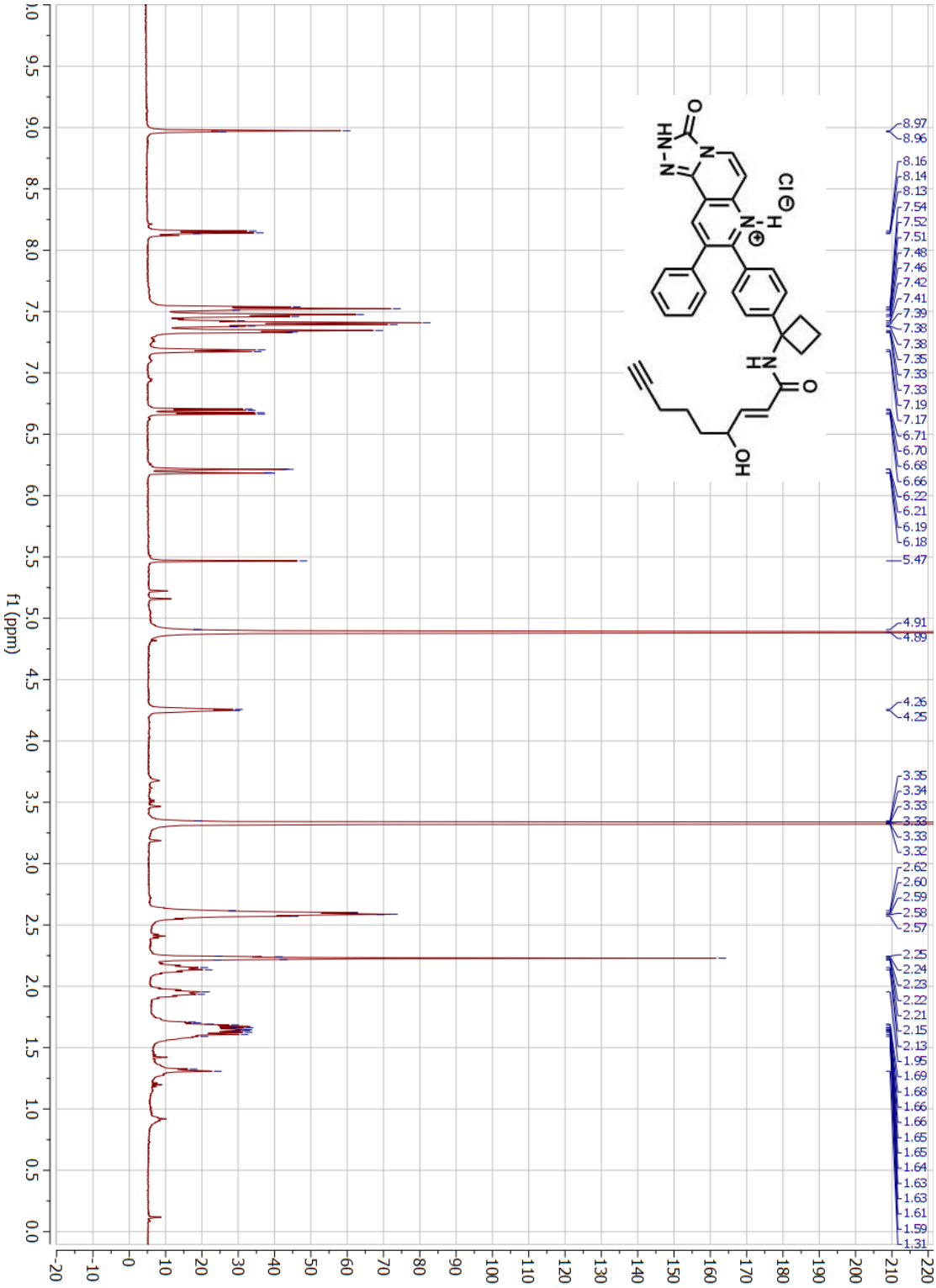

Note: H_2O solvent residue peak is present in this ^{1}H NMR spectrum.

^{13}C NMR spectrum of MK-HNE (HCl salt)

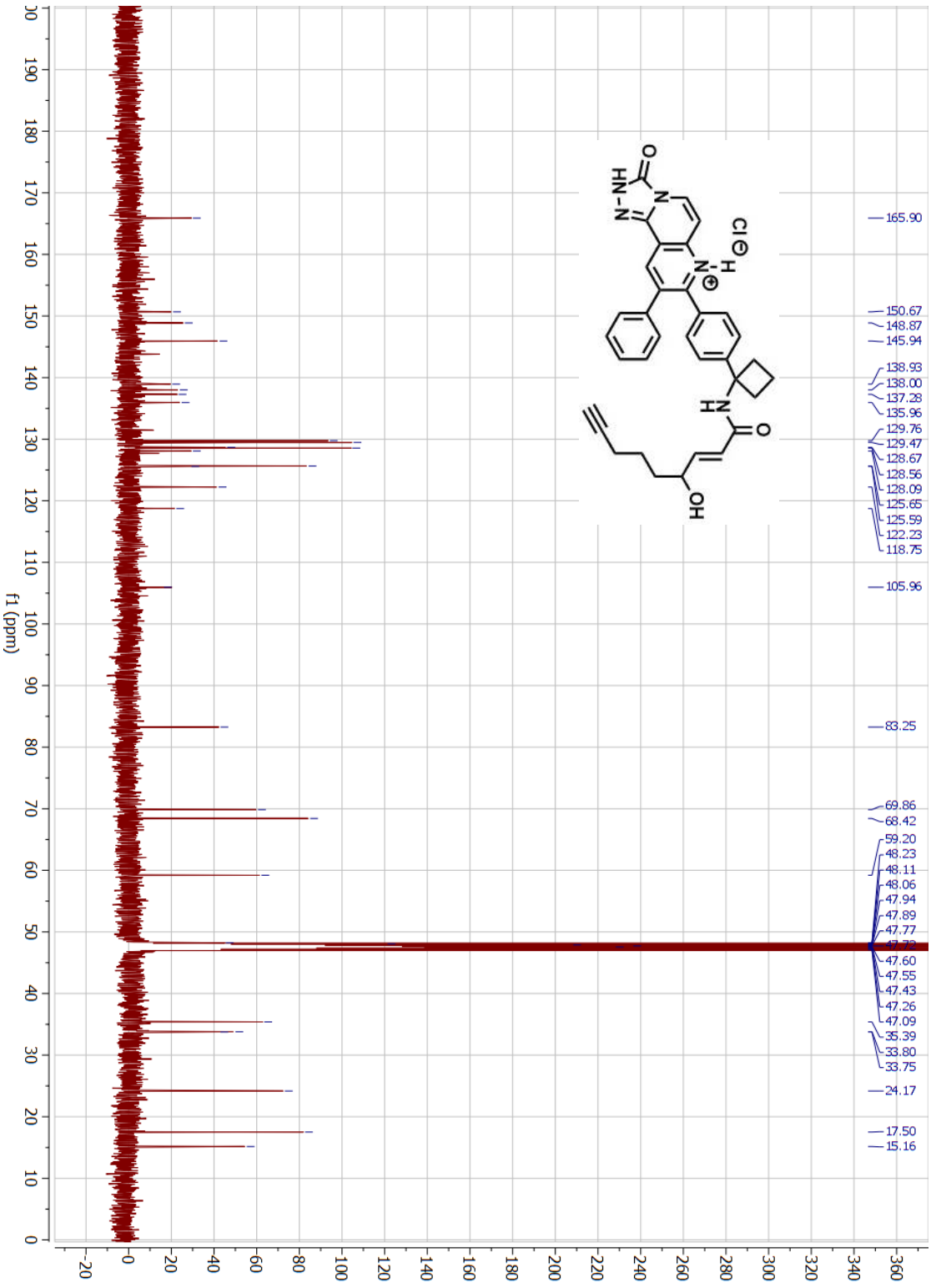

UPLC-MS analysis of MK-HNE

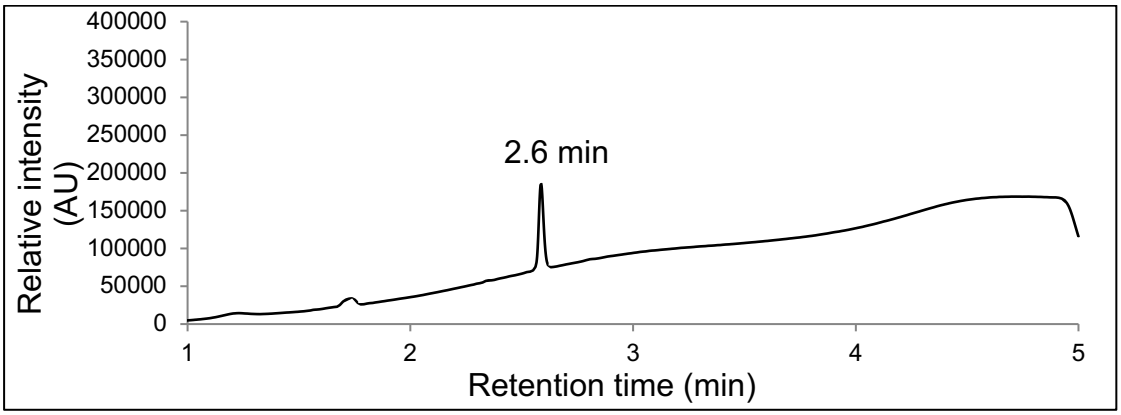

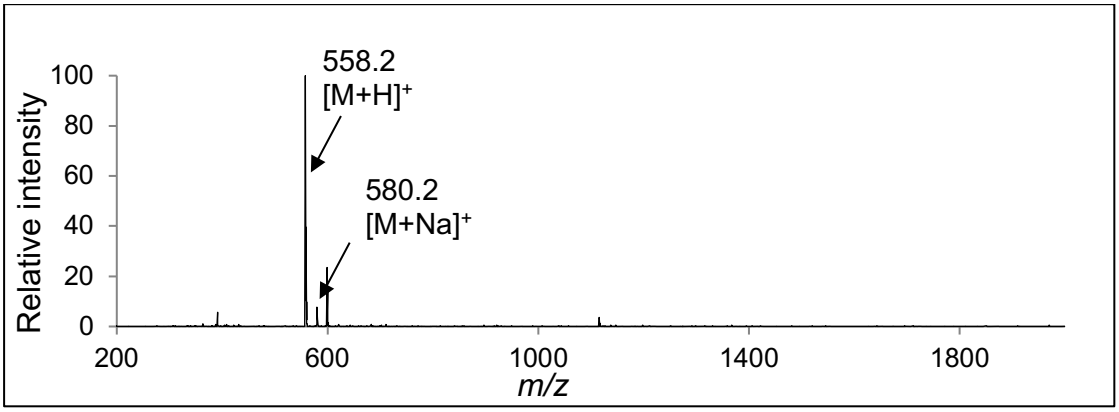

HRMS analysis of MK-HNE

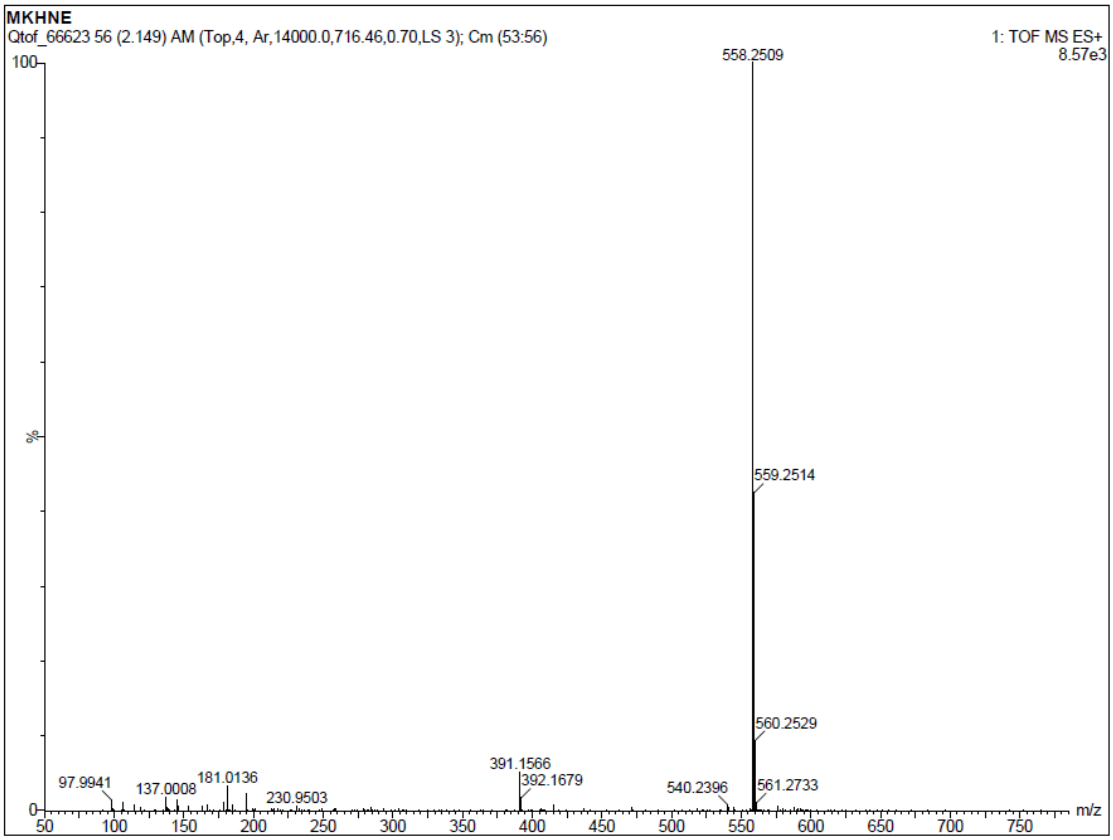

Synthesis of MK-FNE

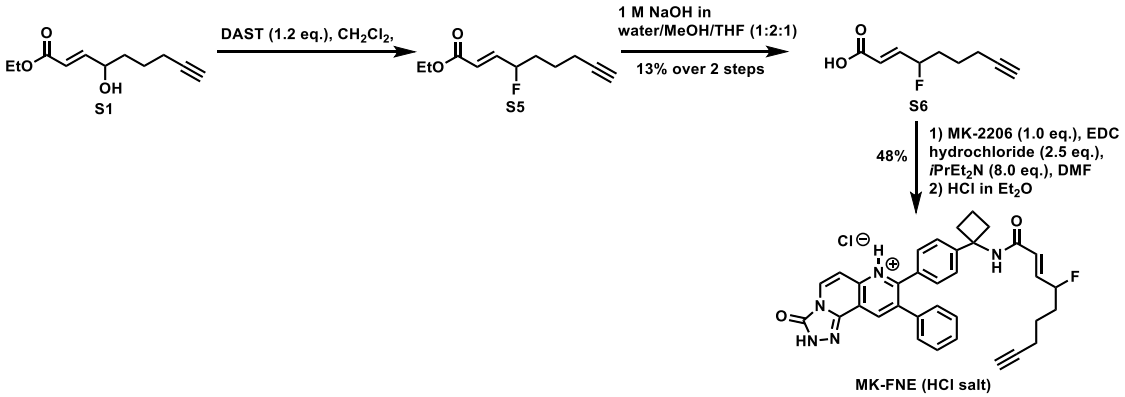

(E)-4-fluoronon-2-en-8-ynoic acid (S6)

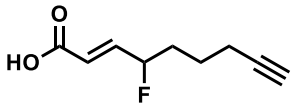

To a solution of ester **S1** (125 mg, 0.64 mmol, 1.0 eq.) in CH_2Cl_2 (2 mL) was added DAST (100 μL, 123 mg, 0.77 mmol, 1.2 eq.) in CH_2Cl_2 (2 mL) dropwise. The resulting solution was stirred for 5 min before addition of sat. $NaHCO_3$ solution (5 mL). The organic fraction was separated, dried over Na_2SO_4 and evaporated in vacuo. The desired ester **S5** was separated from most by-products through flash chromatography (20:1 v/v, hexane/Et_2O). The resulting product was dissolved in MeOH/THF (2:1 v/v, 9 mL) followed by slow addition of 4 M NaOH solution (3 mL). The hydrolysis reaction was monitored by TLC analysis. After completion, 3 M HCl solution was added dropwise until pH reach 2.0. The resulting solution was extracted with Et_2O (3 x 20 mL) and the organic fractions were combined, dried and evaporated. The desired product **S6** as a colorless oil (14 mg, 13%) was afforded through flash chromatography (20:1 v/v, hexane/Et_2O with 1% AcOH). **^{1}H NMR** (500 MHz, $CDCl_3$) δ7.00 (ddd, *J* = 21.1, 15.7, 3.8 Hz, 1H), 6.10 (dt, *J* = 15.6, 1.5Hz, 1H), 5.19 (m, 1H), 2.27 (td, *J* = 6.9, 2.6 Hz, 2H), 1.98 (t, *J* = 2.7 Hz, 1H), 1.94–1.80 (m, 2H), 1.70 (m, 2H). **^{13}C NMR** (125 MHz, $CDCl_3$) δ 171.15, 147.46 (d, *J* = 18.6 Hz, C-F coupling), 120.63 (d, *J* = 11.2 Hz, C-F coupling), 90.73 (d, *J* = 175.3 Hz, C-F coupling), 83.49, 69.29, 33.53 (d, *J* = 21.2 Hz, C-F coupling), 23.51 (d, *J* = 3.6 Hz, C-F coupling) 18.19.

^{1}H NMR spectrum of S6

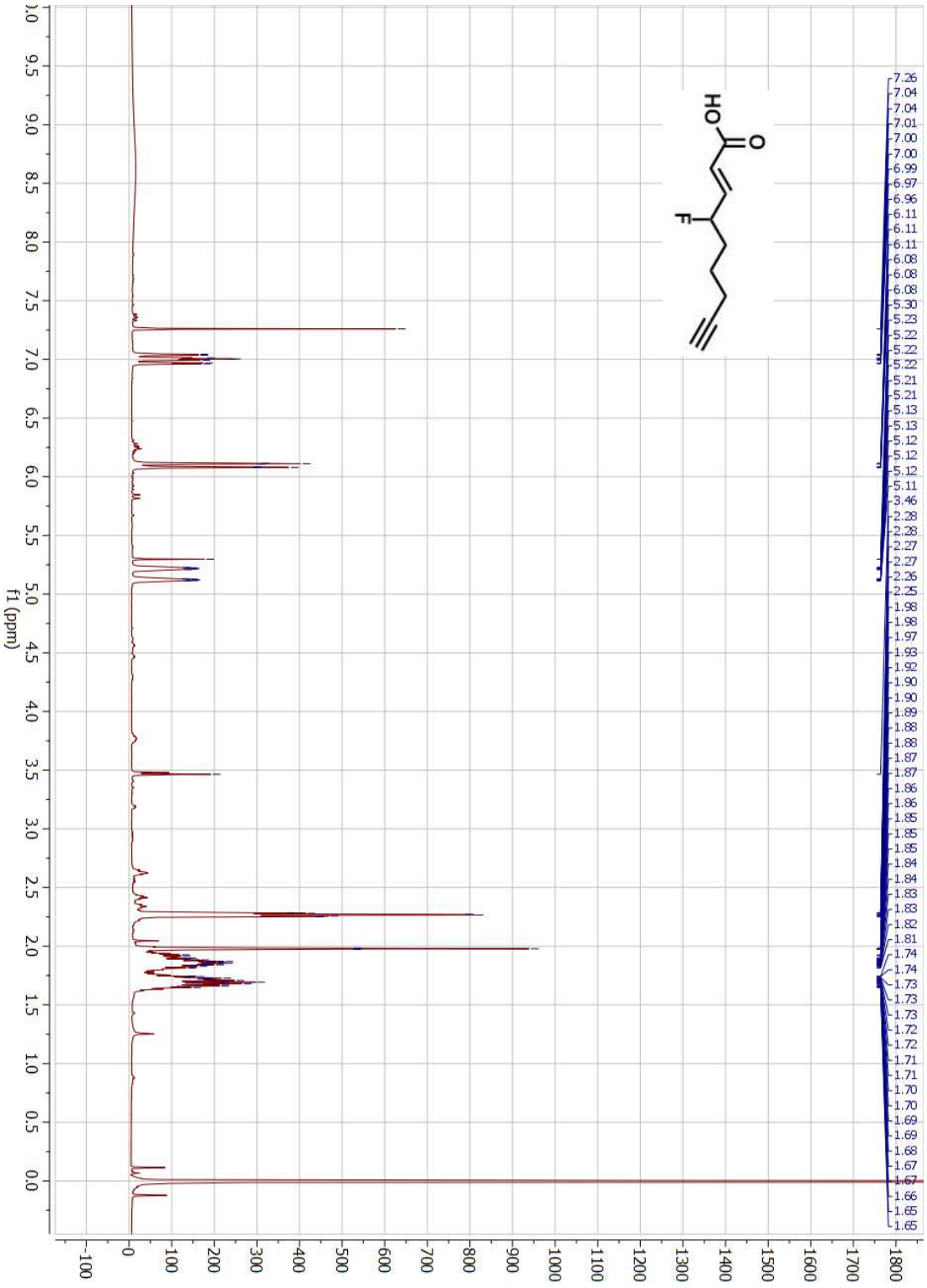

Note: CH_2Cl_2 solvent residue peak is present in this ^{1}H NMR spectrum.

^{13}C NMR spectrum of S6

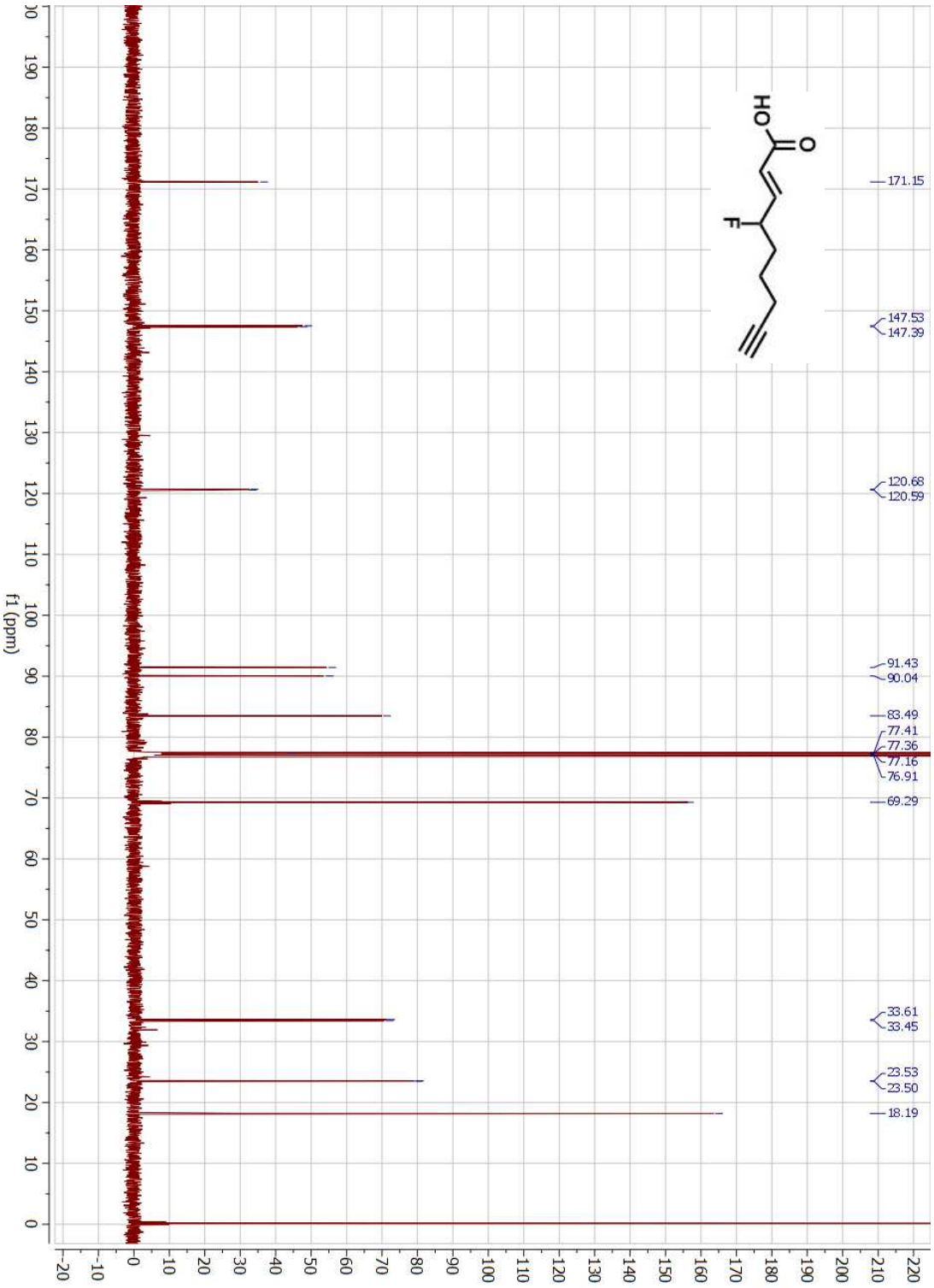

(E)-8-(4-(1-(4-fluoronon-2-en-8-ynamido)cyclobutyl)phenyl)-3-oxo-9-phenyl-2,3-dihydro-[1,2,4]triazolo[3,4-f][1,6]naphthyridin-7-ium chloride (MK-FNE)

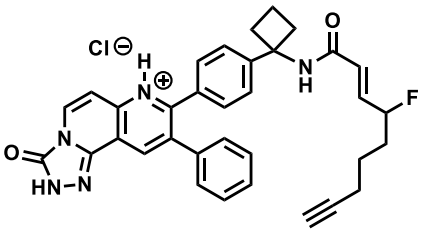

(MK-FNE, HCl salt)

The coupling reaction of **S6** and **MK-2206** was carried out following the general procedure described above. The crude product was first purified by flash chromatography (from 4:1 v/v, toluene:Et_2OAc) followed by HCl precipitation to afford the desired product **MK-FNE** as yellow HCl salt (12 mg, 48%). **^{1}H NMR** (500 MHz, CD_3OD) δ 9.02 (s, 1H), 8.17 (d, *J* = 7.6 Hz, 1H), 7.53 (d, *J* = 8.0 Hz, 2H), 7.46 (d, *J* = 8.4 Hz, 2H), 7.42-7.36 (m, 3H), 7.33-7.31 (m, 2H), 7.16 (d, *J* = 7.7 Hz, 1H), 6.65 (ddd, *J* = 19.9, 15.5, 4.4 Hz, 1H), 6.23 (dt, *J* = 15.6, 1.7 Hz, 1H), 5.09 (m, 1H), 2.64–2.51 (m, 4H), 2.27–2.20 (m, 3H), 2.18–2.09 (m, 1H), 1.98–1.89 (m, 1H), 1.88–1.74 (m, 2H), 1.63 (m, 2H). **^{13}C NMR** (125 MHz, CD_3OD) δ 166.46, 156.64, 151.98, 150.52, 144.56, 142.16, 142.01, 139.97, 139.66, 139.46, 136.88, 131.95, 131.16, 130.84, 130.27, 130.25, 130.01, 127.17, 124.74, 124.66, 120.53, 106.15, 93.11, 91.75, 84.31, 70.08, 60.63, 35.14, 35.06, 35.04, 34.87, 24.84, 24.80, 18.73, 16.54. Analytical UPLC of MK-FNE: Retention time, 3.2 min (0 to 100% Eluent B over 5 min, λ = 230 nm). Mass spectrum (ESI+) of MK-FNE: Calculated mass for $C_{34}H_{31}FN_5O_2^+$ $[M+H]^+$: 560.2; Mass Found $[M+H]^+$: 560.2. HRMS (ESI+) *m/z* calcd. for $C_{34}H_{31}FN_5O_2$ $[M+H]^+$ 560.2462, found 560.2471.

Note, the presence of the fluorine gives more ^{13}C peaks than expected due to ^{13}C-^{19}F coupling. Due to the number of different ^{13}C's in this spectrum, we have not deconvoluted this spectrum.

^{1}H NMR spectrum of **MK-FNE (HCl salt)**

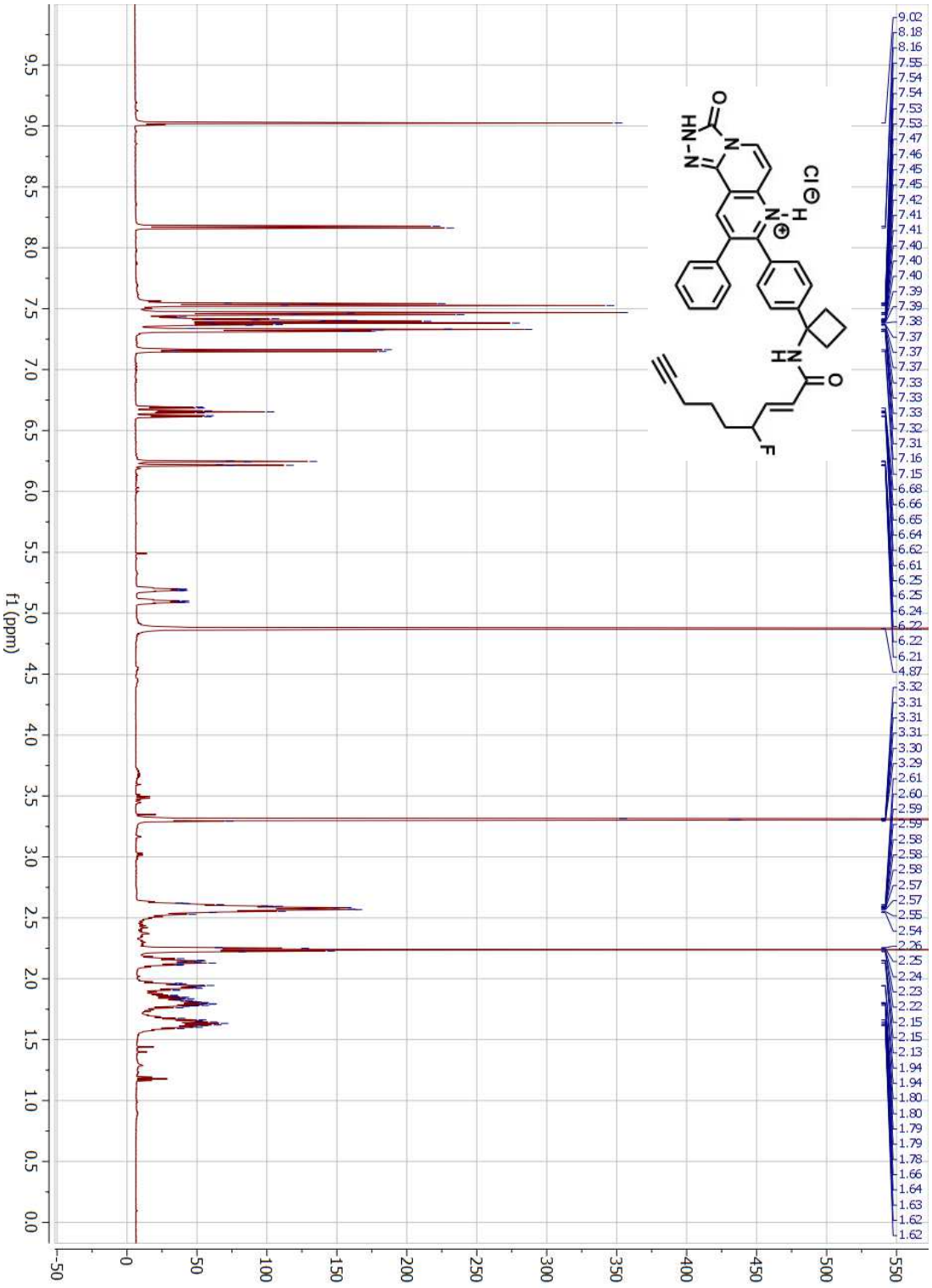

^{13}C NMR spectrum of **MK-FNE (HCl salt)**

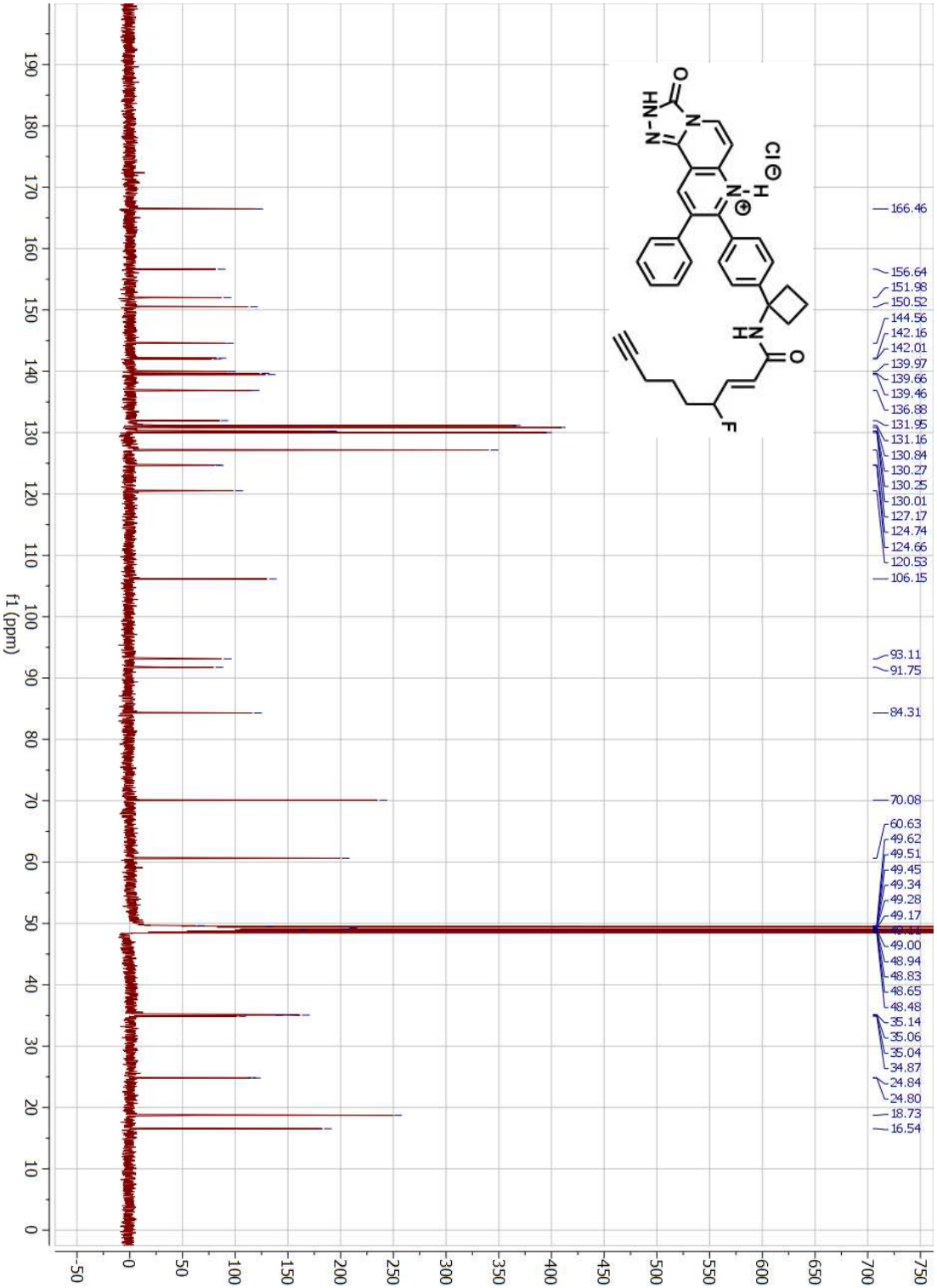

UPLC-MS analysis of **MK-FNE (HCl salt)**

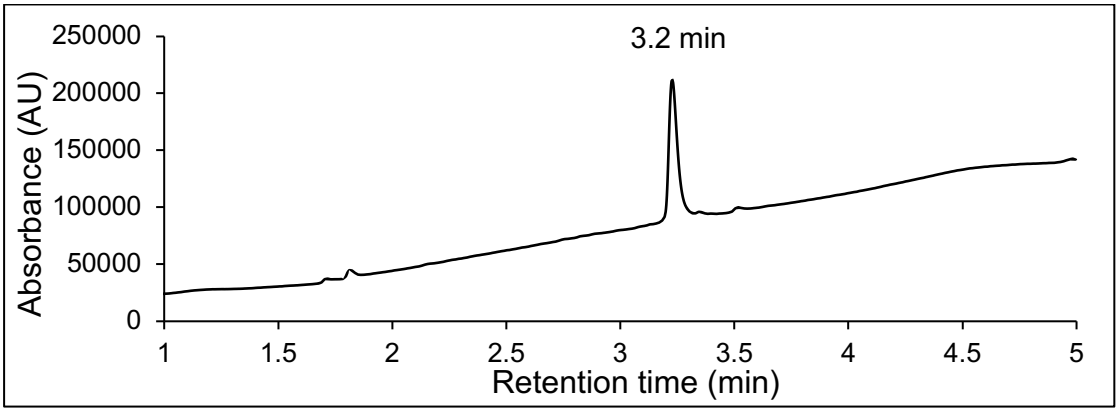

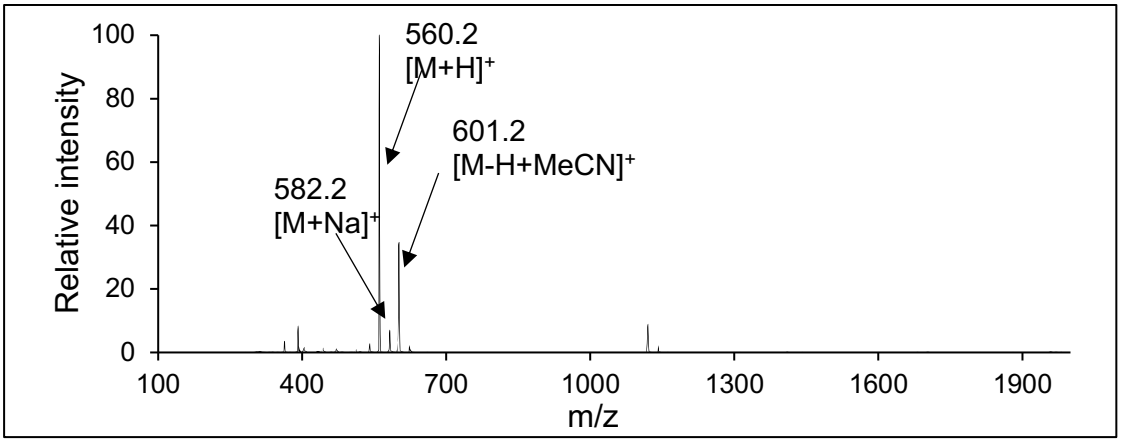

HRMS spectrum of **MK-FNE**

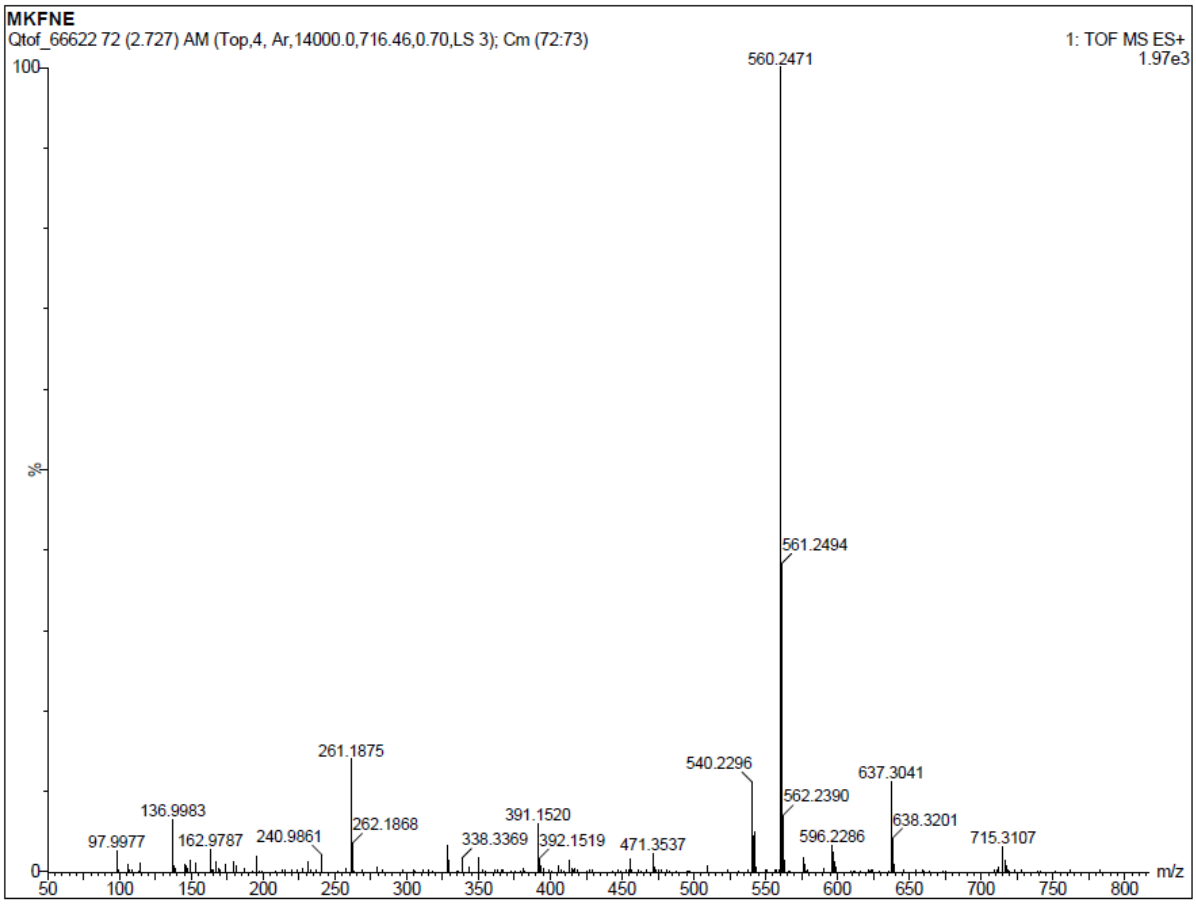

Synthesis of MK-NE

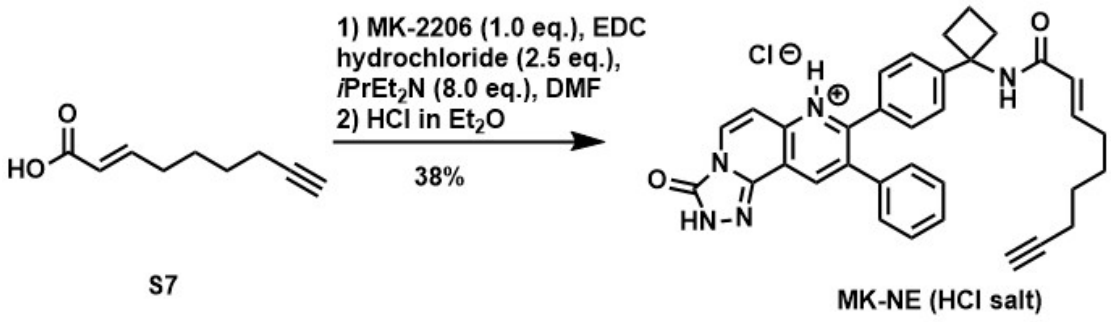

(E)-8-(4-(1-(non-2-en-8-ynamido)cyclobutyl)phenyl)-3-oxo-9-phenyl-2,3-dihydro-[1,2,4]triazolo[3,4-f][1,6]naphthyridin-7-ium chloride (MK-NE)

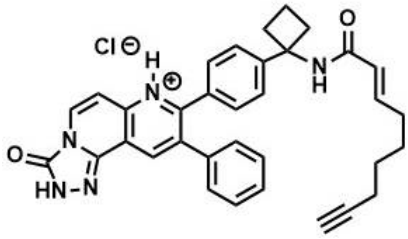

The coupling reaction of **S7** and **MK-2206** was carried out following the general procedure described above. The crude product was first purified by flash chromatography (4:1 v/v, toluene:EtOAc) followed by HCl precipitation to afford the desired product **MK-NE** as yellow HCl salt (10 mg, 38%). **^{1}H NMR** (500 MHz, CD_3OD) δ 8.99 (s, 1H), 8.16 (d, *J* = 7.7 Hz, 1H), 7.53 (d, *J* = 8.5 Hz, 2H), 7.46 (d, *J* = 8.5 Hz, 2H), 7.43 – 7.37 (m, 3H), 7.35-7.33 (m, 2H), 7.16 (d, *J* = 7.8 Hz, 1H), 6.71 (dt, *J* = 15.5, 7.0 Hz, 1H), 6.01 (dt, *J* = 15.2, 1.5 Hz, 1H), 2.65 – 2.52 (m, 4H), 2.28 – 2.17 (m, 3H), 2.14 (m, 1H), 1.95 (m, 1H), 1.65 – 1.50 (m, 4H). **^{13}C NMR** (126 MHz, CD_3OD) δ 167.52, 159.27, 152.28, 149.25, 146.96, 145.16, 141.24, 138.64, 138.61, 135.53, 131.01, 130.79, 129.83, 129.59, 126.72, 125.16, 119.07, 110.34, 84.69, 69.68, 60.53, 35.24, 32.41, 29.11, 28.46, 18.79, 16.56. Analytical UPLC of MK-NE: Retention time, 3.3 min (0 to 100% Eluent B over 5 min, λ = 230 nm). Mass spectrum (ESI+) of MK-NE: Calculated mass for $C_{34}H_{32}N_5O_2^+$ $[M+H]^+$: 542.3; Mass Found $[M+H]^+$: 542.2. HRMS (ESI+) *m/z* calcd. for $C_{34}H_{32}N_5O_2$ $[M+H]^+$ 542.2556, found 542.2579.

^{1}H NMR spectrum of MK-NE (HCl salt)

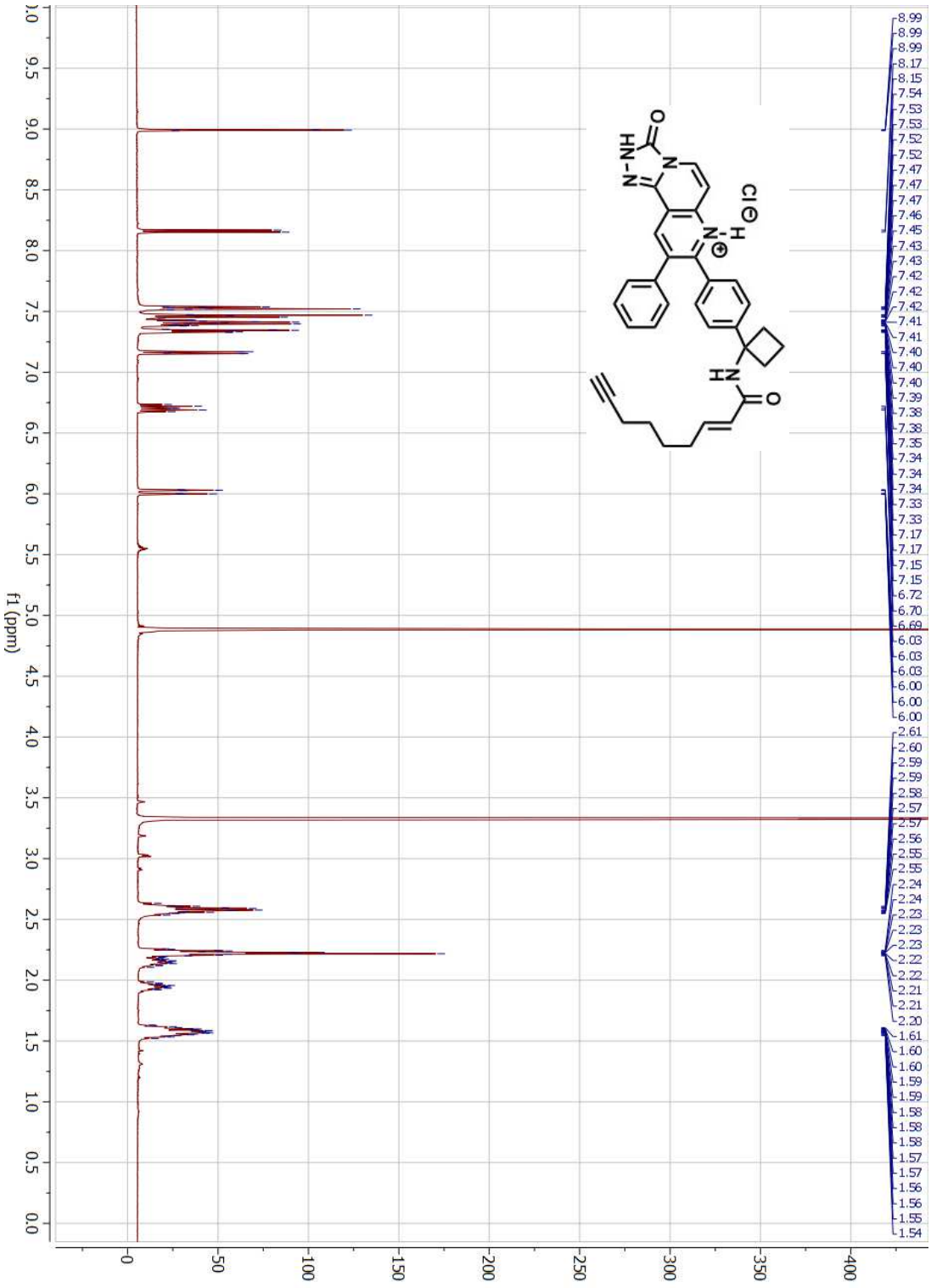

^{13}C NMR spectrum of MK-NE (HCl salt)

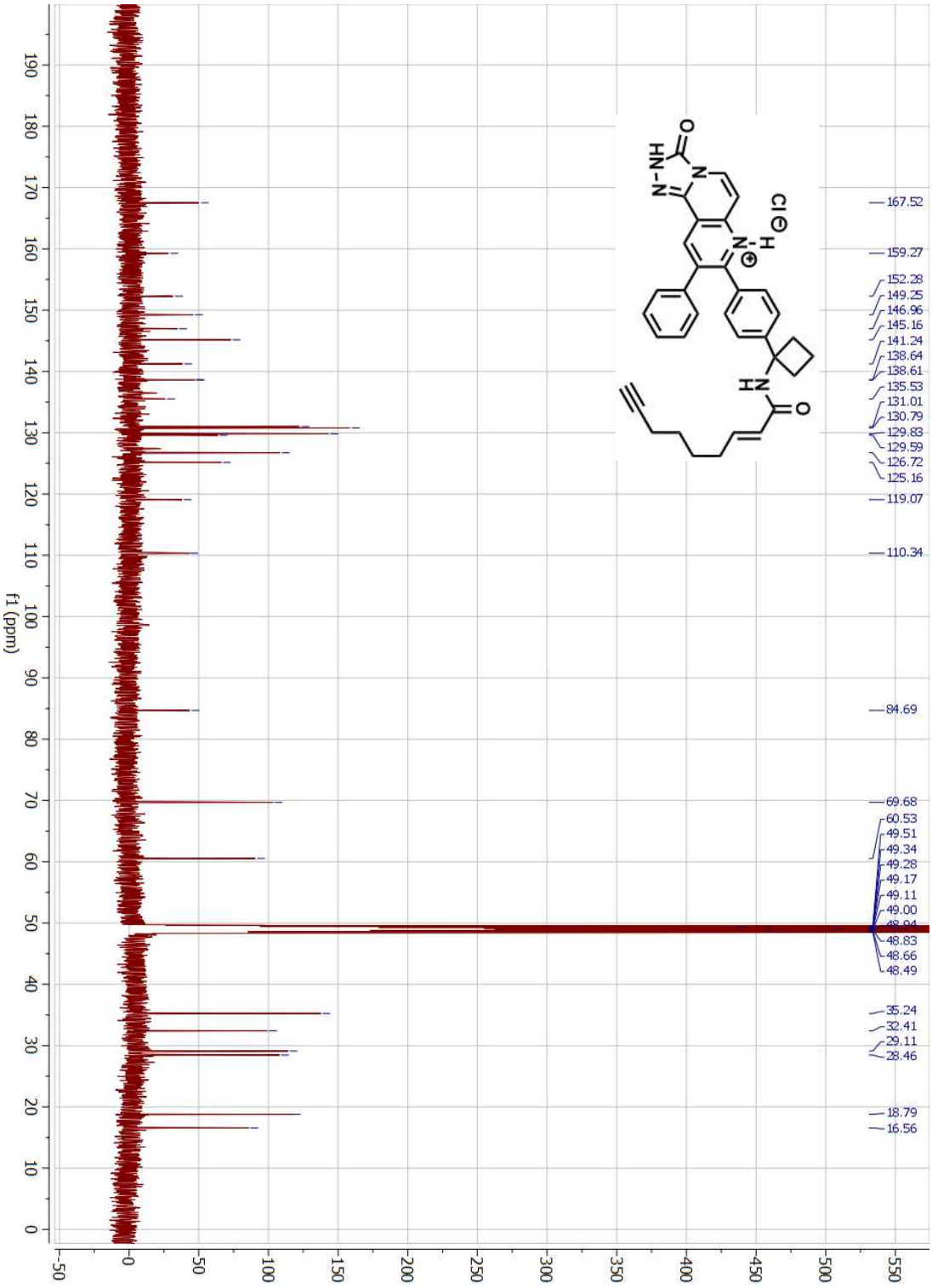

UPLC-MS analysis of **MK-NE (HCl salt)**

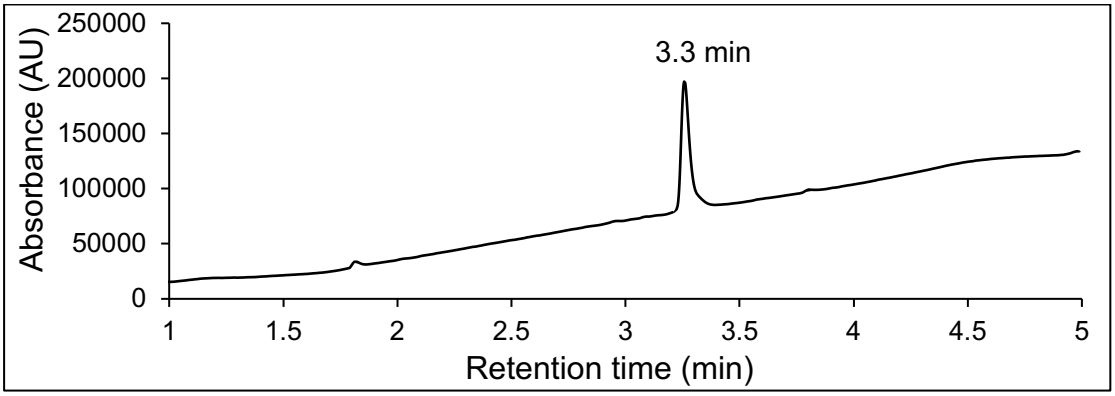

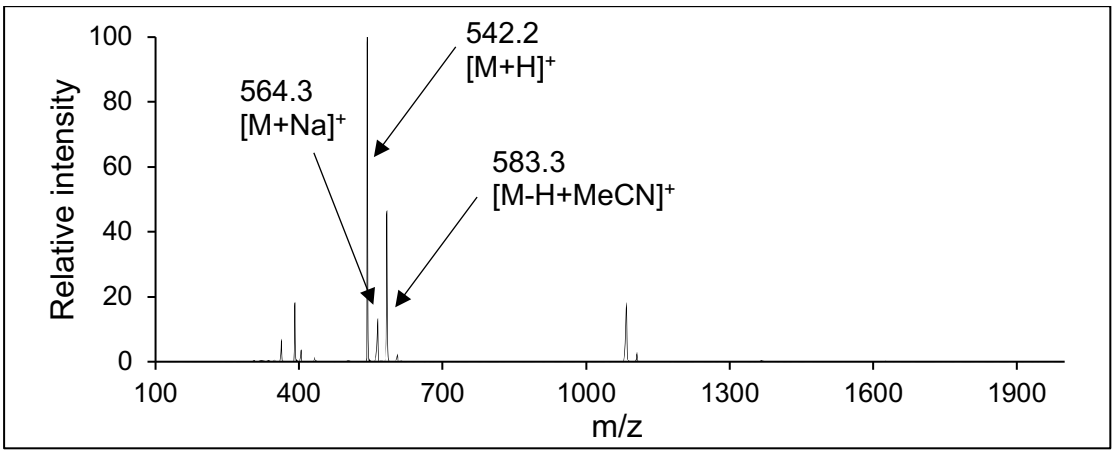

HRMS spectrum of **MK-NE**

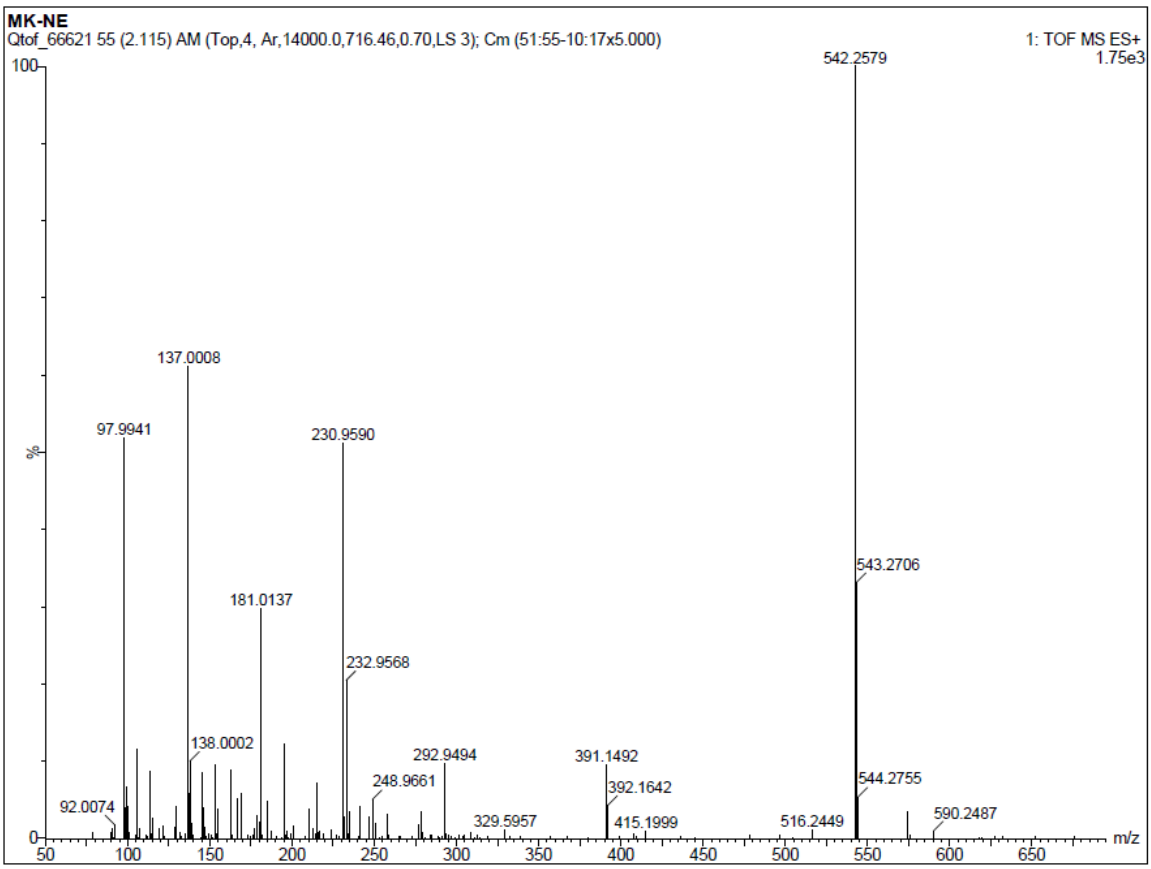

Synthesis of MK-HNA (HCl salt)

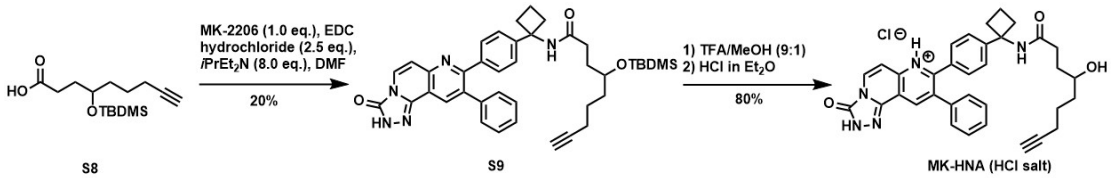

4-((tert-butyldimethylsilyl)oxy)-N-(1-(4-(3-oxo-9-phenyl-2,3-dihydro-[1,2,4]triazolo[3,4-f][1,6]naphthyridin-8-yl)phenyl)cyclobutyl)non-8-ynamide (S9)

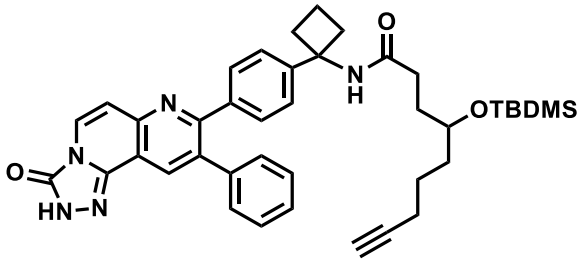

The coupling reaction of **S8** and **MK-2206** was carried out following the general procedure described above. The crude product was purified by flash chromatography (from 4:1 v/v, toluene:EtOAc) to afford the desired product **S9** as a white solid (10 mg, 20%). **^{1}H NMR** (500 MHz, $CDCl_3$) δ 8.56 (s, 1H), 7.91 (d, *J* = 7.6 Hz, 1H), 7.41–7.40 (m, 4H), 7.36–7.34 (m, 3H), 7.32–7.27 (m, 2H), 7.10 (d, *J* = 7.6 Hz, 1H), 3.75 (m, 1H), 2.60–2.49 (m, 4H), 2.30–2.15 (m, 7H), 2.09 (m, 1H), 1.90 (m, 1H), 1.75–1.67 (m, 2H), 1.62–1.52 (m, 4H), 0.93 (s, 9H), 0.09 (s, 3H), 0.08 (s, 3H). **^{13}C NMR** (126 MHz, CD_3OD) δ 173.30, 160.15, 151.13, 147.70, 146.62, 140.97, 138.77, 137.30, 136.30, 132.36, 129.52, 129.34, 128.25, 127.59, 124.87, 123.45, 116.36, 112.69, 83.52, 71.07, 68.29, 59.06, 35.50, 33.82, 33.71, 32.38, 31.53, 25.04, 25.00, 24.05, 17.77, 17.54, 15.16, -5.57, -5.67.

^{1}H NMR spectrum of S9

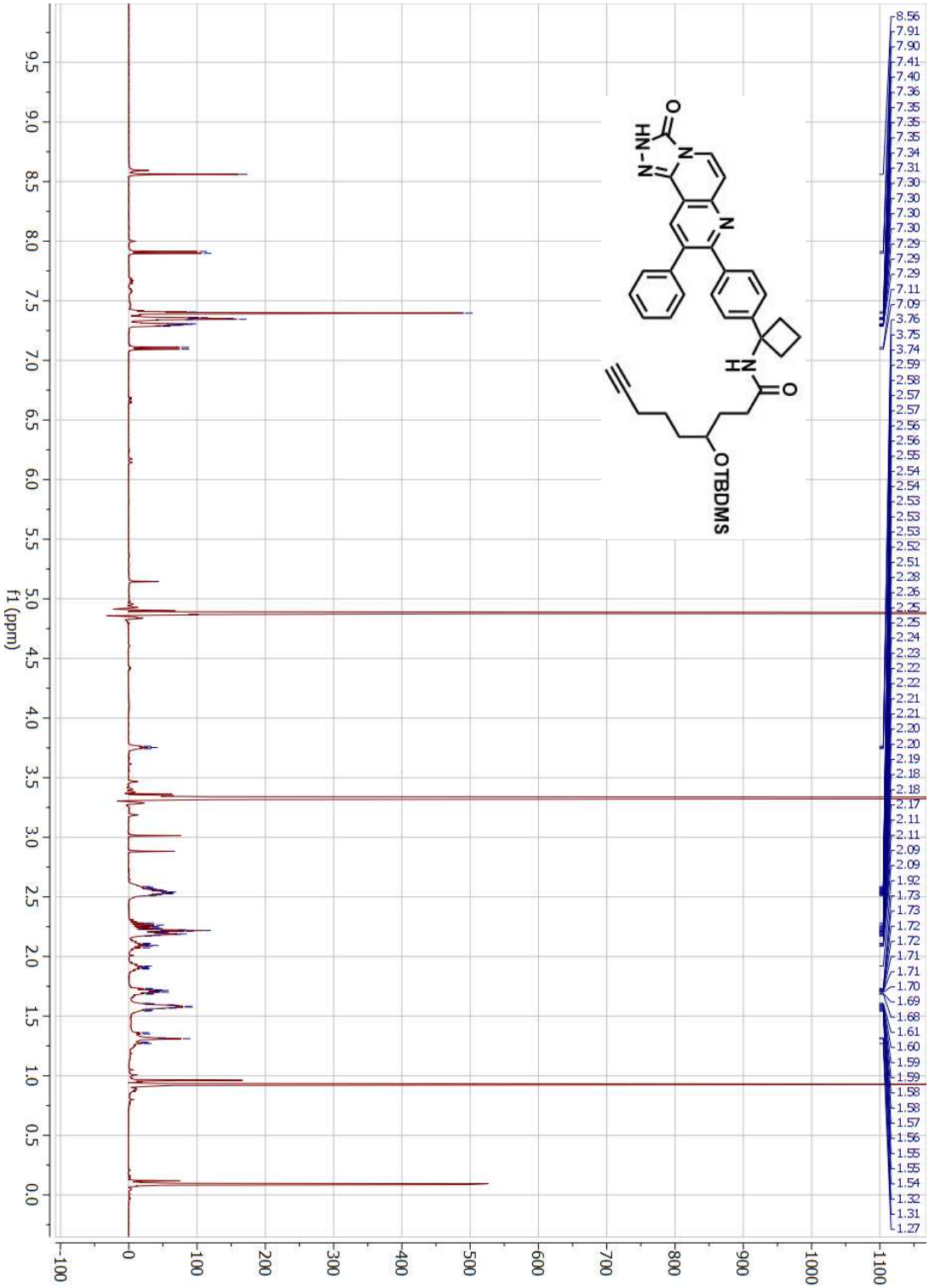

^{13}C NMR spectrum of S9

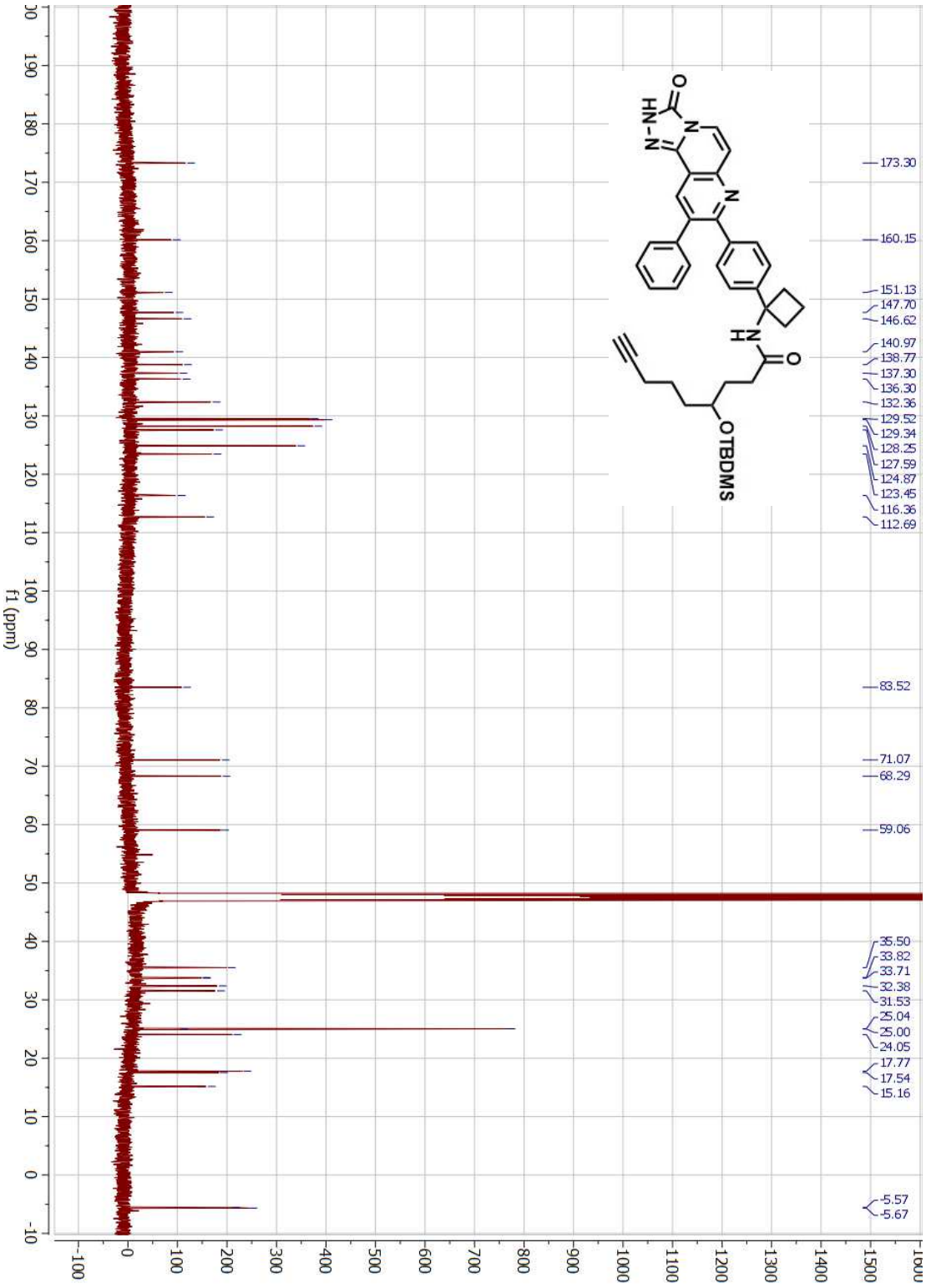

8-(4-(1-(4-hydroxynon-8-ynamido)cyclobutyl)phenyl)-3-oxo-9-phenyl-2,3-dihydro-[1,2,4]triazolo[3,4-f][1,6]naphthyridin-7-ium chloride [MK-HNA (HCl salt)]

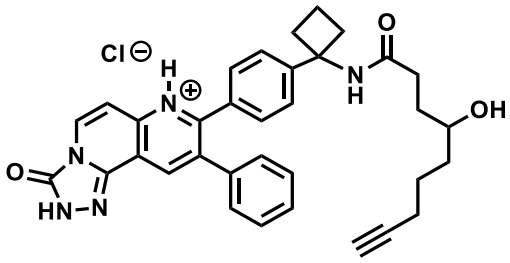

Silyl ether deprotection reaction of **S9** was carried out following the general procedure described above. The resulting crude product was re-dissolved in CH_2Cl_2 and precipitated by slow addition of 1 M HCl in Et_2O to afford MK-HNA as yellow HCl salt (7 mg, 80%). **^{1}H NMR** (500 MHz, CD_3OD) δ 9.10 (s, 1H), 8.23 (d, *J* = 7.7 Hz, 1H), 7.56 (d, *J* = 8.0 Hz, 2H), 7.49 (d, *J* = 8.1 Hz, 2H), 7.46-7.40 (m, 3H), 7.35 (app. d, *J* = 7.1 Hz, 2H), 7.20 (d, *J* = 7.6 Hz, 1H), 3.51 (m, 1H), 2.59-2.49 (m, 4H), 2.38 – 2.25 (m, 2H), 2.24-2.18 (m, 3H), 2.14 (m, 1H), 1.94 (m, 1H), 1.78-1.63 (m, 2H), 1.62-1.50 (m, 4H). **^{13}C NMR** (125 MHz, CD_3OD) δ 140.09, 131.17, 130.86, 130.39, 130.05, 127.17, 105.35, 71.37, 69.70, 60.48, 37.35, 35.13, 34.18, 33.46, 25.94, 19.00, 16.50. Analytical UPLC of MK-HNA: Retention time, 3.1 min (0 to 100% Eluent B over 5 min, λ = 230 nm). Mass spectrum (ESI+) of MK-HNA: Calculated mass for $C_{34}H_{34}N_5O_3^+$ $[M+H]^+$: 560.3; Mass found $[M+H]^+$: 562.3. Calculated mass for $C_{34}H_{32}N_5Na_2O_3^+$ $[M-H+2Na]^+$: 604.2; Mass found $[M-H+2Na]^+$: 603.3.

^{1}H NMR spectrum of **MK-HNA (HCl salt)**

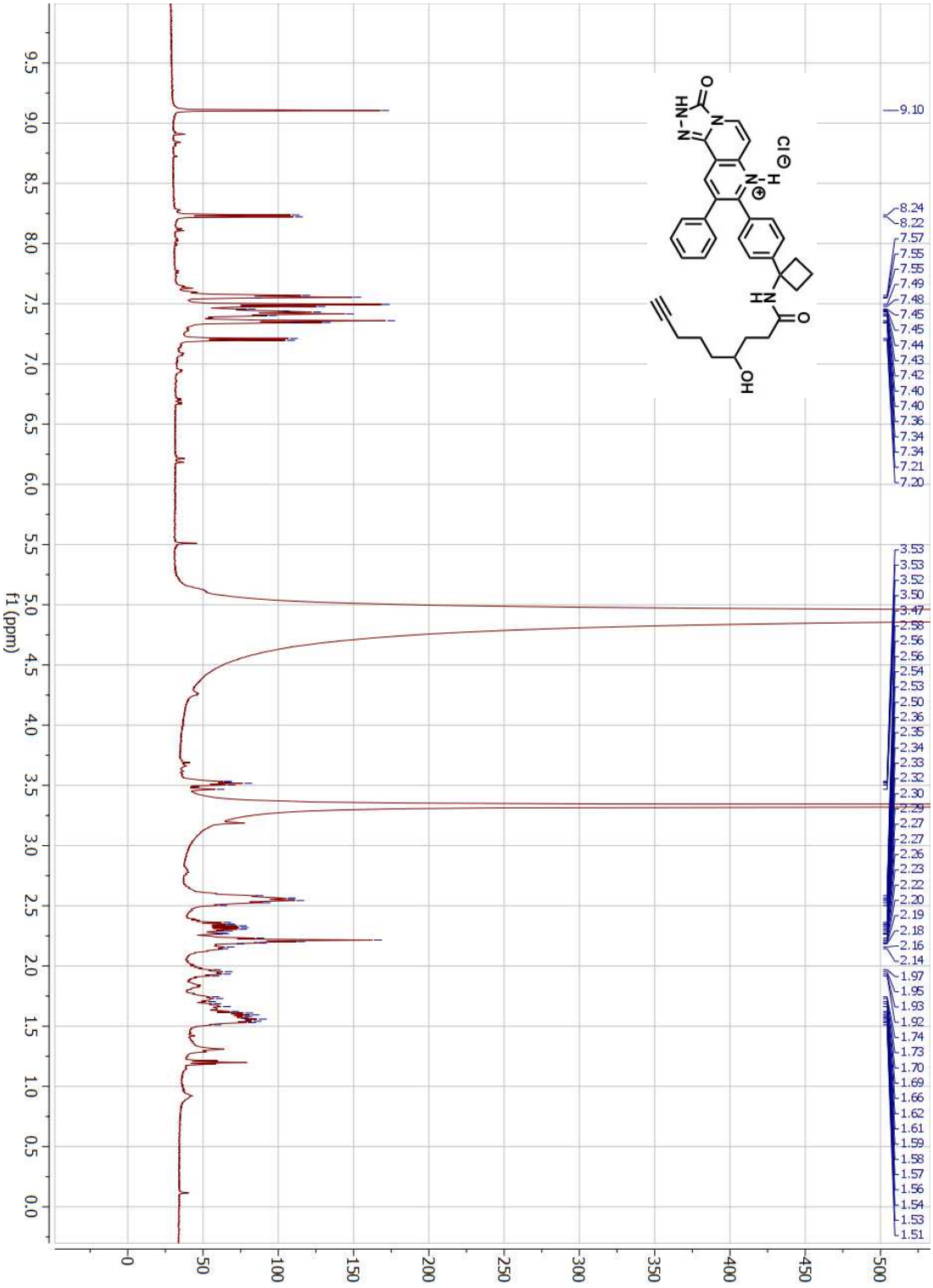

Notes: The minor impurity (5%) in this ^{1}H NMR spectrum is corresponding to the impurity (likely the corresponding α,β-unsaturated lipid) present in the lipid starting material. H_2O solvent residue peak is present in this ^{1}H NMR spectrum.

^{13}C NMR spectrum of **MK-HNA (HCl salt)**

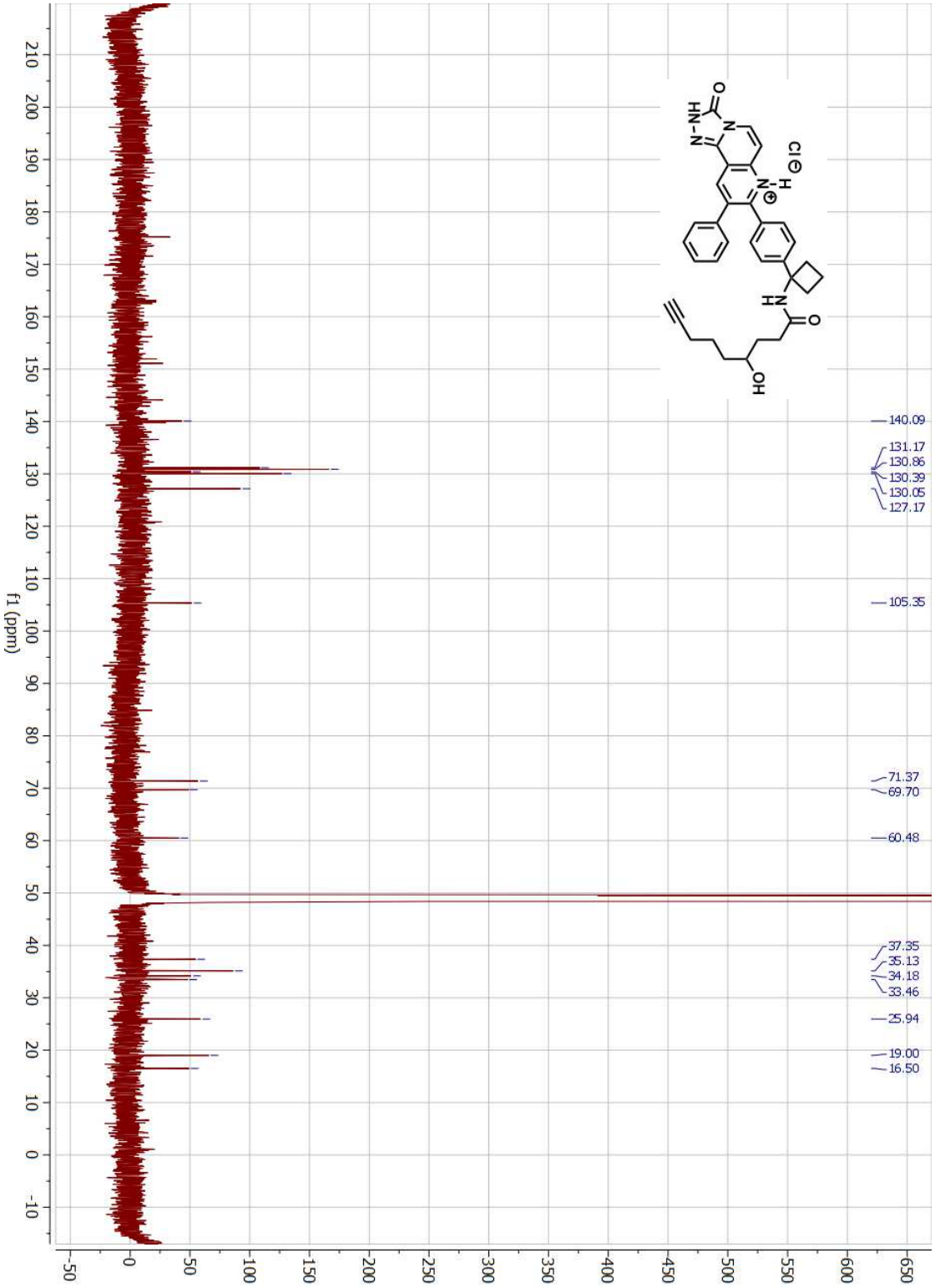

UPLC-MS analysis of **MK-HNA**

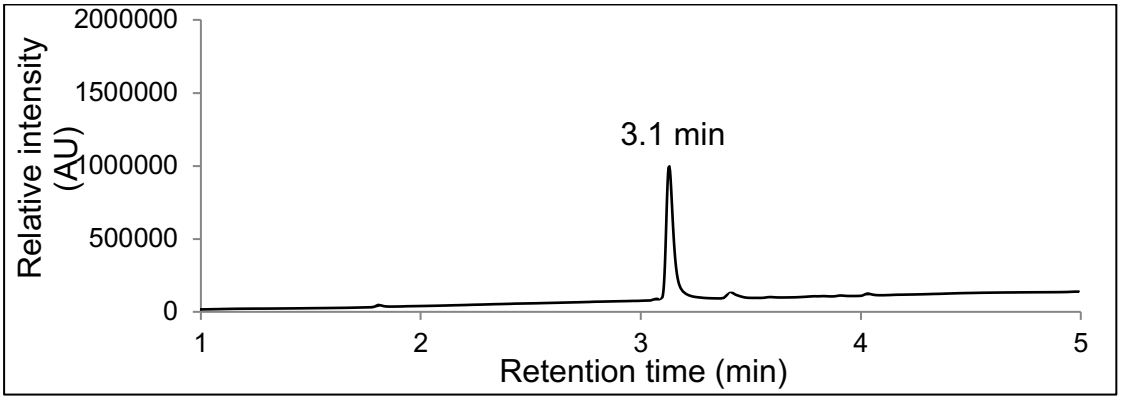

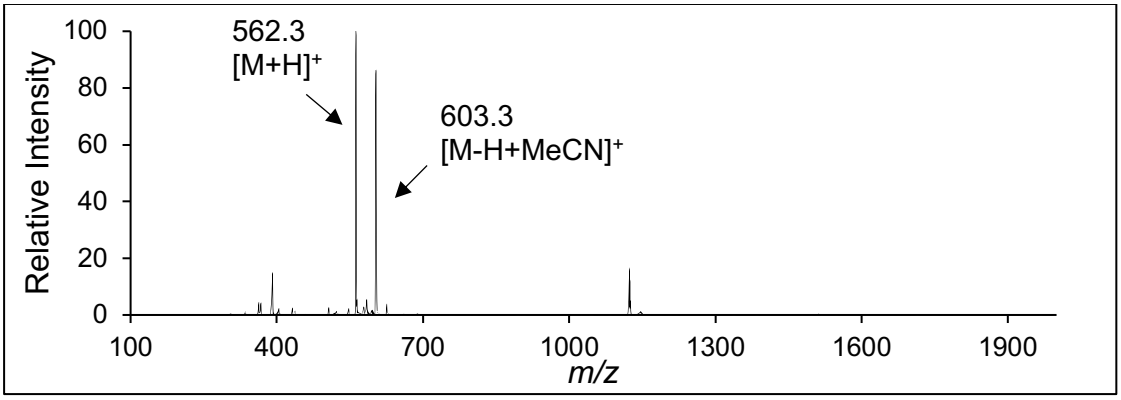

Synthesis of MK-G

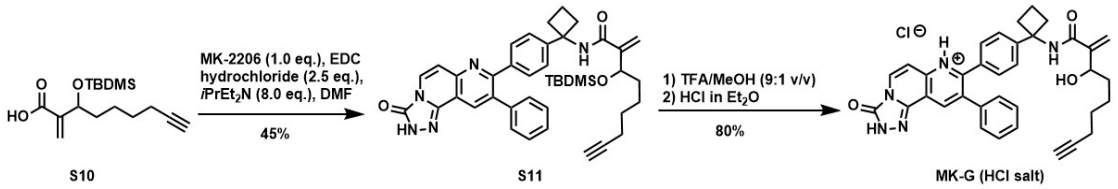

3-((tert-butyldimethylsilyl)oxy)-2-methylene-N-(1-(4-(3-oxo-9-phenyl-2,3-dihydro-[1,2,4]triazolo[3,4-f][1,6]naphthyridin-8-yl)phenyl)cyclobutyl)non-8-ynamide (S11)

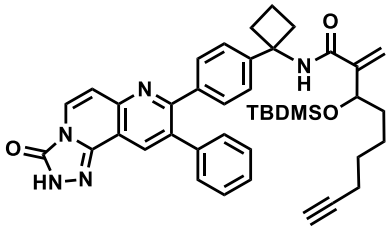

The coupling reaction of **S10** and **MK-2206** was carried out following the general procedure described above. The crude product was purified by flash chromatography (from 4:1 v/v, toluene:EtOAc) to afford the desired product **S11** as a white solid (10 mg, 45%). **^{1}H NMR** (500 MHz, CD_3OD) δ 9.10 (s, 1H), 8.22 (d, *J* = 7.7 Hz, 1H), 7.59 (d, *J* = 8.5 Hz, 2H), 7.51 (d, *J* = 8.5 Hz, 2H), 7.46 – 7.38 (m, 3H), 7.36 – 7.34 (m, 2H), 7.25 (d, *J* = 7.5 Hz, 1H), 5.75 (s, 1H), 5.56 (s, 1H), 4.42 (m, 1H), 2.65 – 2.53 (m, 4H), 2.19 (t, *J* = 2.6 Hz, 1H), 2.17-2.13 (m, 3H), 1.97 (m, 1H), 1.58 – 1.42 (m, 4H), 1.32-1.26 (m, 2H), 0.92 (s, 9H), 0.09 (s, 3H), 0.07 (s, 3H). **^{13}C NMR** (125 MHz, CD_3OD) δ 169.86, 156.16, 151.97, 150.82, 148.88, 144.10, 140.08, 139.86, 139.80, 136.57, 131.27, 131.15, 130.85, 130.68, 130.35, 130.03, 127.16, 120.77, 118.63, 105.51, 84.96, 72.17, 69.65, 60.57, 36.59, 35.30, 35.17, 29.57, 26.32, 26.17, 25.74, 18.96, 16.57,
-3.62, -5.74.

^{1}H NMR spectrum of **S11**

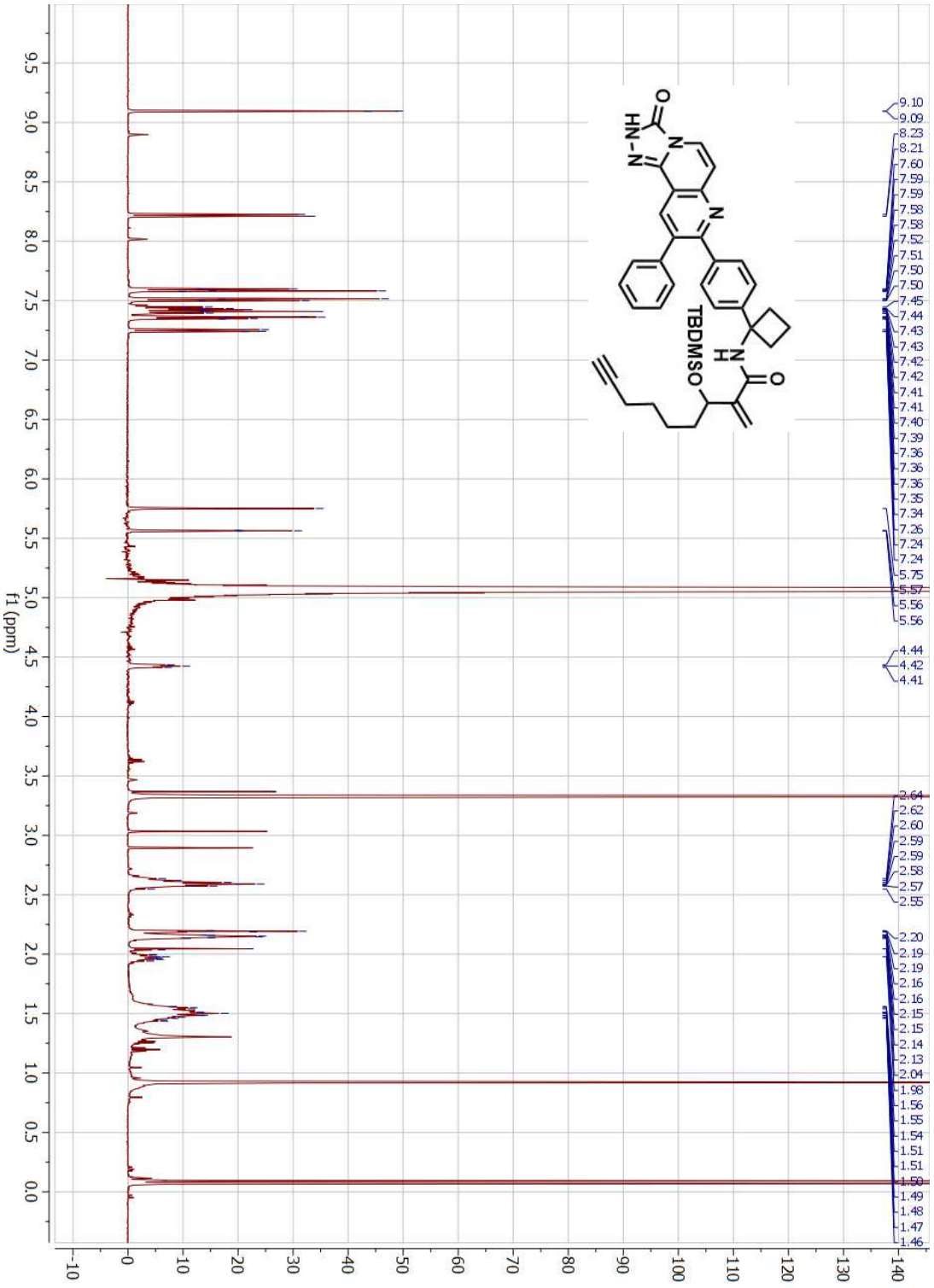

Note: H_2O solvent residue peak is present in this ^{1}H NMR spectrum.

^{13}C NMR spectrum of **S11**

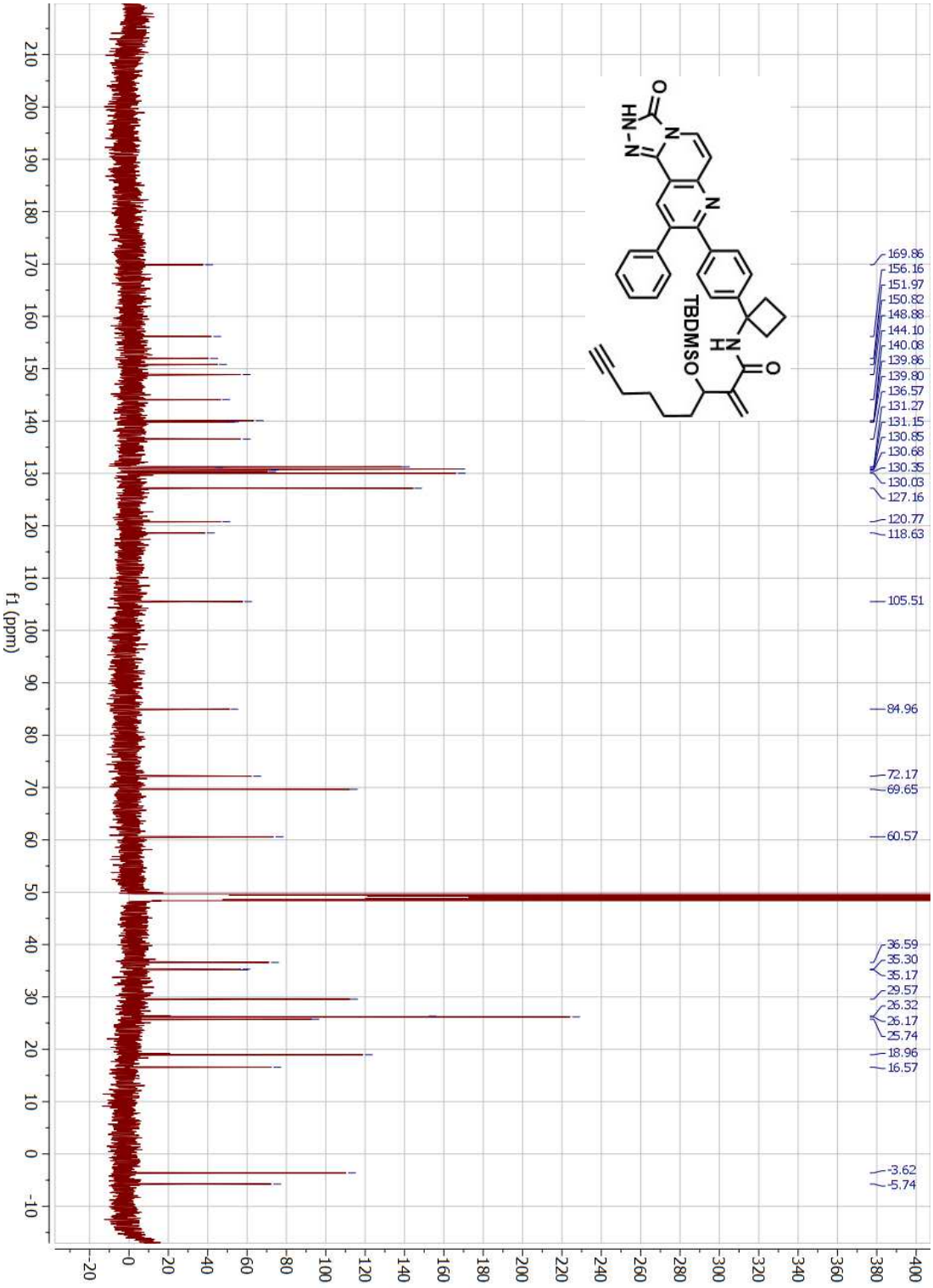

8-(4-(1-(3-hydroxy-2-methylenenon-8-ynamido)cyclobutyl)phenyl)-3-oxo-9-phenyl-2,3-dihydro-[1,2,4]triazolo[3,4-f][1,6]naphthyridin-7-ium chloride [MK-G (HCl salt)]

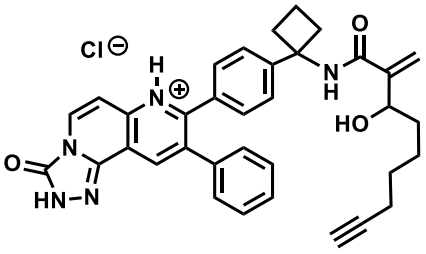

(MK-G, HCl salt)

Silyl ether deprotection reaction was followed the general procedure described above. The resulting crude product was re-dissolved in CH_2Cl_2 and precipitated by slow addition of 1 M HCl in Et_2O to afford **MK-G** as yellow HCl salt (8.5 mg, 80%). **^{1}H NMR** (500 MHz,CD_3OD) δ 8.85 (s, 1H), 8.08 (d, *J* = 7.7 Hz, 1H), 7.52 (d, *J* = 8.4 Hz, 2H), 7.46 (d, *J* = 8.3 Hz, 2H), 7.43 – 7.35 (m, 3H), 7.35 – 7.30 (m, 2H), 7.15 (d, *J* = 7.7 Hz, 1H), 5.74 (s, 1H), 5.55 (s, 1H), 4.42 (m, 1H), 2.65-2.54 (m, 4H), 2.18 (t, *J* = 2.5 Hz, 1H), 2.16 – 2.12 (m, 3H), 1.95 (m, 1H), 1.57 – 1.40 (m, 4H), 1.34 – 1.27 (m, 2H). **^{13}C NMR** (125 MHz, CD_3OD) δ 169.76, 159.16, 152.26, 149.12, 141.22, 138.64, 138.58, 136.50, 131.08, 130.79, 129.84, 129.62, 127.45, 126.70, 119.10, 118.35, 84.93, 72.23, 69.59, 60.60, 36.63, 35.37, 35.16, 29.64, 25.78, 19.00, 16.61. Analytical UPLC of MK-G: Retention time, 3.1 min (0 to 100% Eluent B over 5 min, λ = 230 nm). Mass spectrum (ESI+) of MK-G: Calculated mass for $C_{35}H_{34}N_5O_3^+$ $[M+H]^+$: 572.3; Mass Found $[M+H]^+$: 572.2.

^{1}H NMR spectrum of **MK-G (HCl salt)**

Note: H_2O and CH_2Cl_2 solvent residue peaks are present in this ^{1}H NMR spectrum.

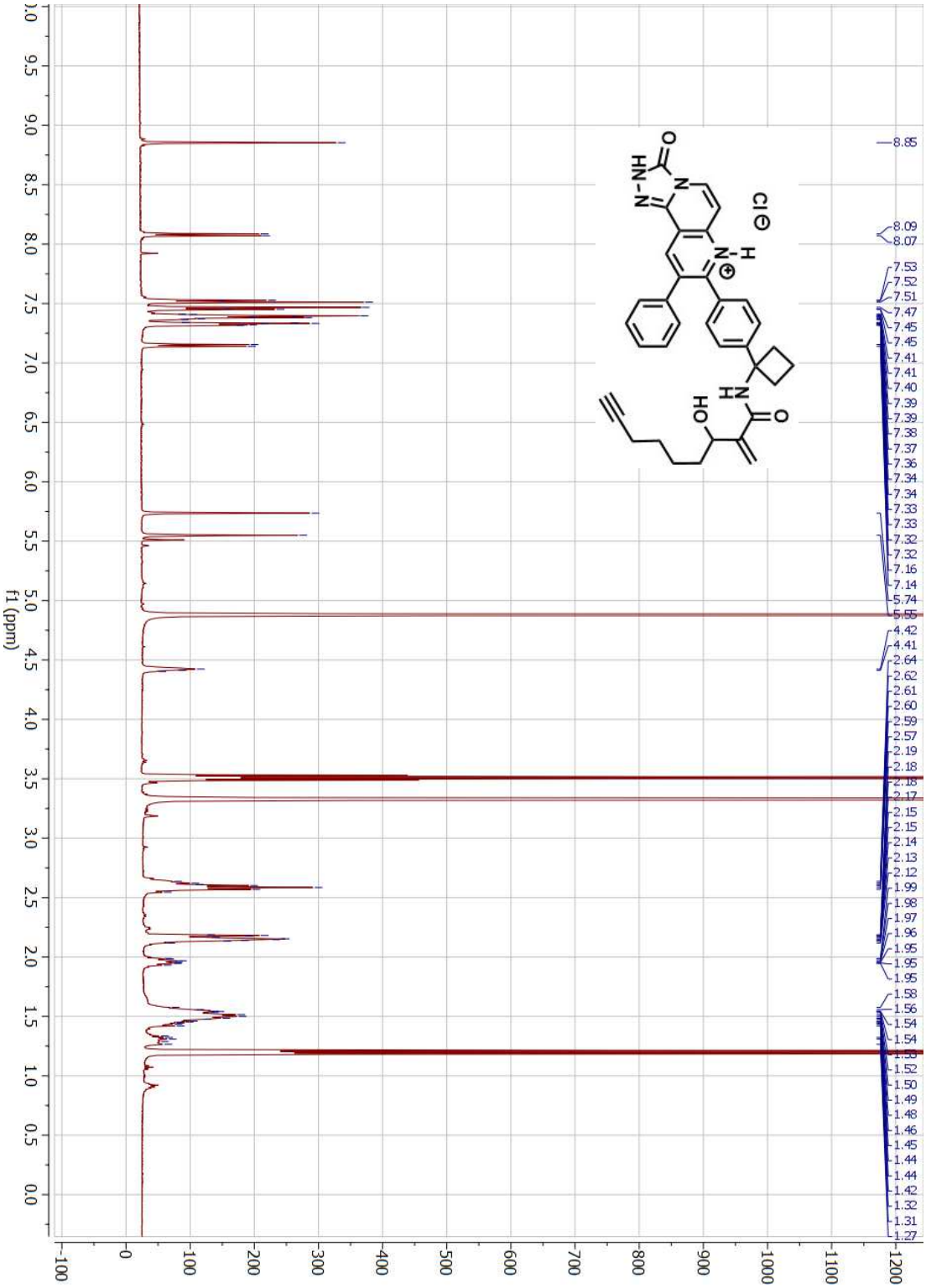

^{13}C NMR spectrum of **MK-G (HCl salt)**

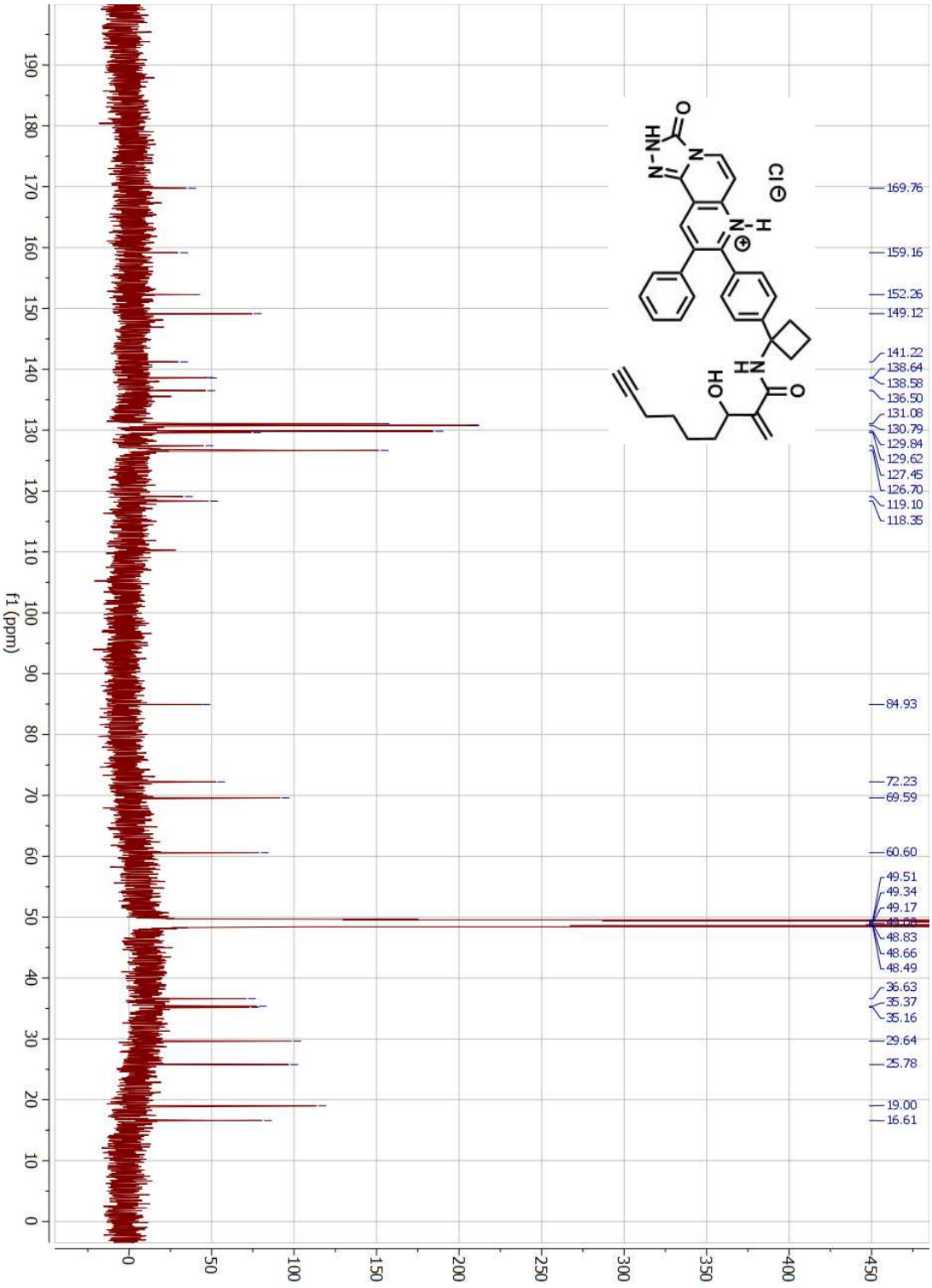

UPLC-MS analysis of **MK-G (HCl salt)**

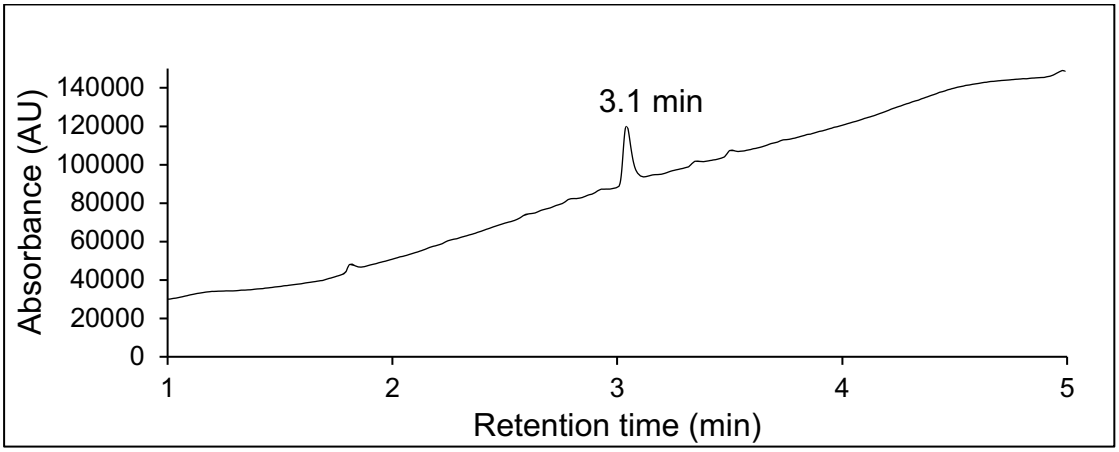

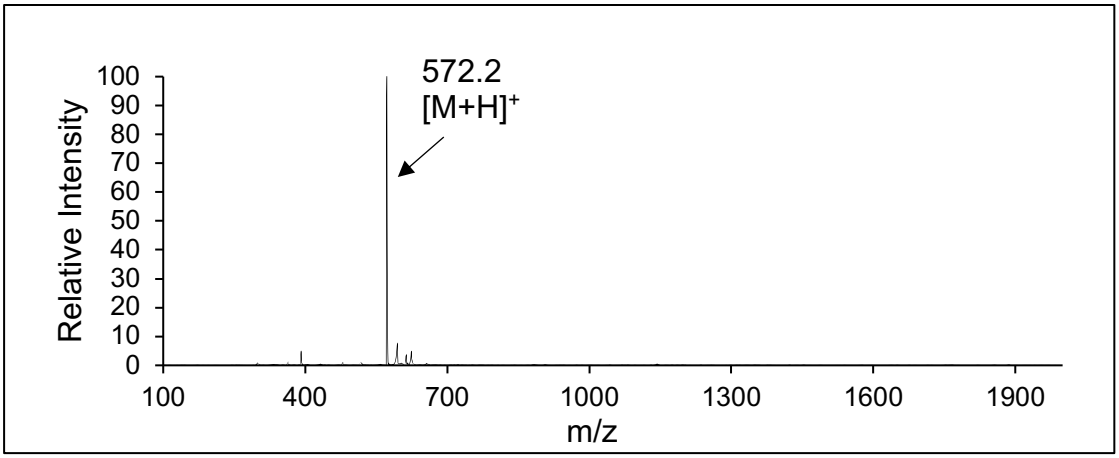

Synthesis of HNE-amide

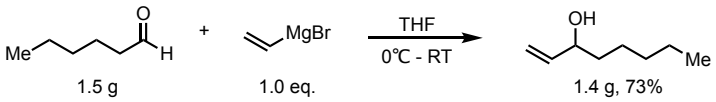

1-Octen-3-ol In an oven-dried round bottom flask, hexanal (1.5 g, 15 mmol, 1.0 equiv.) was dissolved in 10 mL of tetrahydrofuran. To the solution was slowly added vinyl Grignard reagent (15 mL, 15.0 mmol, 1.0 equiv) at 0 °C with an ice bath. The flask was allowed to warm to room temperature and stir for another 2 hours. The reaction mixture was quenched with saturated ammonium chloride aqueous solution (20 mL) and extracted with diethyl ether (3 x 20 mL). The combined organic phase was dried over anhydrous sodium sulfate, filtered and concentrated. The product was isolated by flash column chromatography (ethyl acetate:hexane = 1:8) as a colorless oil (1.4 g, 10.9 mmol, 73% yield). The spectroscopic data matches a previous report[6].

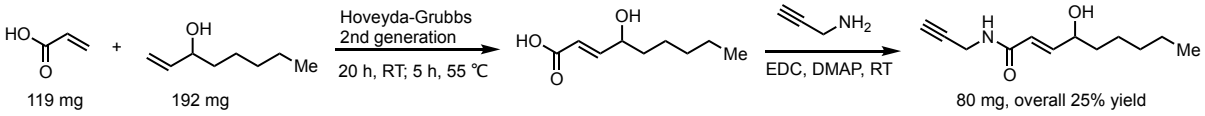

(E)-4-hydroxy-*N*-(prop-2-yn-1-yl)non-2-enamide To an oven-dried 25 mL round bottom flask was added 1-octen-3-ol (192 mg, 1.5 mmol, 1.0 equiv), acrylic acid (119 mg, 1.65 mmol, 1.1 equiv) and dissolved in 5 mL of tetrahydrofuran. To the solution was added Hoveyda-Grubbs 2nd generation catalyst (Hoveyda-Grubbs Catalyst® M72 (C627), 12 mg, 0.019 mmol, 0.013 equiv). The flask was then sealed with a septum, evacuated and backfill with argon. The reaction mixture was stirred at room temperature for 20 hours, and another 5 hours under 55 ℃. The reaction mixture was transferred to a separating funnel containing water (15 mL) and extracted with dichloromethane (3 x 15 mL). The combined organic phase was dried over anhydrous sodium sulfate, filtered and concentrated. To this crude mixture was added propargyl amine (100 mg, 1.8 mmol), EDC hydrochloride (345 mg, 1.8 mmol), DMAP (220 mg, 1.8 mmol) and dichloromethane (10 mL). The reaction mixture was stirred at room temperature overnight. Solvent was removed by rotary evaporator and the product was isolated by flash column (ethyl acetate:hexane = 1:1) as an off-white solid (80 mg with ~6% impurity). Recrystallization in ethyl acetate and hexane afforded the pure compound (off-white solid, 50 mg). **^{1}H NMR** (400 MHz, $CDCl_3$) δ 6.90 (dd, *J* = 15.2, 4.6 Hz, 1H), 6.01 (dd, *J* = 15.3, 1.6 Hz, 1H), 5.66 (br s, 1H), 4.32 (m, 1H), 4.14 (d, *J* = 2.5 Hz, 1H), 4.13 (d, *J* = 2.5 Hz, 1H), 2.25 (t, *J* = 2.5 Hz, 1H), 1.51 – 1.63 (m, 2H), 1.28 – 1.47 (m, 6H), 0.89 (t, *J* = 6.8 Hz, 3H). **^{13}C NMR** (101 MHz, $CDCl_3$) δ 165.5, 147.4, 121.6, 79.6, 71.9, 71.3, 37.0, 31.9, 29.5, 25.1, 22.7, 14.2. **LC-MS** (ESI) $[M+H]^+$ calcd. for $[C_{12}H_{20}NO_2]^+$ 210, 210 found.

^{1}H NMR spectrum of **HNE-amide**

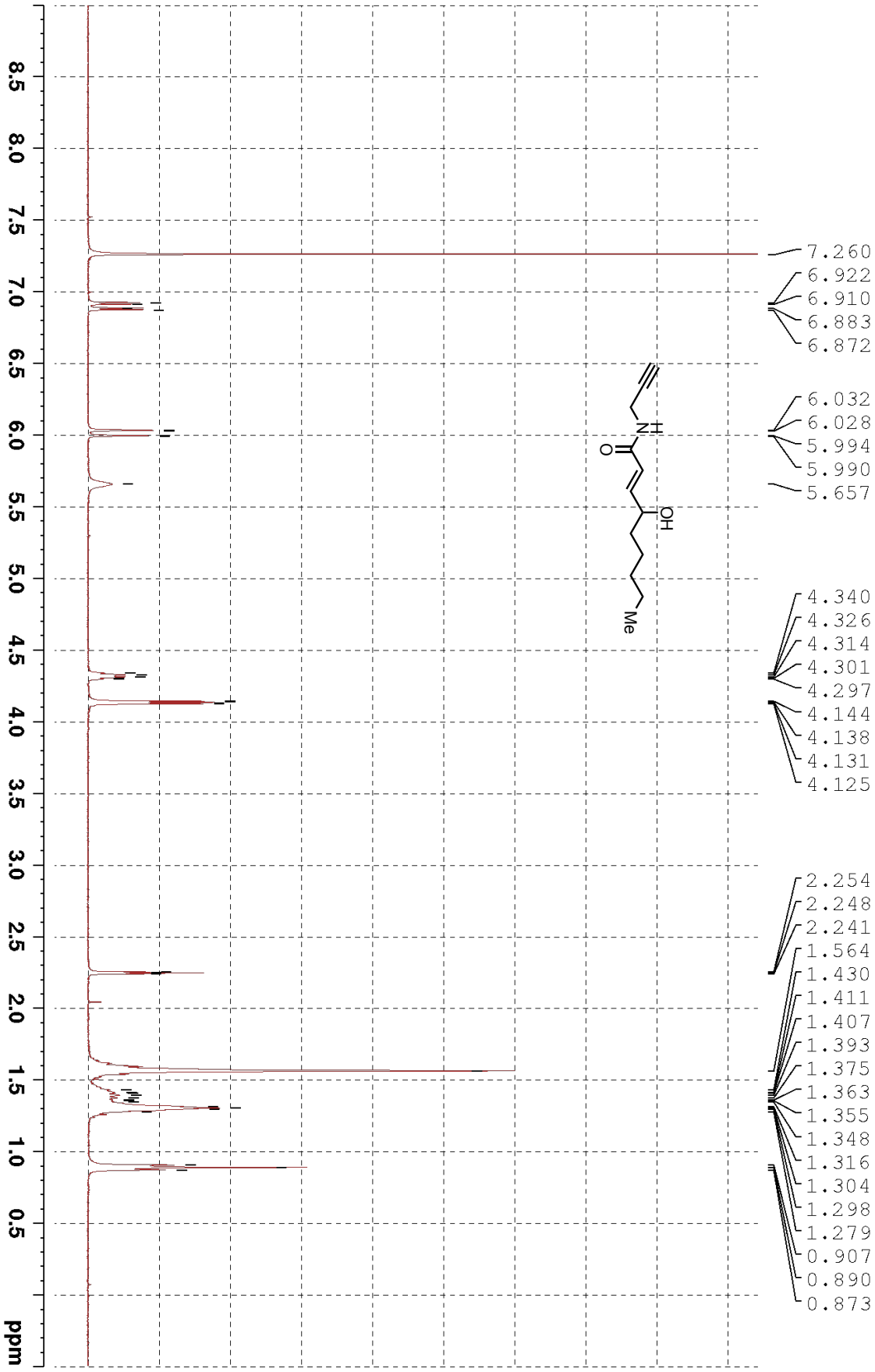

^{13}C NMR spectrum of **HNE-amide**

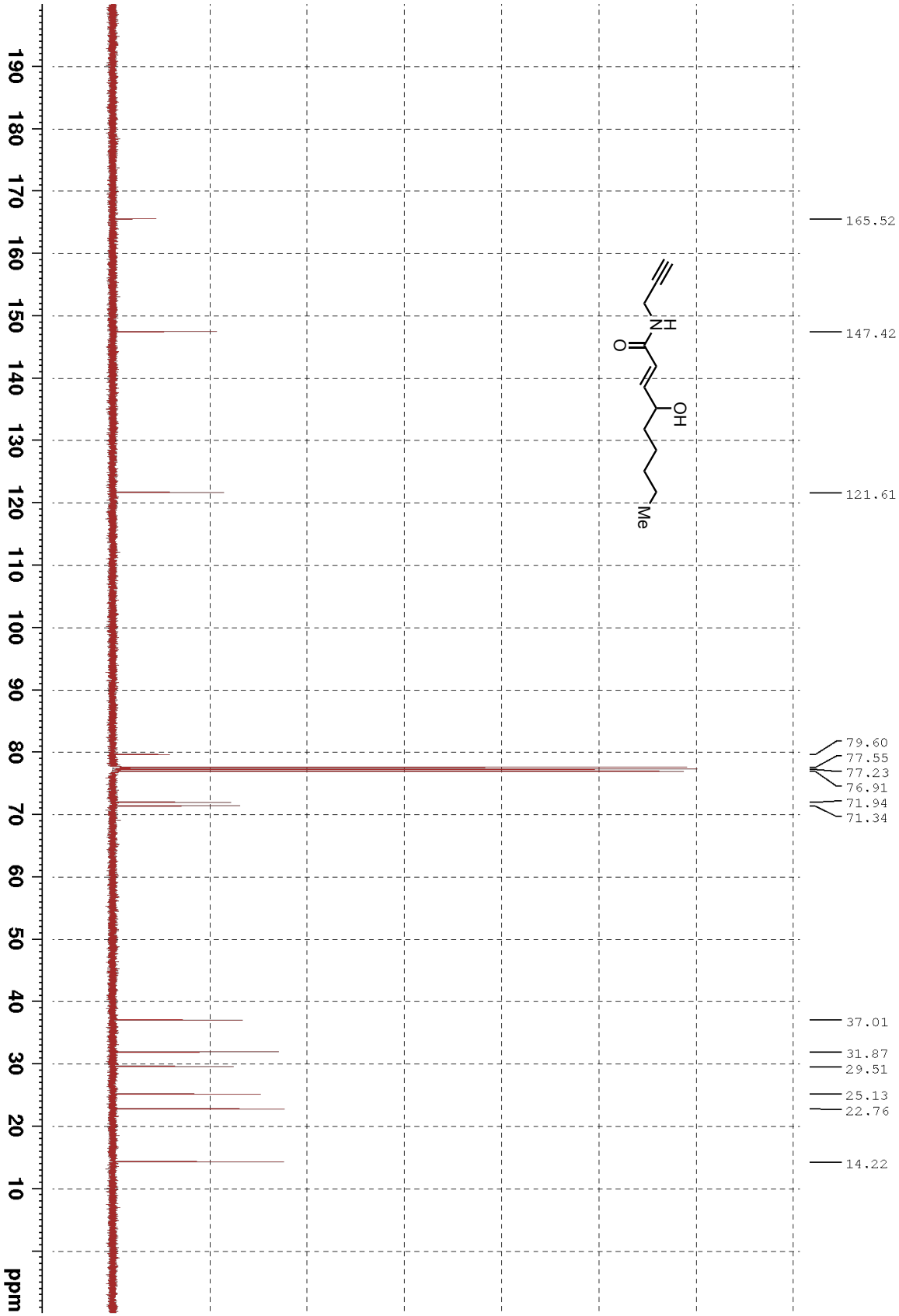

UPLC-MS analysis of **HNE-amide**

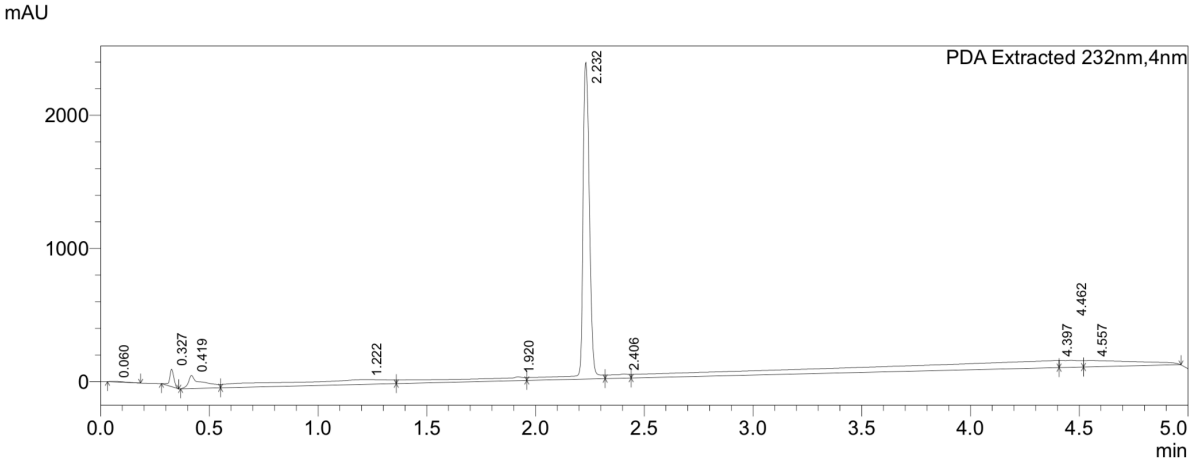

Line#:1 R.Time:2.267(Scan#:681)
MassPeaks:1590
RawMode:Single 2.267(681) BasePeak:251(693552)
BG Mode:None Segment 1 - Event 1

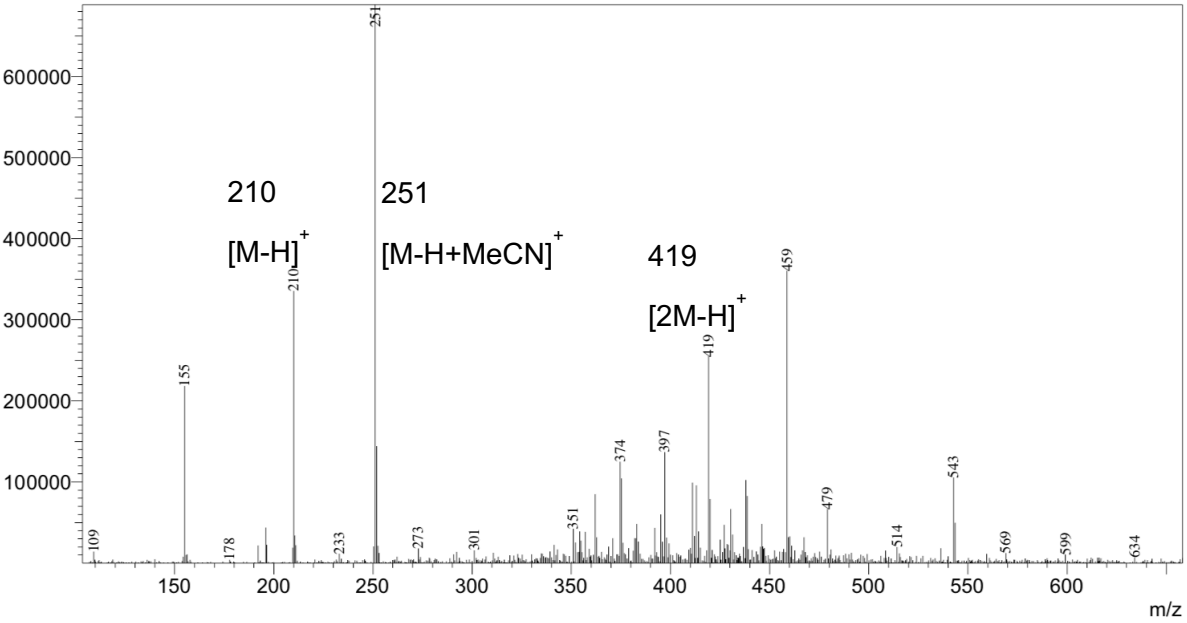

Statistical analysis.

n for imaging experiments represent the number of single cells quantified from at least 7-8 fields of view with controls (empty vector controls for ectopically-overexpressed proteins, sh/siRNA knockdown cell controls for endogenous proteins) as shown in the figures. n for western blot represents the number of lanes on western blots under identical experimental conditions and each lane is from a separate individual replicate/experiment. Unless specified, all *t* tests were two-tailed analysis.

Figure 1, n≥3 independent biological replicates; *t* test of MK-HNE treatment group: p = 0.051 (His_6-Halo-Akt1-2xFlag and His_6-Halo-Akt2-2xFlag), p = $1.6e^{-5}$ (His_6-Halo-Akt1-2xFlag and His_6-Halo-Akt3(wt)-2xFlag), p = $3.5e^{-4}$ (His_6-Halo-Akt2-2xFlag and His_6-Halo-Akt3(wt)-2xFlag), p = $1.7e^{-5}$ (His_6-Halo-Akt3(C119S)-2xFlag and His_6-Halo-Akt3(wt)-2xFlag). *t* test of comparison between MK-HNE and MK-HNA treatment of His_6-Halo-Akt3(wt)-2xFlag: p = $4.8e^{-5}$, and His_6-Halo-Akt2-2xFlag, p = 0.17. *t* test of MK-G treatment group: p = $2.4e^{-4}$ (His_6-Halo-Akt1-2xFlag and His_6-Halo-Akt2-2xFlag), p = 0.007 (His_6-Halo-Akt1-2xFlag and His_6-Halo-Akt3(wt)-2xFlag), p = $6.5e^{-5}$ (His_6-Halo-Akt2-2xFlag and His_6-Halo-Akt3(wt)-2xFlag), p = 0.246 (His_6-Halo-Akt3(C119S)-2xFlag and His_6-Halo-Akt3(wt)-2xFlag). *t* test of each MK-G treatment group vs MK-HNE treatment of His_6-Halo-Akt1-2xFlag: p = 0.025 (His_6-Halo-Akt1-2xFlag), p = 0.05 (His_6-Halo-Akt2-2xFlag), p = 0.016 (His_6-Halo-Akt3(C119S)-2xFlag), p = 0.019 (His_6-Halo-Akt3(wt)-2xFlag).

Figure 2, Cell number analyzed (from left to right panels) = 385, 201, 528, 200, 90, 85, 100, 321, 138 [Akt3(wt)]; and 108, 122, 320, 114, 81, 93, 91, 74, 90 [Akt3(C119S)]; *t* test of compound treatment of Akt3(wt), 24-h treatment: p = $8.5e^{-8}$ (DMSO and MK-2206), p = $1.0e^{-15}$ (DMSO and MK-HNE), p = 0.089 (MK-2206 and MK-HNE); 48-h treatment: p = $1.9e^{-11}$ (DMSO and MK-2206), p = $6.8e^{-8}$ (DMSO and MK-HNE), p = 0.677 (MK-2206 and

MK-HNE); Withdrawal: p = 0.056 (DMSO and MK-2206), p = $4.3e^{-8}$ (DMSO and MK-HNE), p = $3.0e^{-12}$ (MK-2206 and MK-HNE). *t* test of compound treatment of HEK293T expressing Akt3(C119S), 24-h treatment: p = $1.0e^{-15}$ (DMSO and MK-2206), p = $1.0e^{-15}$ (DMSO and MK-HNE), p = 0.005 (MK-2206 and MK-HNE); 48-h treatment: p = $2.9e^{-6}$ (DMSO and MK-2206), p = 0.051 (DMSO and MK-HNE), p = 0.007 (MK-2206 and MK-HNE); Withdrawal: p = 0.062 (DMSO and MK-2206), p = 0.198 (DMSO and MK-HNE), p = 0.002 (MK-2206 and MK-HNE).

Figure 3e, Cell number analyzed (from left to right panels) = 497, 326, 375, 312, 337; *t* test of comparison between each plasmid mixture of Akt3(wt) and Akt3(C119S), p = 0.094 (100:0 and 50:50), p = $1.0e^{-15}$ (100:0 and 25:75), p = $1.8e^{-8}$ (100:0 and 10:90), p = $6.3e^{-14}$ (100:0 and 0:100), p = $1.7e^{-5}$ (50:50 and 25:75), p = 0.0062 (50:50 and 10:90), p = $7.0e^{-5}$ (50:50 and 0:100), p = 0.151 (25:75 and 10:90), p = 0.231 (10:90 and 0:100).

Figure 5d, n ≥ 4 independent biological replicates; *t* test: p = 0.215 (shCont-1 and shCont-2), p = 0.015 (shCont-1 and shKIFC1-1), p = 0.011 (shCont-2 and shKIFC1-1), p = 0.013 (shCont-1 and shKIFC1-2), p = 0.007 (shCont-2 and shKIFC1-2), p = 0.006 (shCont-1 and shKIFC1-3), p = 0.005 (shCont-2 and shKIFC1-3).

Figure 5e, n ≥ 3 independent biological replicates; *t* test, p = 0.039 (MK-FNE and MK-2206).

Figure 6b, n = 14 independent sets of biological replicates; *t* test, p = 0.062 (DMSO and MK-2206), p = 0.032 (DMSO and MK-FNE), p = 0.731 (DMSO and MK-HNE).

Figure 6d, n = 5 independent sets of biological replicates; *t* test, p = 0.018 (MK-2206 and MK-FNE), p = 0.027 (MK-2206 and MK-HNE), p = 0.885 (MK-FNE and MK-HNE).

Figure S4, Cell number analyzed (from left to right panels) = 303, 150, 406, 77, 198, 122, 163, 144 and 98; *t* test of compound treatment of Akt2, 24-h treatment: p = $6.5e^{-12}$ (DMSO and MK-2206), p = $2.0e^{-15}$ (DMSO and MK-HNE), p = 0.845 (MK-2206 and MK-HNE); 48-h treatment: p = 0.0002 (DMSO and MK-2206), p = $2.4e^{-6}$ (DMSO and MK-HNE), p = 0.02 (MK-2206 and MK-HNE); Withdrawal: p = 0.153 (DMSO and MK-2206), p = $8.1e^{-9}$ (DMSO and MK-HNE), p = $9.3e^{-8}$ (MK-2206 and MK-HNE).

Figure S5a, n ≥ 4 independent biological replicates; *t* test, p = 0.0014 (DMSO and MK-2206), p = 0.142 (DMSO and MK-HNE), p = $3.2e^{-5}$ (MK-2206 and MK-HNE).

Figure S5b, n ≥ 3 independent biological replicates; *t* test, p = $2.6e^{-7}$ (DMSO and MK-2206), p = 0.713 (DMSO and MK-HNE), p = 0.021 (MK-2206 and MK-HNE).

Figure S6, n = 4 independent biological replicates; *t* test, p = 0.743 (MK-NE and MK-HNE), p = 0.958 (MK-NE and MK-FNE), p = 0.758 (MK-HNE and MK-FNE).

Figure S9(b), Cell number analyzed (from left to right panels) = 139, 177, 159, 140; *t* test of comparison between each plasmid mixture of Akt2 and Akt3(C119S), p = 0.466 (100:0 and 50:50), p = 0.583 (100:0 and 25:75), p = 0.979 (100:0 and 0:100), p = 0.001 (50:50 and 25:75), p = 0.045 (50:50 and 0:100), p = 0.472 (25:75 and 0:100).

Figure S9(d), Cell number analyzed (from left to right panels) = 76, 121, 164, 142; *t* test of comparison between each plasmid mixture of Akt2 and Akt3(C119S), p = 0.087 (100:0

and 50:50), p = 0.340 (100:0 and 25:75), p = $1.2e^{-8}$ (100:0 and 0:100), p = 0.157 (50:50 and 25:75), p = $1.2e^{-14}$ (50:50 and 0:100), p = $2.7e^{-9}$ (25:75 and 0:100).

Figure S9(f), Cell number analyzed (from left to right panels) = 170, 107, 158, 148; *t* test of comparison between each plasmid mixture of Akt2 and Akt3(C119S), p = $9.5e^{-8}$ (100:0 and 50:50), p = $1.0e^{-15}$ (100:0 and 25:75), p = $1.0e^{-15}$ (100:0 and 0:100), p = $4.9e^{-7}$ (50:50 and 25:75), p = $9.0e^{-7}$ (50:50 and 0:100), p = 0.723 (25:75 and 0:100).

Figure S10

n ≥ 7 independent biological replicates; *t* test, p = 0.0002 (MK-2206 and MK-2206 wd), p = 0.7523 (MK-HNE and MK-HNE wd), p = 0.1598 (MK-FNE and MK-FNE wd), p = 0.184 (MK-2206 and MK-HNE), p = 0.262 (MK-2206 and MK-FNE).

Figure S11

8 independent biological replicates; *t* test, p = 0.748 ([MK-2206]:[HNE-amide], 0:0 and [MK-2206]:[HNE-amide], 0:100), p = 0.018 ([MK-2206]:[HNE-amide], 0:0 and [MK-2206]:[HNE-amide], 0:200), p = 0.052 ([MK-2206]:[HNE-amide], 0:100 and [MK-2206]:[HNE-amide], 0:200), p = $8.3e^{-5}$ ([MK-2206]:[HNE-amide], 0:0 and [MK-2206]:[HNE-amide], 0.5:0), p = $6.9e^{-8}$ ([MK-2206]:[HNE-amide], 0:0 and [MK-2206]:[HNE-amide], 0.5:100), p = $1.3e^{-8}$ ([MK-2206]:[HNE-amide], 0:0 and [MK-2206]:[HNE-amide], 0.5:200), p = $5.6e^{-10}$ ([MK-2206]:[HNE-amide], 0:0 and [MK-2206]:[HNE-amide], 1.0:0), p = $1.0e^{-9}$ ([MK-2206]:[HNE-amide], 0:0 and [MK-2206]:[HNE-amide], 1.0:100), p = 5.1 e^{-8} ([MK-2206]:[HNE-amide], 0:0 and [MK-2206]:[HNE-amide], 1.0:200).

Figure S12, n ≥ 3 independent biological replicates; *t* test, p = 0.271 (Akt1: wt and MK-res), p = 0.986 (Akt2: wt and MK-res), p = 0.033 (Akt3: wt and MK-res).

Figure S13, n ≥ 3 independent biological replicates; *t* test of Akt3 gene silencing with the respective siRNA followed by western blot probing with anti-Akt3 antibody, p = 0.260 (siCont-1 and siCont-2), p = 0.003 (siCont-1 and siAkt3-1), p = 0.0008 (siCont-1 and siAkt3-2), p = 0.106 (siCont-2 and siAkt3-1), p = 0.0096 (siCont-2 and siAkt3-2). *t* test of Akt2 gene silencing with the respective siRNA followed by western blot probing with anti-Akt2 antibody, p = 0.237 (siCont-1 and siCont-2), p = 0.004 (siCont-1 and siAkt2-1), p = 0.0003 (siCont-1 and siAkt2-2), p = 0.002 (siCont-2 and siAkt2-1), p = 0.0001 (siCont-2 and siAkt2-2), p = $1.0e^{-5}$ (siCont-1 and siAkt2-3), p = $1.2\ e^{-11}$ (siCont-1 and siAkt2-4), p = $4.3e^{-10}$(siCont-1 and siAkt2-5). *t* test of Akt1 gene silencing with the respective siRNA followed by western blot probing with anti-Akt1 antibody, p = 0.324 (siCont-1 and siCont-2), p = 0.035 (siCont-1 and siAkt1-1), p = 0.039 (siCont-1 and siAkt1-2), p = 0.001 (siCont-2 and siAkt1-1), p = $6.0e^{-5}$ (siCont-2 and siAkt1-2).

Figure S16, n ≥ 4 independent biological replicates; *t* test of Grsf1 gene silencing followed by western blot probing with anti-Grsf1 antibody, p = 0.137 (shCont-1 and shCont-2), p = 0.031 (shCont-1 and shGrsf1-1), p = 0.360 (shCont-1 and shGrsf1-2), p = 0.405 (shCont-1 and shGrsf1-3), p = 0.002 (shCont-2 and shGrsf1-1), p = 0.019 (shCont-2 and shGrsf1-2), p = 0.052 (shCont-2 and shGrsf1-3). *t* test of JUP gene silencing followed by western blot probing with anti-JUP antibody, p = 0.034 (shCont-1 and shCont-2), p = $1.4e^{-7}$(shCont-1 and shJUP-1), p = 0.073 (shCont-1 and shJUP-2), p = $2.0e^{-4}$ (shCont-1 and shJUP-3), p = $1.0e^{-5}$ (shCont-2 and shJUP-1), p = 0.363 (shCont-2 and shJUP-2), p = 0.001 (shCont-2 and shJUP-3).

Figure S22b, n = 14 independent biological replicates; *t* test, p = 0.014 (DMSO and MK-2206), p = 0.006 (DMSO and MK-FNE), p = 0.341 (DMSO and MK-HNE).

Supplementary References:

1. Shechter, D.; Dormann, H. L.; Allis, C. D.; Hake, S. B., Extraction, purification and analysis of histones. *Nat. Protoc.* **2007,** *2* (6), 1445-1457.
2. Hornbeck, P. V.; Zhang, B.; Murray, B.; Kornhauser, J. M.; Latham, V.; Skrzypek, E., PhosphoSitePlus, 2014: mutations, PTMs and recalibrations. *Nucleic acids research* **2015,** *43* (Database issue), D512-D520.
3. Goldman, M.; Craft, B.; Hastie, M.; Repečka, K.; Kamath, A.; McDade, F.; Rogers, D.; Brooks, A.; Zhu, J.; Haussler, D., The UCSC Xena platform for public and private cancer genomics data visualization and interpretation. bioRxiv: 2018.
4. Yang, Y.; Anderson, E.; Zhang, S., Evaluation of six sample preparation procedures for qualitative and quantitative proteomics analysis of milk fat globule membrane. *Electrophoresis* **2018,** *39* (18), 2332-2339.
5. Harman, R. M.; He, M. K.; Zhang, S.; Van De Walle, G. R., Plasminogen activator inhibitor-1 and tenascin-C secreted by equine mesenchymal stromal cells stimulate dermal fibroblast migration in vitro and contribute to wound healing in vivo. *Cytotherapy* **2018,** *20* (8), 1061-1076.
6. Whittaker, A. M.; Lalic, G., Monophasic Catalytic System for the Selective Semireduction of Alkynes. *Organic Letters* **2013,** *15* (5), 1112-1115.

Acknowledgement:

Swiss National Science Funding (SNSF) Project Funding (310030_184729); NCCR Chemical Biology (SNSF); NIH Director's New Innovator (1DP2GM114850); Novartis Medical-Biological Research Foundation (Switzerland); Swiss Federal Institute of Technology Lausanne (EPFL) (to Y.A.). Miss Sanjna Surya (a former undergraduate researcher in Y.A. team, and now an MD-student at Perelman School of Medicine, University of Pennsylvania) for her assistance in initial studies. Dr. Sheng Zhang and staff members at Cornell University proteomics facility for assistance with SILAC-data processing and analysis and NIH SIG grant 1S10 OD017992-01 grant for the Orbitrap Fusion mass spectrometer. The FRET reporter images were created with Biorender.